VSB – TECHNICAL UNIVERSITY OF OSTRAVA

FACULTY OF METALLURGY AND MATERIALS ENGINEERING

Fracture Mechanics

Study Support

Stanislav Lasek

Ostrava 2015

Title: Fracture Mechanics (Introduction)

Code: 636 – 3005/01

Author: doc. Ing. Stanislav Lasek, Ph.D.

Edition: First, 2015

Number of pages: 93

Academic materials for the Advanced Engineering Materials study programme at the Faculty of Metallurgy and Materials Engineering.

Proofreading has not been performed.

Execution: VŠB – Technical University of Ostrava

Preface

This study support is intended primarily for students of the combined form of the bachelor's degree study, who have limited direct instruction with a teacher. This support is suitable for an introductory study of the Fracture Mechanics course (in the 1st year of master's degree study, specialization Diagnostics and Design of Materials, field of study – Advaced Engineering Materials) and should also motivate to further and more extensive study of the subject.

The Fracture Mechanics course follows mainly in the courses of Physics, Materials Science and Fundamentals of Strength and Elasticity. Fracture mechanics is a multidisciplinary technical field of material failures due to cracks and fractures. It is also closely related to diagnostics, defectoscopy and quality of products.

Findings from the fracture mechanics course are applied in assessment of material or structural failure, to increase reliability and a lifetime of components and devices. Knowledge of the subject can be used in designing and construction of many components with requirements for weight reduction (especially vehicles), energy saving and reducing total operational cost of equipment. Findings in fracture mechanics are also used in research and development of new progressive materials, particularly high-strength alloys and ceramic materials.

The study support is divided into 8 main chapters, each containing prescribed particulars: time dedicated to study, study objectives, interpretation itself, summary of knowledge or principal terms. At the end of each chapter, there are questions, solved problems or exercises for individual solving with results for a check. At the end of this study support, there is also provided a bibliography and other sources of knowledge and information for the study.

Students can consult solving techniques and results of exercises directly with the teacher in his office or via e-mail or by phone.
In case of doubts, questions or observations, please contact the author of the support at the e-mail address (stanislav.lasek@vsb.cz) or by phone at 596995205.

The author of the support wishes you to master the Fracture Mechanics successfully.

doc. Ing. Stanislav Lasek, Ph.D.

Table of Contents

1. INTRODUCTION TO THE FRACTURE BEHAVIOUR OF MATERIALS

Time dedicated to the study of this chapter is approximately 2 hours.

Design of components or structures is usually associated with the requirement to minimize potential failure, to reduce material consumption and total cost. Therefore, it is essential to understand behaviour of materials in practice and processes of failures - e.g. brittle fractures, fatigue failures or stress corrosion cracking. It is also necessary to respect the principles to be used to prevent failures in operation.

Objective:
After studying this chapter, you will be able to

- Express and apply true strains and true stresses.
- Characterize brittle and ductile fractures from the macroscopic and microscopic point of view.
- Describe basic conditions for crack initiation for the brittle and ductile failure mode.
- Define the concepts of fracture mechanics

Interpretation

A big boom in production and use of steel structures in the last century was accompanied by failures and breakdowns of structures (bridges, large tanks, vessels, boilers, railway vehicle wheelsets, etc.). Incidence of defects in materials, in some cases also poor structural designs or unforeseen operational conditions were the main cause of such breakdowns.

Other problems (even catastrophic incidents in the last century) happened due to sudden brittle fractures in welded structures. Main initiators of dangerous fractures ranked among **material defects and structural notches**, wherein strain concentration and the **triaxial state of stress** occur. Fractures were of brittle nature; changes in composition and structure of material in welded joints contributed to their occurrence. To reduce or eliminate the risk of brittle fracture, welding technologies have been improved and crack detection methods have been introduced. Reducing the incidence of areas with high strain concentration was also significant.

Development of high-strength steels enabled to implement structures with lower weight, smaller transverse dimensions. A disadvantage of these steels lies in relatively lower toughness, i.e. lower resistance to unstable crack propagation and hence a brittle fracture.

In an originally solid material, crack propagation causes creation of new surfaces, i.e. fracture surfaces.

A fracture is a degradation process, inhomogeneous in time and space, consisting of the initiation stage (formation, in a number of localized points) and the phase of propagation and coalescence of cracks.

Besides the negative role of fracture processes, it is necessary to mention the practical use with a beneficial or positive result, such as quarrying of mineral deposits, breaking ice by an icebreaker, separation of material by breaking off, crushing brittle materials etc.

The following first subchapter suits to repeat the basic concepts from the field of materials science, elasticity and strength, needed for the study of further chapters from the field of material failures and fracture mechanics.

1.1. Main Stress-Strain Characteristics

Description of the stress-strain and of other fracture behaviour of materials is usually based on tensile tests and diagrams, **Fig. 1.1**. A tensile test consists in slow loading of a testing rod (of a sample, a product), usually up to a rupture.

Engineering (conventional) diagram $\sigma = f(\varepsilon)$.   True (real) diagram $\sigma' = g(\varepsilon')$

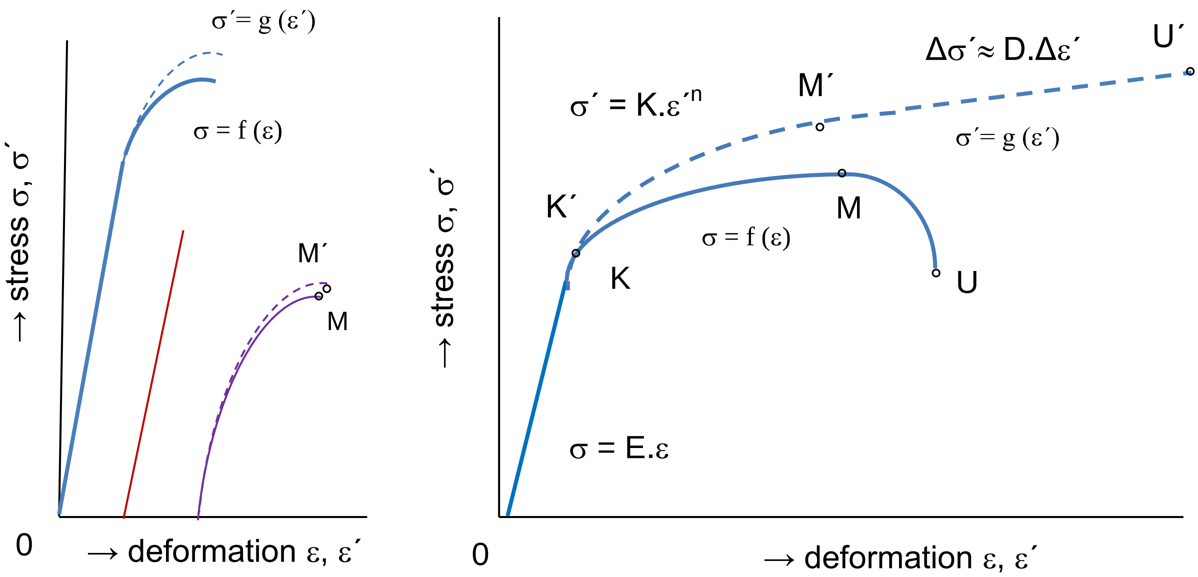

Fig. 1.1*. Comparison of engineering and true stress-strain diagrams of brittle and ductile metal materials. Differences in the yield strength (between the engineering and the true graph - dashed line) are negligible.*

Basic mechanical properties are determined based on the engineering diagram in the coordinates of stress σ - deformation (relative strain) ε, and using the measured values of prescribed dimensions of a sample:

The yield limit:	$R_p = \frac{F_p}{S_0}$ [MPa], where S_o is the initial load-bearing cross-section, F_p – a force at the yield stress (point K)
The tensile strength:	$R_m = \frac{F_m}{S_0}$ [MPa], where F_m is a force at the engineering ultimate strength (point M – at maximum of diagram $\sigma = f(\varepsilon)$)
Ductility	$A = \frac{Lu-Lo}{Lo}$.100 [%], where L_o is the initial measured length of the rod, L_u – length after the rupture
Contraction	$Z = \frac{So-Su}{So}$.100 [%], where S_o is the initial cross-section $S_o \perp F$, S_u – in the rupture point

The engineering ultimate strength is useful for classification and comparing of materials, for structural calculations of load-bearing capacity.

To describe fracture behaviour of material more accurately, true stresses shall be considered

$$\sigma' = \frac{F}{S}, \tag{1.1}$$

where S is a true cross-section, perpendicular to the applied force F, and true (logarithmic) strain

$$\varepsilon' = \ln \frac{L}{L_o}, \tag{1.2}$$

where L is the length of the rod under loading by force F and L_o is the initial length of the rod (when F = 0). Between engineering and true parameters following relations can be derived: $\sigma' = \sigma(1+\varepsilon)$ and $\varepsilon' = \ln(1+\varepsilon)$. An engineering graph can be transformed into a true one and vice versa by these relations.

True stress, or fracture stress

$$\sigma'_u = \frac{F_{u'}}{S_u}. \tag{1.3}$$

True strain in the rupture point (in the middle of a neck) - i.e. rupture strain

$$\varepsilon'_u = \ln \frac{1}{1-Z}. \tag{1.4}$$

Hooke's law is applied within the limit of proportionality, i.e. linear dependence between stress and elastic strain

$$\sigma = E.\varepsilon \quad \text{or} \quad \sigma' = E.\varepsilon', \tag{1.5}$$

where E is the modulus of elasticity in tension. With increasing strain, the stress necessary for further strain continuation increases - hardening occurs. In terms of running physical processes, manifesting themselves by hardening, it is advantageous to monitor the dependence of the actual stress on the actual strain. Empirical Hollomon's equation

$$\sigma' = K.\varepsilon'^n \tag{1.6}$$

applies in the field of smooth plastic deformation (between points K' and M '), where the material constant K is also called strength parameter (coefficient) and **n is the strain hardening exponent** characterizing intensity of hardening by plastic deformation. Generally, n = 0 - 1, for metals and alloys usually: n = 0,1 - 0,5.

For an ideal elastic-plastic material n = 0, for linear elastic material n = 1.

For uneven deformation after formation of a neck (K' - U') it is possible to use rough approximate relation between stress and strain increments $\Delta\sigma' \approx D.\Delta\varepsilon'$, where D is the hardening modulus.

True stress here is average tensile uniaxial stress in the middle of a neck (at the time prior to rupture); in microscopic volumes of material, local maxima of stress are much higher, mainly due to stress concentration on particles around microcavities, microcracks, etc.
For comparison, at the engineering strength of steel R_m = 500 MPa, the true strength (fracture stress) can be σ_u' = 1000 MPa, while the theoretical strength of iron $\sigma_t' \approx \frac{E}{10} \simeq 20000\ MPa$.

Density of elastic strain energy is given by the known relation $w_e = \frac{\sigma.\varepsilon_e}{2}$, where ε_e is the elastic component of strain, and stress $\sigma = E.\varepsilon_e$. Work of an external force exerted on deformation of material is equal to an internal elastic energy W_e and plastic strain energy W_p, resp. its increments.
The total energy $W_c = W_e+W_p$ or similarly for the energy density $w_c = w_e + w_p$, which is proportional to the area under the tensile diagram in the coordinates of true strain - true stress:

$$\mathbf{w_c} = \int_0^{\varepsilon_u'} \sigma'\, d\varepsilon' \qquad (1.7)$$

Using the equation $\sigma' = K.\varepsilon'^n$ then $w_c = \int_0^{\varepsilon_u'} K.\varepsilon'\, d\varepsilon' = \frac{K}{1+n}(\varepsilon_u')^{1+n}$. From the physical point of view, the plastic strain energy density, which is proportional to the area under the true diagram (graph), expresses toughness of material.

1.2.Basic Knowledge of Fractures

In this chapter, there is repeated some findings from material science or elasticity and strength.

Fractures and limit states can be classified according to several criteria:
According to size of plastic deformation: ductile (tough), brittle (cleavage), mixed.
According to capability and speed of propagation: Cracks and fractures, stable or unstable.
According to conditions for degradation processes: fatigue fractures, stress corrosion cracking, hydrogen cracking, creep fractures, cracks formed at wear.
According to development respective to grain boundaries: intercrystalline, transcrystalline, mixed.

Examples of several typical fractures and details of fracture surfaces are shown in **Fig. 1.2 - 1.4.**
Fractography examines cracks and fracture surfaces with regard to causes and mechanisms of failures.

Macrofractography gives an integral picture of a fracture process on the basis of macroscopic features of a fracture surface, visible to the naked eye, with a magnifying glass or a light microscope (stereomicroscope) with the maximum magnification of 100 times.

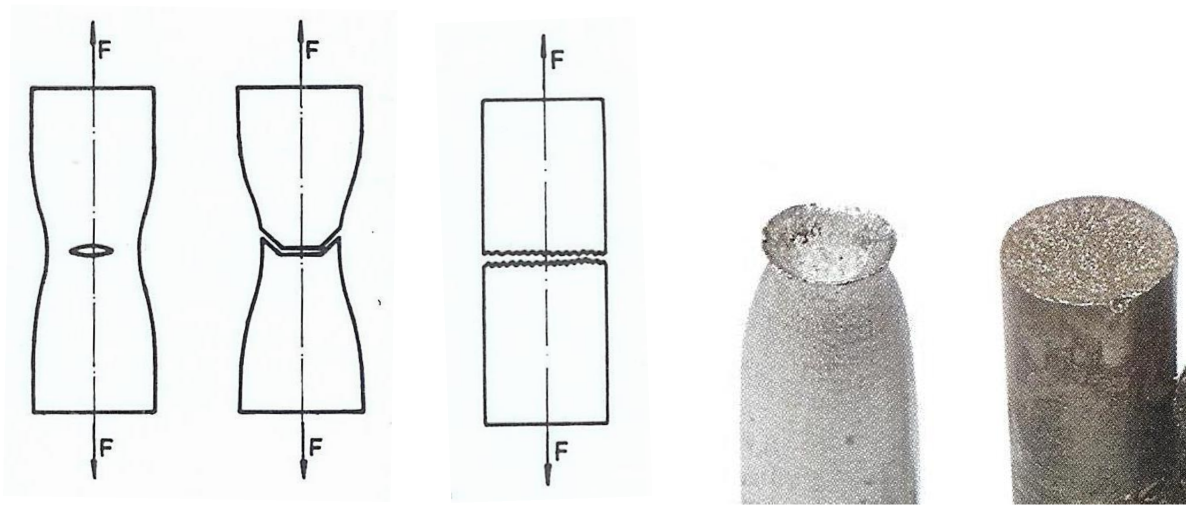

Fig. 1.2. Scheme of a ductile and a brittle fracture – a macroscopic view

Ductile fractures (tough) fractures are preceded or accompanied by permanent plastic deformation. Tough fractures consume more energy – high- energy fractures.

***Fig. 1.3**. A blade coupled with a shaft by welding was operated for a relatively short time in a piping of a pumping system till failure occurred (crack and fracture) at a weld joint*

Microfractography studies a fracture surface at high magnification and gains information concerning a mechanism of material failures on the basis of microscopic features (traces), such as cleavage planes, intercrystalline or transcrystalline facets (**Fig. 1.4 and 1.6**), secondary microcracks, microscopic cavities (Figure 1.6) etc.

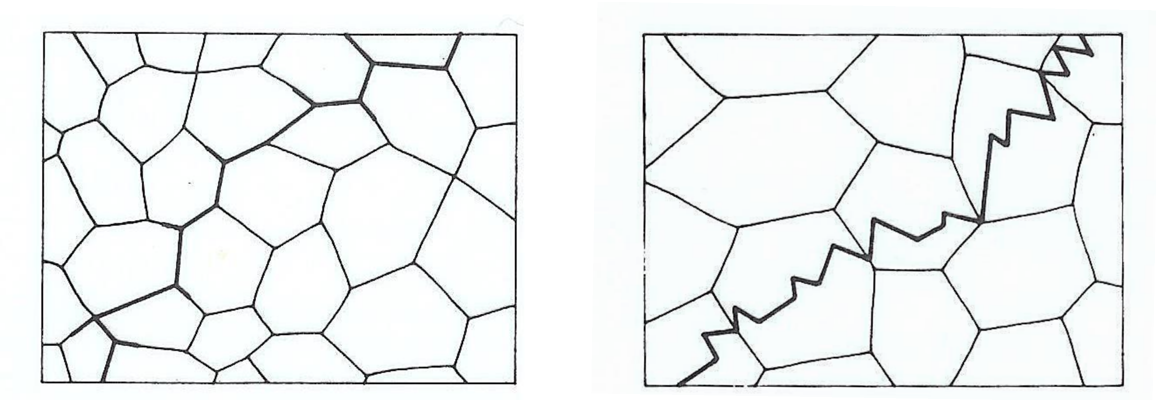

a) *b)*

Fig. 1.4. *Scheme of an intercrystalline and a transcrystalline cleavage brittle fracture. The fracture profile of a surface is marked in bold.*

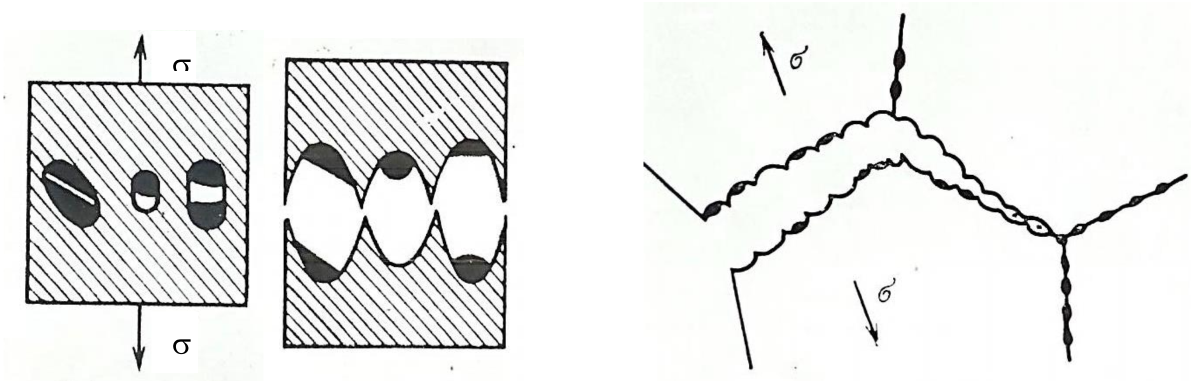

a) b)

Fig. 1.5. *Scheme of a dimple transcrystalline mechanism of ductile failure (a). Scheme of intercrystalline cavity failure, crack propagation (b)*

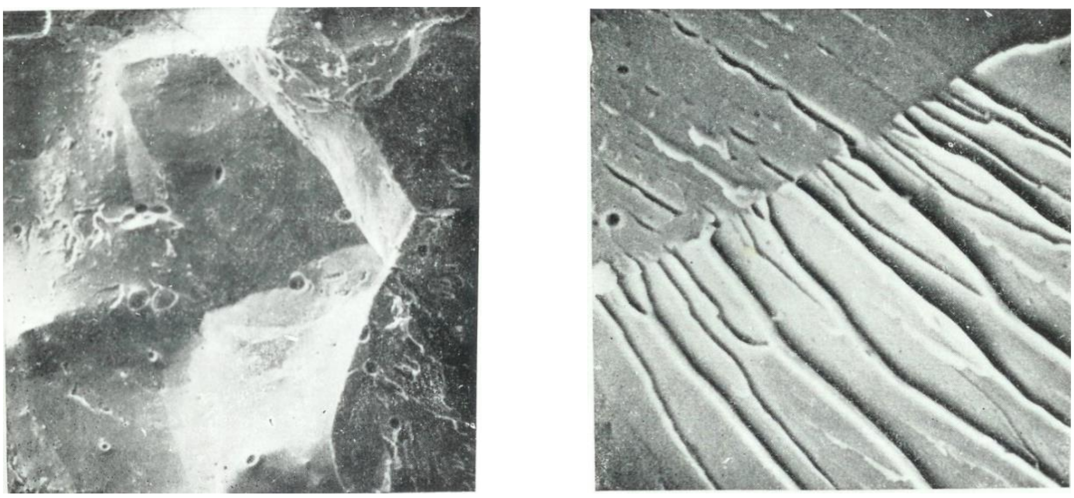

a) b)

Fig. 1.6. *A brittle fracture a) intercrystalline, b) transcrystalline. In metals with a body centered cubic lattice, transcrystalline cleavage takes place along the crystallographic planes of the type of {100 }. A scanning electron microscope (magn. 1000x)*

a)

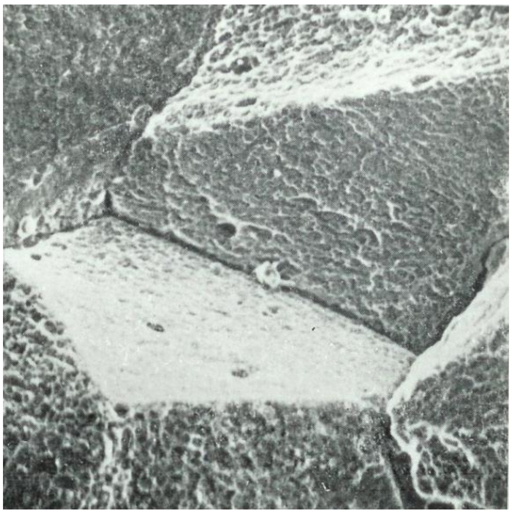

b)

Fig. 1.7. *Area of cavity transcrystalline ductile failure (a), SEM, 800 x. Cavity intercrystalline failure, evoked by precipitation of phases along grain boundaries (1000 x)*

Formation and development of microscopic cavities is accompanied by plastic deformation and energy consumption. In cases of extensive plastic deformation, **high-energy fractures** occur.

By means of a fractographic analysis of disrupted parts and/or pieces of equipment, we can find out what caused the failure or who is to be blamed for the breakdown (a technologist, a designer, a keeper). Results of a fractographic analysis as an objective evidence material can be used in legal or arbitration proceedings.

1.3.Development of Fractures in Metals

Difference in values between ideal and real strength of metals is not only due to existence of lattice defects, but also due to different mechanism of fracture formation and propagation in real polycrystalline materials, compared to the idea of sudden failure in entire cross-section in so called ideal metals. A fracture in real metals is carried out by a process of deformation and local failure at the front of a slowly or rapidly propagating crack. This implies that **the fracture process is performed in multiple phases (stages)**, which can be briefly summarized as follows:

a) Formation (Initiation) of a Crack

A crack may occur already in a manufacturing process (an a priori crack) or during body loading. The term **a crack** means permanent detachment of atomic bonds concurrently with formation of new surfaces. A crack may occur as a result of mechanical, thermal or chemical action. These factors may act simultaneously, e.g. corrosive cracking at elevated temperatures.

Mechanisms of crack initiation at different types of stress are described in the following chapters.

b) Stable Growth (Propagation) of a Crack

At stable propagation, a crack length increases continuously at low speed. A crack may grow when the stress value is:

- increasing, e.g. at tensile test
- constant (e.g. at creep),
- time-variable (cyclic stress at fatigue).

Stable crack growth is also practically applied in a ductile (tough) fracture of metal materials (except the aforementioned cases of creep and fatigue).

c) Initiation of an Unstable Crack

The initiation stage of an unstable crack is a point in time at the beginning of transition from a stable crack or stable growth of a crack to its unstable propagation. According to the principles of fracture mechanics, a crack will propagate unstably when the elastic stress energy reaches the value of surface energy of newly emerging surfaces of a diverging crack. This state appears in cases when a crack length or a value of applied stress reaches a critical size.

d) Unstable Growth (Propagation) of a Crack

Unstable crack propagation takes place at constant stress at increasing speed and by action of elastic energy accumulated in a body. An unstable crack disrupts the body partially or completely into two or more parts. Excessive free elastic energy, which was not consumed by crack propagation, is converted to kinetic energy of separated parts of the body and to a sound effect accompanying the failure.

e) Stopping an Unstable Crack

An unstable crack stops during its growth when conditions that affect its unstable propagation are changed, that means

- when the resistance to unstable propagation increases (by increasing temperature, increasing toughness of material, etc.)
- when stress suddenly decreases (a crack passes to a larger cross-section),
- when the elastic stress energy suddenly drops to a negligible value.

Operational **failure conditions,** arising from material causes, occur especially under difficult conditions of stress:

- under dynamic stress of welded structures at low temperatures,
- under cyclic loading,
- when material stressed at high temperatures (at creep)
- in interaction with a corrosive environment, including hydrogen cracking.

1.4. Resistance to Brittle Failure

Brittle failure can be considered a separation (detachment) of a part of material of a body, which occurs when nominal stress is lower than the yield strength of the material, determined by static tensile test.

Brittle failure is characterized by the following main features:

a) it arises when stress is lower than the yield strength of material ($\sigma < R_p$),
b) no larger macroplastic deformation occurs prior to failure and during a fracture,
c) it arises suddenly and propagates rapidly (even above 1000 m/s),
d) a fracture surface is oriented perpendicularly to the largest normal tensile stress
e) plastic strain energy consumed by failure is minimal (a low-energy fracture),
f) it is carried out by a cleavage transcrystalline mechanism or intercrystalline separation (cleavage) and it usually has a crystalline appearance.

Failure of a part of a machine or a structure usually has unfavourable consequences. It appears often at the beginning of a structure lifetime without previous symptoms. Most commonly, it is present in welded steel structures, rarely in aluminum alloys.
Based on an analysis of many cases of damage by a brittle fracture, the following **key factors and conditions that promote formation of a brittle fracture** may be mentioned:

a) microscopic and macroscopic concentrators of stress (notches, cracks, sudden changes in a cross-section, etc.),
b) large thicknesses of material,
c) dynamic loading,
d) large elastic strain energy in a stressed body (cumulated in a system),
e) low temperatures.

Brittleness is not a typical characteristic for all metals and conditions. It appears only in some metals under certain conditions of loading and state of a structure. From this point of view, brittleness can be defined not as a property but as a condition of material under given conditions of loading.

Microscopic nature of failure of metals and their alloys is mainly explained in the context of physical metallurgy. Therefore, physico-metallurgical aspect is an important supplement to knowledge of a brittle fracture of metals and their alloys, which it explains from the microscopic structural point of view, including causes of stability loss of a fracture process. A core of the explanation lies in a microscopic analysis of causes of **change in a micro-mechanism of failure**, and thus also the amount of energy consumed on failure.

In terms of physical metallurgy, there will be certain differences for different materials in the definition of brittle failure. We mention hereinafter definitions of brittle failure for three most widely used groups of metallic structural materials, for which a risk of brittle failure exists, namely for steels of low and medium strength, high-strength steels and aluminum alloys of higher strength.

Steels of Low and Medium Strength

In low-carbon and low-alloy steels, brittle failure appears by an unstable fracture at nominal stress lower than their yield strength. Brittle failure of these steels relates to a change in a failure micromechanism due to temperature decrease or increase in speed of loading. As a consequence of temperature and loading speed, the fracture micromechanism changes from ductile cavity to cleavage and the energy consumed on failure decreases. From the microscopic point of view, an unstable fracture is carried out by a cleavage mechanism.

High-Strength Steels

In high-strength and tool steels, brittle failure occurs by an unstable fracture at load, which is lower than the load corresponding to the yield strength. Effect of temperature and speed of loading on a failure micromechanism of these steels is much smaller and depends on composition and heat treatment of the steel. From the microscopic point of view, failure may be carried out by an intercrystalline or a transcrystalline cleavage fracture, but also by a ductile fracture and the proportion of a cleavage and a ductile fracture may differ in different areas of a fracture surface.

Aluminum Alloys of Higher Strength

Brittle failure of aluminum alloys is carried out by an unstable fracture under load, which is lower than the load corresponding to the yield strength. In aluminum alloys, failure micromechanisms do not change due to temperature (within the temperature range of conventional use of known alloys).

Besides these most widely used and known structural materials, the risk of a brittle fracture occurs also in other alloys, intermetallic compounds, in ceramics, composite materials, in powder metallurgy products and in amorphous materials (glass). Also plastics, especially in the vitreous state, wood and wood materials, building materials (concrete), and last but not least bones succumb to brittle failure.

Criteria and the Concepts of Resistance to Brittle Failure

From an analysis of the mechanism of brittle failure it implies that brittle fractures, including criteria of resistance to its formation, can be studied and assessed from several points of view:

a) **energy** (amount of energy consumed on a fracture),
b) **stress** (critical fracture stress, at which cracks initiate or propagate)
c) **kinetic** (stable or unstable crack propagation),
d) temperature (transition temperature level),
e) morphological (a failure mechanism)

On this basis, different concepts and criteria according to which the material resistance to a brittle fracture is assessed, were determined. In practice, two groups of criteria were verified and have proved themselves:

- Criteria based on defects propagation (according to fracture mechanics).
- Criteria based on transition temperature.

1.5.Fracture Mechanics Concept

A large amount of knowledge of failures and fractures, collected from both practice and material testing, contributed to the creation of a separate technical field - fracture mechanics.

Fracture mechanics is a scientific discipline of fracture formation of defects that occur in a stressed body. It studies the behaviour regularities of cracks when a body is stressed under various conditions, especially in terms of brittle failure creation.
The objective of fracture mechanics is to determine the stressed-body critical size of a defect that would cause sudden brittle failure of a component under stress.

By area of deformation under load, fracture mechanics is divided into:

- **Linear elastic fracture mechanics** (LEFM), applicable for stress of bodies in the elastic strain area,
- **Elastic-plastic fracture mechanics** (EPFM), extended to stress in the elastic-plastic strain area.
- Dynamic fracture mechanics is considered in cases of dynamic and shock loads.

Cases of catastrophic fractures indicate that the real conditions for stress of structures are more complex than those in laboratory testing of mechanical properties, which are used in design calculations. The fact that materials in practice often break down at lower stress than the yield strength, fracture mechanics reflects by introducing existence of defects to strength calculations and qualifying the strength of a stressed body according to processes and regularities that determine the initiation and propagation of cracks.
Therefore, the criteria of fracture mechanics are based on the physico-mechanical quantities, expressing the stability of cracks.

Linear elastic fracture mechanics assumes that a crack propagates **in the elastic state of stress.** A fracture in a compact body (without cracks, defects, faults) can theoretically occur only when the acting stress reaches the ideal strength ($R_{m,id} = (E\gamma/a_o)^{1/2}$). In bodies containing stress concentrators type of a crack, the ideal strength value at the crack front (tip) can be reached at lower nominal stress. At the same time, a lattice parameter (a_o) is much smaller than a length of a defect (c), thus ($a_o << c$).

The above mentioned shows that in bodies with a crack at nominal stress lower than the yield strength of material, the maximum stress concentrated by the crack can highly exceed the yield strength value and also the ultimate strength in materials that break down in the ductile state.

The fundamental role of fracture mechanics is to use this knowledge to set appropriate criteria for evaluating the resistance of materials to brittle failure of bodies with a crack.
For structural metallic materials, allowable stress is often chosen according to the value of yield strength and it is approximately 2/3 of R_p. If this stressed component contains a crack of a certain size, it may unstably propagate and cause brittle failure. Strength of the component containing the crack will be correlative of resistance of the material to initiation of brittle failure in a localized mass at the crack tip. In this context, attention shall be paid to small mass of material at the crack tip and processes that take place by action of concentrated stresses shall be analysed.

Plastic deformation occurs in the area where stress exceeds the yield strength. Thereby a plastic zone, whose size depends on the ratio σ_y/R_p, occurs at the crack tip. A plastic zone in high-strength materials is very small. In materials with lower yield strength or at higher temperatures, plastic zone may reach dimensions comparable to thickness of a body and a crack will not propagate under elastic conditions.

Deeper theoretical analyses proved by experiments show that in metallic materials in relation to their crystalline structure, it is impossible to induce an ideally brittle fracture even under extremely unfavourable stress conditions. Any brittle failure is carried out at small accompanying plastic deformation.

Σ Summary of Terms

After reading this chapter, you should understand contents of the following technical terms:
Engineering and true stress and strain. Hollomon's equation, a strain hardening exponent. Fracture stress and strain. Strain energy density
A crack, a fracture, stable and unstable crack propagation. A brittle fracture, a ductile fracture, a tough fracture, an intercrystalline and a transcrystalline fracture. Fractography. Micromechanisms of failure.
Main features and conditions for brittle failure.
Fracture mechanics, Linear elastic fracture mechanics, Elastic-plastic fracture mechanics.

? Questions to Chapter 1

1.1 How are true stresses and true strains during tensile test defined?
1.2 How may the fracture strain and the fracture stress be defined?

1.3 How may the density of strain energy be calculated?
1.4 In which area of the tensile diagram does Ramberg-Osgood law hold true?
1.5 What are the conditions for formation of a brittle fracture of steel?
1.6 Along which crystallographic planes does the growth of a cleavage fracture in a body centred cubic lattice take place?
1.7 What are the stages (phases) of development of the fracture process?
1.8 What does the stable development of a crack characterize?
1.9 What are the differences between linear elastic and elastic-plastic fracture mechanics?
1.10 Which groups of metallic materials are susceptible to brittle failure?

Exercises to Chapter 1

1.1. Calculate the true stress and the true strain at the yield strength $R_p0{,}2$ = 190 MPa of austenitic steel with the modulus of elasticity E = 190 GPa
1.2. What values do true stress and strain reach at the engineering ultimate strength R_m = 600 MPa at smooth deformation of 30% of austenitic steel (according to exercise No. 1.1)?
1.3. Calculate the true stress in a rod of an Al alloy stressed by uniaxial tension, when the engineering stress σ = 140 MPa, the modulus of elasticity E = 70 GPa, and Poisson's ratio ν = 0,33.
1.4. Calculate density of the elastic strain energy of a component made of steel stressed by uniaxial tension, when the elastic strain is 0,05%.
1.5. Cleavage in bcc crystals appears mainly along planes (100). Consider what can happen with the fracture energy of a randomly oriented polycrystalline structure, when the grain size was reduced several times.

Answers to the Questions

1.1. True stress $\boldsymbol{\sigma' = \frac{F}{S}}$, where S is a true cross-section perpendicular to the applied force F, and true strain $\boldsymbol{\varepsilon' = \ln\frac{L}{L_o}}$, where L is a length of a rod under load by the force F and L_o is the initial length.
1.2. The true strength i.e. fracture stress is given by the equation $\boldsymbol{\sigma'_u = \frac{F_u}{S_u}}$, where F_u is the force at the time prior to a fracture. True strain at a fracture (in a neck) - i.e. fracture strain $\boldsymbol{\varepsilon'_u = \ln\frac{1}{1-Z}}$.
1.3. Generally using the relation $w_c = \int_0^{\varepsilon_u'} \sigma' \, d\varepsilon'$, for elastic deformation: $w_e = \frac{\sigma.\varepsilon_e}{2}$.
1.4. In the area of smooth elastic-plastic deformation of the true diagram.

1.5. Stress concentration, low temperature, high strain rate, triaxial tensile stress (larger wall thickness).
1.6, Cleavage crystallographic planes in the bcc lattice are type of {100}.
1.7. Usually the initiation stage of stable (micro) cracks, propagation of a stable crack, initiation of an unstable fracture, propagation of an unstable fracture.
1.8. It is necessary to supply energy for the slow growth of a crack.
1.9. Linear fracture mechanics considers linear dependences of stress - strain. Elastic-plastic fracture mechanics (EPFM) is extended to elastic-plastic deformations of a body.
1.10. High-strength steels, structure steels of medium strength at low temperature (except of austenitic), high-strength Al alloys, intermetallic alloys (compounds).

Results of the Exercises

1.1. For ε_p = 0,20% = 0,002 is σ'= 190,38 MPa, strain ε_p' = 0,1998 %, ε_e = 0,1 %.
1.2. Stress σ'= 780 MPa, strain ε_p' = 26,2 %,
1.3. For elastic deformations for ($\sigma < R_p0,2$) $\sigma' = \sigma/(1-\nu\varepsilon_x)^2$, where ε_x = 0,002 = 0,2%, stress σ'= 140,185 MPa
1.4. Density of elastic energy w_e = 26,2 kJ/m^3 = 0,187 Jmol^{-1}.
1.5. Clue: Watch the crack path across grain boundaries.

2. STRESS AROUND NOTCHES AND CRACKS

Time dedicated to the study of this chapter is approximately 2 hours.

Objective: After studying this chapter, you will be able to

- Determine stress concentrations for simple notches and defects
- Name various stress concentrators
- Characterize stress intensity factors
- Explain why the strength of brittle material is much lower than its theoretical strength.

Interpretation

During the historic development, it is possible to consider two main concepts in the field of study of fracture processes - stress and energetic:

a) Determination of stress around a defect – local exceeding of the ultimate strength of material at the crack tip leads to disruption of cohesion of the material, to crack propagation and to initiation of a fracture.
b) Energy balance - surplus of potential energy of a system will be used on creation of a new fracture surface (Chapter 5). Both approaches provide approximately the same results.

2.1. Stress Concentration in the Vicinity of Notches

When loading parts, flow-around and concentration (thickening) of a power flow appears around notches and holes, where maximum stresses that can cause material failure are forme, see **Fig. 2.1**. To express the highest stress at a notch, **the stress concentration factor** (α) was introduced, defined as a ratio of maximum stress (σ_{max}) to nominal or mean stress σ. Nominal stress is defined as a force (F) acting perpendicularly to the weakened true cross-section in a defect site S_d, thus $\sigma_{nom} = F/S_d$. Mean stress $\sigma = F/S_o$, where S_o is a cross-section considered without a notch resp. defect (and occurs in the plane with the notch or the defect). Therefore, we can distinguish two types of stress concentration factors:

$$\alpha_n = \frac{\sigma_{max}}{\sigma_{nom}} \quad , \quad \alpha_g = \frac{\sigma_{max}}{\sigma}, \qquad (2.1)$$

whose values significantly differ at relatively large notches (c/W > 0,2), differently reflect the impact of final dimensions of a body on a size of stress concentrations. In general, $\alpha_n \leq \alpha_g$.
Values of these stress concentration factors are almost identical in cases when the size of notches (the length c) is very small relative to the width of the body (c <<W), usually for c/W < 0,05. Or else, at a given size of a notch, this concerns large bodies, theoretically

from the mathematical point of view infinite, semi-infinite. In these cases, the following applies: $\boldsymbol{\alpha_n} = \boldsymbol{\alpha_g} = \boldsymbol{\alpha}$ and to simplify, in further interpretation the stress concentration factor $\boldsymbol{\alpha}$ is considered. Note: Stress concentration factor may also be referred to as K_t.

For an elliptical hole (a notch, a defect) with the length **c** and the radius of curvature ρ, the stress concentration factor at tensile stress may be calculated according to the formula (under the condition c << W)

$$\boldsymbol{\alpha = 1 + 2\sqrt{\frac{c}{\rho}}} \tag{2.2}$$

A similar simple relation applies in case of bending stress $\alpha = 1 + \sqrt{\frac{c}{\rho}}$. These relations apply for the configuration where the hole axis, the major axis of the ellipse and the direction of stress are mutually perpendicular.
Also homogeneous and isotropic material is considered.

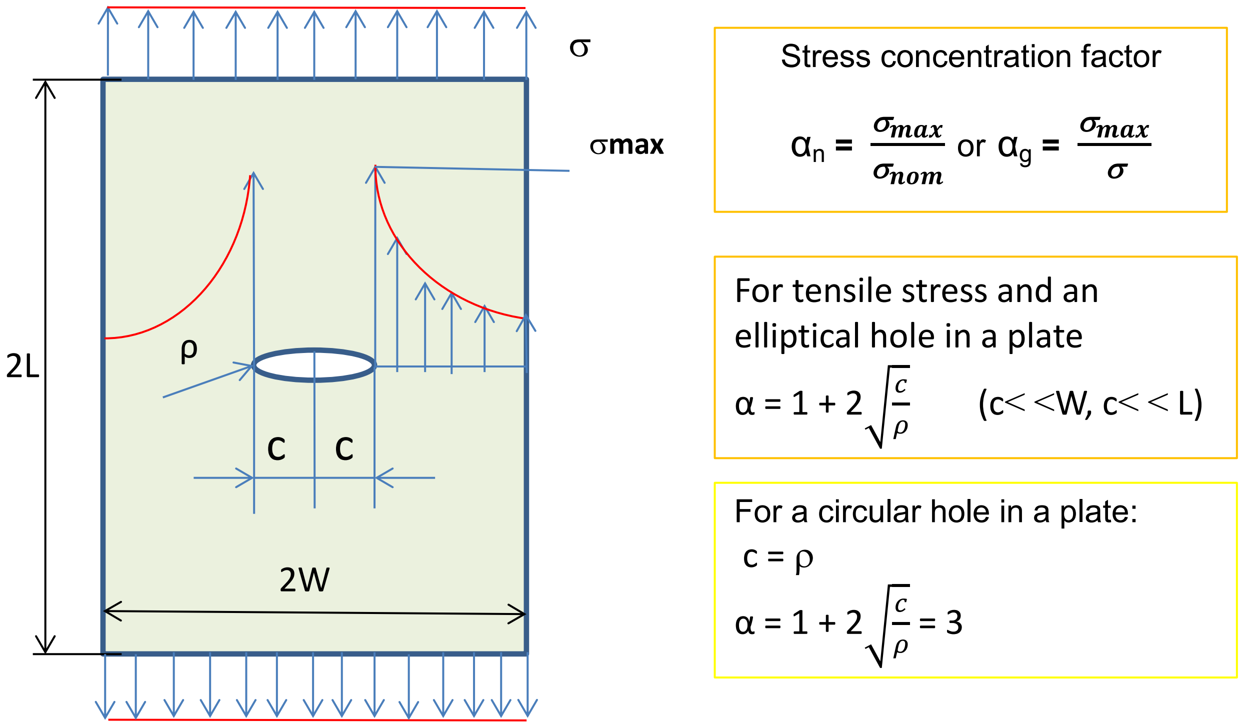

Fig. 2.1. *Scheme of a plate with an elliptical hole, the main hole axis is oriented perpendicularly to tensile stress. The longer and sharper the notch or defect, the higher stress concentration occurs.*

Note: Solution of elastic stress around a circular hole was given by Kirsch in 1898 and thus he laid the foundations for calculations of stress concentration around notches and cracks. Stress concentrations of various notches were systematically explored by Neuber, the founder of teaching about stress concentrations at notches. For a spherical shape of a defect (e.g. bubbles, pores) within material, α = 2,24.

In general, **calculations of stress concentrations** and stress-strain elastic fields in the vicinity of notches and cracks are relatively difficult. In terms of the theory of elasticity and mathematics, it is necessary to solve systems of partial differential equations. At the same time, it is necessary to respect relations between components of a displacement vector and components of a strain tensor (Cauchy relations), compatibility equations, differential equations of equilibrium, generalized 3D Hooke's law, conditions for plane strain and plane stress. For solving, Airy function is used, the method of complex stress potentials, etc. These issues are beyond the scope of this support and will not be further expanded; those interested can find them in the relevant listed literature.

The stress concentration factor $\boldsymbol{\alpha}$ applies to both elastic and elastic-plastic stress field. In case of linear elastic behaviour of material, $\boldsymbol{\alpha}$ is referred to as a theoretical stress concentration factor $\boldsymbol{\alpha_t}$, in case of elastic-plastic behaviour it is $\boldsymbol{\alpha_\sigma}$.

Similarly, for maximum strain ε_{max} the strain concentration factor in the form $\boldsymbol{\alpha_\varepsilon} = \frac{\varepsilon_{max}}{\varepsilon}$ was introduced, where ε is mean or nominal strain. **Neuber** equation $\boldsymbol{\alpha_t^2} = \boldsymbol{\alpha_\sigma} . \boldsymbol{\alpha_\varepsilon}$ applies among the factors stated above. According to the relation, an increase in plastic deformation leads to a reduction of stress peaks. An example of stress distribution at a structural notch is shown in **Fig. 2.2**.

The picture shows a comparison of stress at elastic and elastic-plastic behaviour of material. At inception of plastic deformation, more complex courses of stress are formed, maximum stress peaks are blunted, lowered and shifted under the surface.

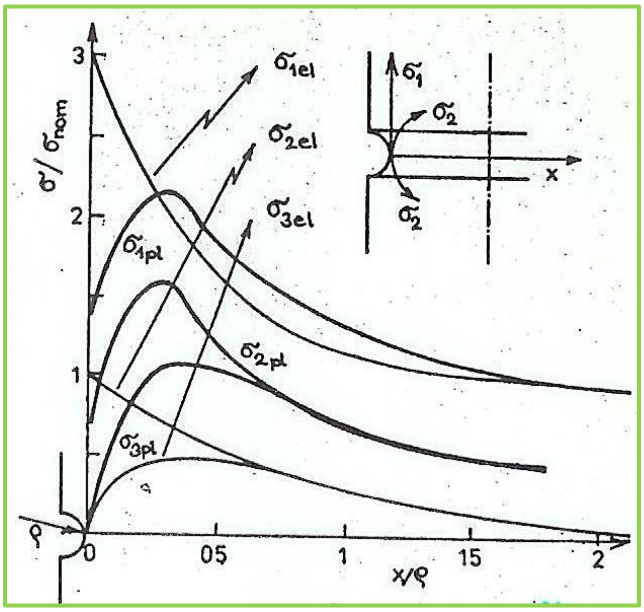

Components of the stress tensor:
σ_1 – axial stress,
σ_2 – tangential stress
σ_3 – radial stress, $\sigma_3 || x$
σ_{nom} – nominal (mean) stress,

σ_{iel} – elastic state of stress,
σ_{jpl} – elastic-plastic state of stress
i = 1,2,3; j = 1,2,3
ρ – radius of curvature of a notch

For a decrease in axial elastic stress components from the front of a notch (Fig. 2.2), the correlation is applicable:

$$\sigma_{1el} = \sigma_{nom} \left[1 + 2.\left(\frac{\rho}{\rho + x}\right)^3\right]$$

Fig. 2.2. *Courses of triaxial stresses before a semicircular circumferential notch on a cylindrical shaft. Differences between linear elastic and elastic-plastic solution.*

It is necessary to use **numerical calculation methods** when calculating stress concentrations at notches or defects in case of elastic-plastic behaviour, especially the finite element method (FEM). For the research and visualization of strain or stress fields, also suitable experimental methods are used (**Figure 2.3**, photo-elasticimetry, moiré patterns), in the research of stress concentrations and stress state it is possible to use the methods of roentgenography (diffraction), tensometry, interferometry.

Determination of stress concentrations is of great importance at brittle materials, where maximum stresses can reach high values and cause a fracture. In these materials, the maximum stresses (stress peaks) are not reduced by plastic deformation. Stress concentrations are also important in cases of cyclic loading of machine parts, where they significantly affect fatigue characteristics. In this context we talk about the shape (dimensional) strength under alternating stress.

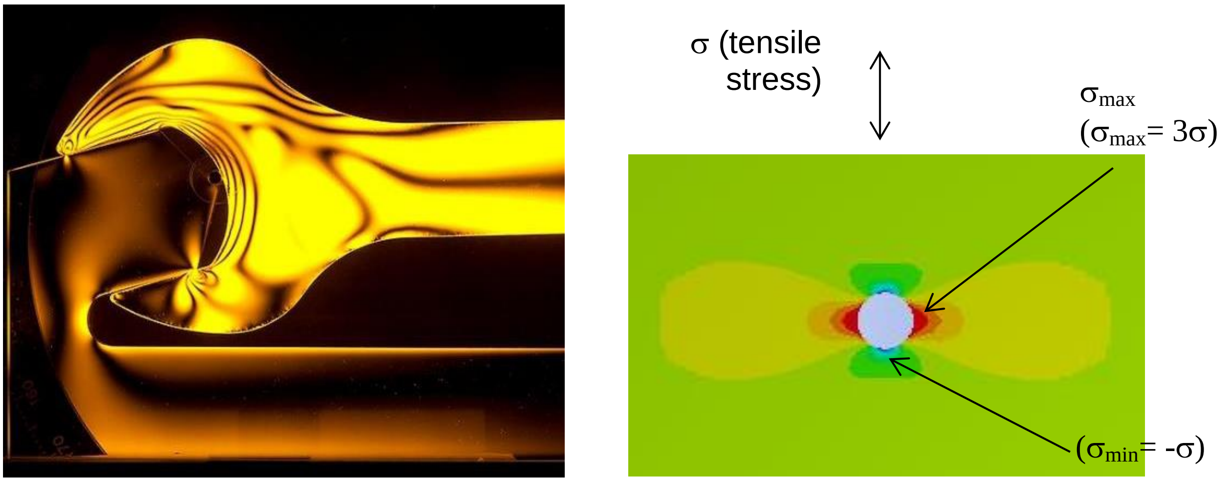

***Fig. 2.3**. Depiction of fields and stress concentrations using photoelasticimetry (with polarized light) and calculation methods (FEM) at a circular hole.*

Areas and Reasons for Occurrence of Stress Concentration (Summary)

- *A sudden change in body shape* leads to a change from simple or uniaxial stress to multiaxial and complex stress
- *Structural notches* (intentionally created, they have a certain function in a structure) cause stress concentrations and multiaxial stress states
- *contact local areas* (important in some types of wear, deformation).

- *Material defects*- they act in a similar notch effect
- Inclusions, precipitates
- Pores, bubbles
- Cracks (they can occur e.g. during manufacturing or at cyclic stress, fatigue)

- *Effects of a surface* (dents after machining, a rough surface, unevenness and corrosion pitting).

For sharp defects or cracks, it applies $\rho << c$ and stress concentration α and maximum stress σ_{max} reach high values in the front of a defect. If σ_{max} exceeds the theoretical strength, propagation of a crack and a fracture occur. In an extreme case according to relation (2.2), for

$\rho \rightarrow 0$ at a given length of a defect, then would $\alpha \rightarrow \infty$ and also $\sigma_{max} \rightarrow \infty$, stress here shows the so called singularity. If we consider a distance between atoms (a), resp. a size of an atom as the smallest possible radius of curvature (a = ρ), then $\sigma_{max} = \sigma\ (c/a)^{1/2}$, concurrently a<< c. In case that σ_{max} achieves the theoretical resp. ideal strength of material ($R_{m,id} = (E\gamma/a_o)^{1/2}$), then a brittle fracture appears.

2.2. Stress Intensity Factors

Linear elastic fracture mechanics is based on an analysis of the size and distribution of stress and strain in the vicinity of a crack tip. It is based on **linear dependence** between stress and strain.

In the stress analysis of bodies with a crack, there are distinguished three basic types of stress (modes) of a body with a crack with the option of material separation in its front, which are schematically shown in **Fig. 2.4**.

Mode I corresponds with load and opening of a crack by tensile stress perpendicular to the crack. In doing so, depending on thickness of the body, two different states of stress in the front of a crack may appear:

State of plane stress (thin bodies and free surfaces)

State of plane strain (central part of bodies of greater thickness)

Definition of these conditions is mentioned hereinafter.

Mode II is characterized by plane shear deformation caused by shear stress perpendicular to a crack tip.

Mode III represents shear stress parallel to a crack tip (antiplane shear deformation).

According to these three basic modes of crack loading, values of the stress intensity factor are distinguished by designations: K_I, K_{II} and K_{III}.

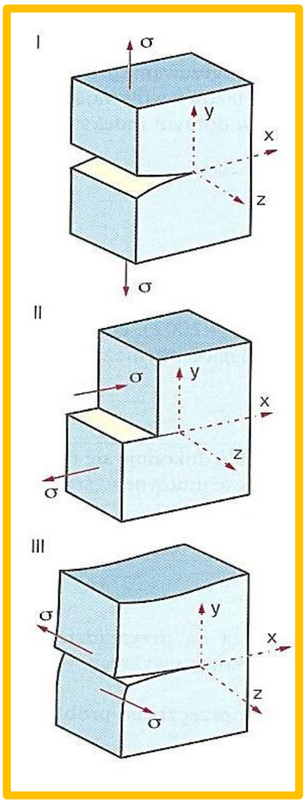

Fig. 2.4. *Loading modes of cracked material: I – tensile mode (tension), II – plane shear mode (sliding, Translator's Note: in-plane shear), III – antiplane shear mode (tearing, TN: out-of-plane shear)*

By use of the stress analysis in the area of a crack tip, dependences of stress tensor components in the vicinity of the crack tip on a size of nominal stress $\boldsymbol{\sigma}$, a crack length **c**, a distance vector **r** and an angle $\boldsymbol{\varphi}$, can be determined, **Fig. 2.5**. For a plate of a large width b containing a central crack of a length of 2c (in condition b >> 2c) stressed by tensile stress, basic stresses in the element of volume are described by the polar coordinates of **r** and φ. Sizes of these stresses for the first type of loading are expressed by the following relations:

$$\boldsymbol{\sigma_y(r,\varphi) = \frac{\sigma\sqrt{c}}{\sqrt{2r}}\left(1+\sin\frac{\varphi}{2}\sin\frac{3\varphi}{2}\right)\cos\frac{\varphi}{2}};\quad \sigma_x(r,\varphi) = \frac{\sigma\sqrt{c}}{\sqrt{2r}}\left(1-\sin\frac{\varphi}{2}\sin\frac{3\varphi}{2}\right)\cos\frac{\varphi}{2}, \tag{2.3}$$

$$\tau_{xy}(r,\varphi) = \frac{\sigma\sqrt{c}}{\sqrt{2r}}\sin\frac{\varphi}{2}\cos\frac{\varphi}{2}\cos\frac{3\varphi}{2},\quad \sigma_z(r,\varphi) = 2\nu.\frac{\sigma\sqrt{c}}{\sqrt{2r}}\cos\frac{\varphi}{2}\ (RD),\ \sigma_z(r,\varphi) = 0\ (RN),\ \tau_{xz}=0,\ \tau_{yz}=0$$

Calculations and analyses of stress fields and their concentrations in the front of a sharp crack in linear elastic isotropic material led to **introduction of the stress intensity factor** according to **the definition** for the three modes.

$$\boldsymbol{K_I = \lim_{r\to 0}(2\pi r)^{1/2}\sigma_y(r,0)},\quad K_{II} = \lim_{r\to 0}(2\pi r)^{1/2}\tau_{xy}(r,0),\quad K_{II} = \lim_{r\to 0}(2\pi r)^{1/2}\tau_{yz}(r,0) \tag{2.4}$$

The stress intensity factor implemented this way represents certain average concentration of stress in the front of a sharp crack and has a finite value at $r \to 0$ (when $\sigma_{ik} \to \infty$).

The stress intensity factor K_I can be used to describe components of a stress tensor at a crack tip (for linear elastic material), see relations (2.6), or in general $\sigma_{ik} = \frac{K_I}{\sqrt{2\pi.r}} . f_{ik}(\varphi)$.
On the other hand, K_I relates to external stress and a length of an inner crack by the relation

$$\boldsymbol{K_I = \sqrt{\pi c}}, \tag{2.5}$$

which derives from the comparison of relations (2.3) and (2.4). Similar relations as for the mode I are applicable for loading modes II and III: $K_{II} = \tau.\sqrt{\pi c}$ and $K_{III} = \tau.\sqrt{\pi c}$. The main unit for a stress intensity factor is **[MPa $\sqrt{m}$],** as it follows e.g. from equation (2.5). For short surface cracks $K_I = 1{,}12.\sigma\sqrt{\pi c}$.

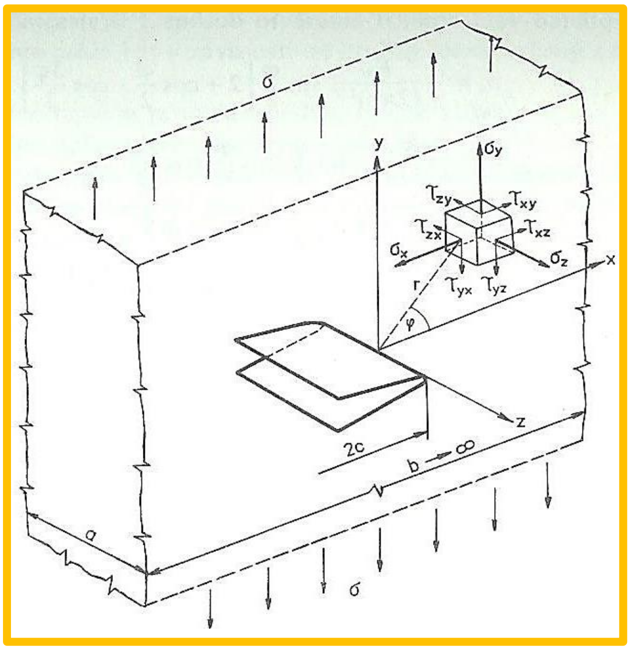

$$\sigma_x = \frac{K_I}{(2\pi r)^{1/2}}\cdot\cos\frac{\varphi}{2}\left[1-\sin\frac{\varphi}{2}\cdot\sin\frac{3\varphi}{2}\right]$$

$$\sigma_y = \frac{K_I}{(2\pi r)^{1/2}}\cdot\cos\frac{\varphi}{2}\left[1+\sin\frac{\varphi}{2}\cdot\sin\frac{3\varphi}{2}\right]$$

$$\sigma_z = \nu(\sigma_x+\sigma_y),\qquad \tau_{xz} = \tau_{yz} = 0$$

$$\tau_{xy} = \frac{K_I}{(2\pi r)^{1/2}}\cdot\sin\frac{\varphi}{2}\cdot\cos\frac{\varphi}{2}\cdot\cos\frac{3\varphi}{2}$$

$$u = \frac{K_I}{G}\left(\frac{r}{2\pi}\right)^{1/2}\cdot\cos\frac{\varphi}{2}\left[1-2\nu+\sin^2\frac{\varphi}{2}\right]$$

$$v = \frac{K_I}{G}\left(\frac{r}{2\pi}\right)^{1/2}\cdot\sin\frac{\varphi}{2}\left[2-2\nu-\cos^2\frac{\varphi}{2}\right]$$

$$w = 0 \tag{2.6}$$

Fig. 2.5. *Components of a stress tensor around a crack tip for mode I. Formulas for calculating components of stress and displacement at a crack tip, linear elastic deformations of material.*

According to the listed equations (2.6), stress at a crack tip increases with the decreasing distance *r*, in general according to the relation $\sigma = K_i/\sqrt{r}$, and at $r \to 0$ would $\sigma \to \infty$ (i = I, II and III).

If an examined element of material is in a plane, wherein the angle $\varphi = 0$ ($y = 0$), the basic stresses, which may cause crack propagation, will be determined by the product of acting stress and a crack length. For example for the mode I, it will apply:

$$\sigma_x = \sigma_y = \frac{K_I}{\sqrt{2\pi r}} = \sigma\sqrt{\left(\frac{c}{2r}\right)},\ \sigma_z = 2\nu\sigma\sqrt{\left(\frac{c}{2r}\right)},\text{ and } \tau_{xy} = 0. \tag{2.7}$$

In practice, the tensile loading mode perpendicular to the plane of a crack is most important. Depending on thickness of a body, state of stress at this loading mode can be biaxial or triaxial.

The first case applies to the **state of plane stress**, i.e. biaxial stress, which can be represented by a very thin plate loaded in its plane by real values of stress σ_x and σ_y, while stress $\sigma_z = 0$ (Fig. 2.5). Deformation in the direction *z* will not equal to zero, because according to Hook's law, it applies $\varepsilon_z = \frac{1}{E}[\sigma_z - \nu(\sigma_x + \sigma_y)]$, which means that for $\sigma_z = 0$:

$$\boldsymbol{\varepsilon_z = -\frac{\nu}{E}(\sigma_x + \sigma_y)}, \tag{2.8}$$

It follows from the derived state that in the direction perpendicular to the plane of a plate, negative deformation appears (thickness reduction in tension), which is important in crack propagation in a stressed body. State of plane stress is also on a surface of bodies of any thickness. Under atmospheric pressure (p) component $\sigma_z = -p < 0$ and usually $|\sigma_z| << \sigma_x$ and $|\sigma_z| << \sigma_y$, i.e. $\sigma_z \to 0$, practically $\sigma_z = 0$.

The second case, i.e. **state of plane strain** occurs, when strain components ε_x and ε_y are larger than 0, but in the direction *z* of strain $\varepsilon_z = 0$. This means that both basic strains ε_x and ε_y act in one plane, out of which the term plane strain has been derived. If $\varepsilon_z = 0$, according to Hook's law or the aforementioned equation, it may be derived that

$$\boldsymbol{\sigma_z = \nu(\sigma_x + \sigma_y)}, \tag{2.9}$$

and the plate is loaded by tri-axial tensile stress. In this state of stress, possibility of formation of plastic deformation is limited. Load of a rough plate, i.e. with high thickness, corresponds to the given case.

It follows from the aforementioned that the pure plane stress would be created at loading of a very thin plate and pure plane strain in a very thick plate, in the central part. In real components, there may be plane strain conditions at the centre, and it changes to plane stress towards the free surface. Therefore, in the wider (thicker) test samples or structures, there may be plastically deformed areas formed on the surface, while there is a state of elastic stress inside.

So far, in considerations of the stress intensity factor, we have considered a crack in a so called semi-infinite body (Fig. 2.5), or assumed that the crack length c is much smaller than dimensions of a body (in the direction of crack propagation and perpendicularly to the crack, $c << W$ or $c << b$). In these cases value of K_I (K_{II}, K_{III}) is not affected by body dimensions.

If a length or a size of a crack is not small enough relative to determinative body dimensions, then values of an intensity factor are also affected by dimensions and a loading mode of a body according to the relation

$$\boldsymbol{K_I = \sigma\sqrt{\pi a}.\mathrm{f}} \tag{2.10}$$

where **f is a shape function** , dependent on geometry of a body, mainly on the proportional length of a crack (a/W), its position and the mode of loading. Shape function f is also referred to as the **shape factor Y**.

The shape function is a dimensionless function. Usually the higher value of the shape function is, the longer the crack is (while keeping the other parameters of stress and dimensions of samples). Several relations for the shape function were derived, e.g. for a central crack of a length of 2a in a plate of finite dimensions, **Fig. 2.6**. For general notation $K_I = \sigma\sqrt{\pi a}.f_I$, the shape function is

$$f_I\left(\frac{a}{W}\right) = \left[\cos\frac{\pi a}{2W}\right]^{-\frac{1}{2}} \quad \text{for a/W≤0,8 with an accuracy of 1\%} \tag{2.11}$$

or $f_I\left(\frac{a}{W}\right) = 1 + 0{,}128\left(\frac{a}{W}\right) - 0{,}288\left(\frac{a}{W}\right)^2 + 1{,}525\left(\frac{a}{W}\right)^3$, true for a/W≤0,7.

Similarly for an edge crack (Fig. 2.6), relation in the form of a polynomial is often used, respectively of first members of function development into a line.

$$f_I\left(\frac{a}{W}\right) = 1{,}12 - 0{,}231\left(\frac{a}{W}\right) + 10{,}55\left(\frac{a}{W}\right)^2 - 21{,}72\left(\frac{a}{W}\right)^3 + 30{,}39\left(\frac{a}{W}\right)^4 \tag{2.12}$$

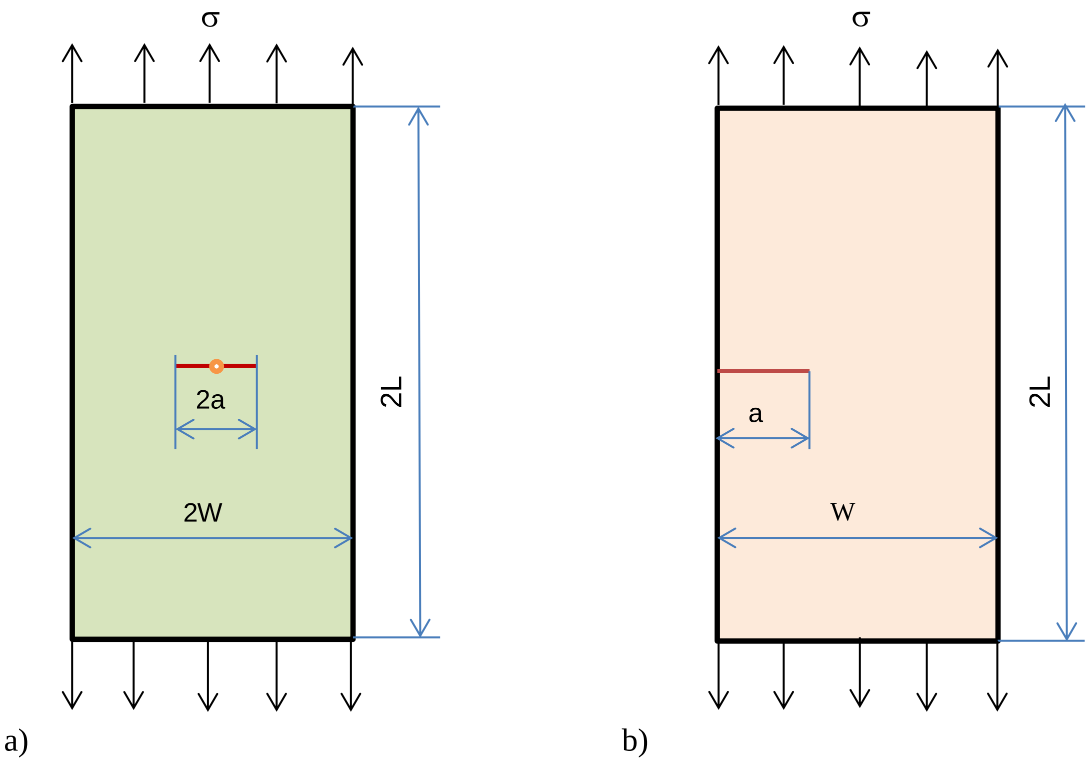

Fig. 2.6*. A central-cracked body of finite dimensions stressed by tensile stress (a). An edge-cracked finite body (b). Through direct cracks - the same length and orientation across the thickness of the plate.*

A stress intensity factor also depends on the orientation of a crack to the main tensile stress. E.g. for a crack whose plane forms an angle β with the direction of tensile stress, it is $K_I(\beta) = K_I.\sin^2\beta$.

Equations for calculation of the shape function are complex and sometimes ambiguous, even for relatively simple shapes of a sample and a crack. Therefore, more transparent graphical dependences are used. Analytical methods, numerical (FEM) and experimental (photoelasticimetry, resistance tensometry, moiré patterns, yielding measuring, etc.) can be used to determine the shape function.

For stress intensity factors, the so called **principle of superposition** applies, which is used to solve certain combined loads of bodies or multiaxial states of external stresses.
If a certain value of the stress intensity factor K_{ij}, where i = I, II, III, j = 1,2, …n, corresponds to each of n acting external loads (i.e. forces, torques), then the resulting stress intensity factor is given by the sum of individual contributions in the given mode (method) of loading, i.e.

$$K_i = \sum_{j=1}^{n} K_{ij} \tag{2.13}$$

In a similar way, the superposition principle can be applied also for the calculation of components of a stress tensor, a strain tensor and a displacement vector.

As already mentioned, the occurrence of a notch, a crack or other discohesions in material has an important role in brittle failure. Each material defect causes stress increase in its vicinity, which may result in initiation or propagation of unstable failure. At the same time, the term defect does not mean only a crack, a cavity, foreign particle in mass but also in the field of material where sudden local and undesirable change in structure and properties exists, which means the failure of homogeneity, such as a heat-affected zone during welding, heterogeneous coarse-grained structure.

Σ Summary of Terms

After reading this chapter, you should understand these terms and concepts.
Structural notches. Stress field. Stress concentration. Stress concentration factor. A strain concentration factor, Neuber equation. Methods of determining stress field and concentrations. Stress distribution at crack tip.
Components of a stress tensor, state of plane stress, state of plane strain.
Three modes of loading of a cracked body, stress intensity factor (K_I, K_{II}, K_{III}), shape functions (factors), the principle of superposition.

Questions to Chapter 2

2.1 Define the stress concentration factors.
2.2 What value does α reach for a small circular hole inside a large plate?
2.3 In which materials can high stress concentrations emerge?
2.4 What is the dependence of a stress concentration factor on a length and curvature of an elliptical notch?
2.5 What methods are used to determine fields of stresses or strains around notches and cracks in components?
2.6 Name the basic modes of loading of a cracked component.
2.7 What are the differences between the state of plane strain and plane stress?
2.8 What is the definition and what does a stress intensity factor characterize?
2.9 How does K_I relate to a length of a defect and external stress?
2.10 What purposes is the shape function used for?

Exercises to Chapter 2

2.1. Calculate the maximum stress at the front of an internal elliptically shaped defect of a length of 10 mm and radius of curvature (curvature ρ = 2,0 mm), when the external tensile stress has the value of 100 MPa and acts perpendicularly to the major axis of the defect.

2.2. Calculate the stress in a distance of 3.0 mm from the surface of a cylindrical shaft (Fig. 2.2), equipped with a circumferential semi-circular notch having a radius of curvature of 2,0 mm, at a tensile stress of 200 MPa. We assume elastic deformations.

2.3. What value of the stress concentration factor α does a V-notch of a sample for the impact test approximately have under static load in the elastic region of bending? A depth of the notch h = 2,0 mm, radius of curvature of the notch ρ= 0,25 mm, outer dimensions of the cross-section of the sample 10 x 10 mm (angle between walls of the notch 45°).

2.4. What is the maximum value of stress that exists at the front of an internal crack of a length of $3{,}8.10^{-2}$ mm and with radius of curvature $1{,}9.10^{-4}$ mm, when nominal tensile stress is 140 MPa ?

2.5. What course does the shape function have for a central crack and what value does it reach for the half proportional length of the crack a/W = 0,5?

2.6. In a structure in different areas with tensile stress, three cracks were detected by use of ultrasound. The first one of a length of 16 mm in region of stress of 100 MPa with the shape function f = 1,2; the second crack of a length of 9,0 mm under stress of 150 MPa (value f = 1,1) and the third one of a length of 25 mm in region of stress of 70 MPa (f = 1,3). Which of these cracks is the most dangerous one?

Answers to the Questions

2.1. The stress concentration factor $\alpha_n = \sigma_{max}/\sigma_{nom}$ or $\alpha_g = \sigma_{max}/\sigma$

2.2. For a circular hole and under certain conditions, α = 3,0 (for tensile load, $\rho \ll W$)

2.3. High stress concentrations can occur in brittle materials, in materials with limited plastic deformation.

2.4. Stress concentration is proportional to a length and inversely proportional to a radius of the notch, i.e. proportional to sharpness of the defect. For the elliptical internal notch or the defect at the tensile stress $\alpha = 1 + 2(c/\rho)^{1/2}$

2.5. Calculation methods analytical and numerical (FEM, complex stress potentials) experimental methods (photoelasticimetry, tensometry)

2.6. We distinguish 3 modes: I – tensile mode (tension), II – plane shear mode (sliding; *TN: in-plane shear*), III – antiplane shear mode (tearing; *TN: out-of-plane shear*))

2.7. For plane stress (i.e. biaxial stress, on a surface), one normal component of the stress tensor is zero ($\sigma_z = 0$), components of strain (ε_x, ε_y, ε_z) are nonzero. For a plane (biaxial) deformation, one component of the strain tensor is zero ($\varepsilon_z = 0$).

2.8. K – factor characterizes the average concentration of stress at the crack tip. Definition for mode I:

$K_I = \lim (2\pi r)^{1/2}\sigma_y(r,0)$, for $r \to 0$. Similarly for K_{II} and K_{III}. (equation 2.4)

2.9. In general, $K_I = \sigma\sqrt{\pi a}.f$ (the shape function f = f(a/W))

2.10. For more precise and correct calculations of the stress intensity factor and related parameters of fracture mechanics.

Results of Exercises

2.1. [σ_{max} = 416 MPa]

2.2. [$\sigma(x)$ = 318 MPa]

2.3. [α = 3,25]

2.4. [σ_{max} = 4100 MPa]

2.5. [monotonically nonlinearly increasing, f(0,5) = 1,19]

2.6. [K_{I1} = 15,2 MPa$\sqrt{m}$, K_{I2} = $\underline{15{,}7}$ MPa$\sqrt{m}$, K_{I3} = 14,4 MPa$\sqrt{m}$, second crack]

3. FRACTURE TOUGHNESS

Time dedicated to the study of this chapter is approximately 2 hours.

Objective: After studying this chapter, you will be able to

- Define fracture toughness in the state of plane strain
- Distinguish the fracture behaviour of material at the state of plane strain and plane stress.
- Calculate the critical defect size by a value of fracture toughness
- Assess values of fracture toughness of important materials

Interpretation

3.1. Definition and Importance

When the dimension of the plastic deformation area (zone) at the crack tip compared to the crack size and body dimensions in the direction of crack propagation is very small ($r_p \leq a/50$), the plastic zone can be omitted and stability of the crack can be addressed in the context of linear elastic fracture mechanics. The elastic state of stress applies to values of the acting nominal stress $\boldsymbol{\sigma_n \leq (0{,}6\text{-}0{,}8)R_p}$.

Fracture toughness can be defined as the critical value of the stress intensity factor K_I at the time of an unstable crack propagation, i.e. $\mathbf{K_I = K_{Ic}}$.

Fracture toughness is material characteristic that quantitatively expresses resistance of material to initiation of an unstable fracture in case there is a crack in the material. Designation of fracture toughness K_{Ic} means that a crack is being opened during loading (loading mode I) and the state of stress at the crack tip meets the condition for plane strain. Condition of unstable fracture creation of a crack is given by the relation $\mathbf{K_I \geq K_{Ic}}$. It is necessary to know the expression for the stress intensity factor of a specimen of finite dimensions and the loading mode (tension, bending) so that the value of K_{Ic} may be experimentally determined.

Since the value of K_I is expressed by two parameters (σ, a) according to the known (simplified) equation $\mathbf{K_I = \sigma \sqrt{\pi . a}}$, the above mentioned condition can be expressed as follows: In a body with a crack of a length a, loaded by stress σ, brittle failure appears when one of the parameters (σ or a) reaches such a value that the corresponding value of K_I exceeds material resistance to unstable crack propagation, K_{Ic}.

The relation between fracture toughness K_{Ic}, nominal stress σ and a crack length a, is schematically depicted in **Fig. 3.1**. The full curve shows course of the function $\sigma_c = K_{Ic}/\sqrt{\pi . a}$ at constant values of K_{Ic} and represents the stress limits and crack sizes above which brittle failure occurs. In fact, critical value of K_{Ic} may be reached by various combinations of stress and a crack length.

$$\mathbf{K_{Ic} = \sigma_1 \sqrt{\pi . a_1} = \sigma_2 \sqrt{\pi . a_2} = \dots = \sigma_n \sqrt{\pi . a_n}} \qquad (3.1)$$

This also means that for a given crack size a_i, a brittle fracture occurs when stress reaches a critical value σ_i or vice versa. Below the curve, there are permissible combinations of stress and lengths of cracks that do not lead to brittle unstable failure ($K_I < K_{Ic}$). It is necessary to consider the shape function f (i.e. the shape factor Y) and the equation $K_{Ic} = \sigma_c \sqrt{\pi . a}.f(a)$ or similarly $K_{Ic} = \sigma \sqrt{\pi . a_c}.f(a_c)$ for more precise application of K_{Ic}.

In the picture, there is also highlighted limitation of LEFM for metallic materials in relation to plastic deformation of the load-bearing cross-section (dotted line) and possibility to use the EPFM criteria.

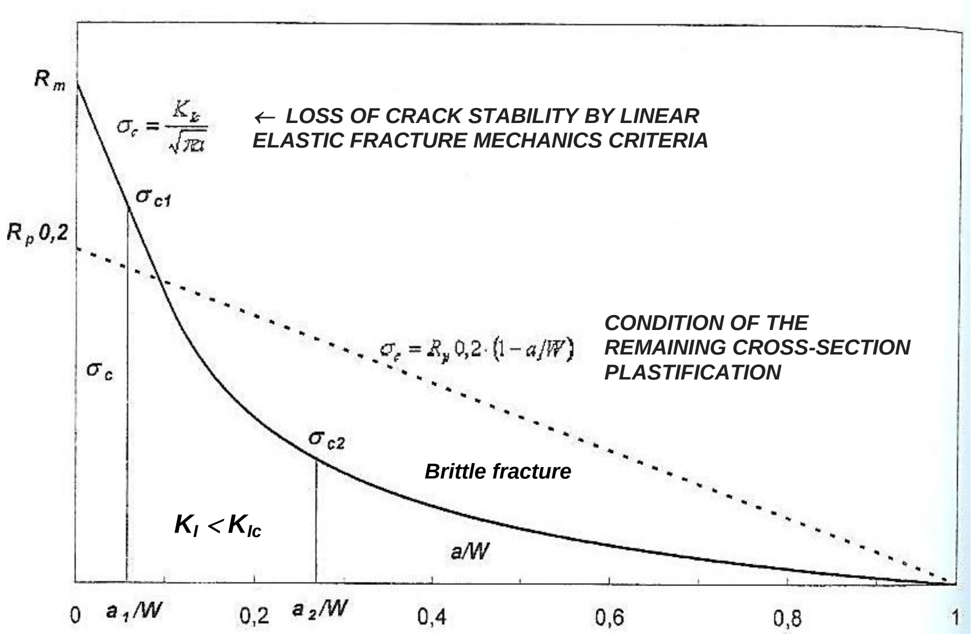

Fig. 3.1. *Dependence of the critical stress σ_c on the proportional length of a crack a/W using the criterion of linear elastic fracture mechanics.*

Limitations - linear fracture mechanics cannot be used for

- materials with low fracture toughness in the region of short cracks,
- materials with high fracture toughness,
- limitations of linear fracture mechanics at $\boldsymbol{\sigma_c < \frac{2}{3} R_p}$ (R_p – the yield strength)

Fracture toughness can be derived from energetic considerations of initiation of crack propagation. From the equivalence of K_I values and the crack driving force G_I, it follows that the fracture toughness can be expressed using the rate of release of elastic strain G_I (Chapter 5). It is then applicable for the critical values and the state of plane strain,

$$G_{Ic} = \frac{K_{Ic}^2}{E}(1-\nu^2), \tag{3.2}$$

where E is modulus of elasticity and ν - Poisson ratio.

Fracture toughness K_{Ic}, resp. G_{Ic} is material property that relies on chemical composition and state of metal structure. Its value is also dependent on temperature and loading rate.

3.2. Effects of Temperature, Strain Rate

General temperature dependence of fracture toughness is shown in **Figure 3.3**. With decreasing temperature, the value of fracture toughness sharply decreases, which means that the curve has transition character. Similarly to Vidal curve for notch toughness. At higher temperatures, the yield strength reduces and consequently size of a plastic zone and macroscopic plastic deformation increases. Therefore, validity of the value of K_{Ic} is limited only to certain temperature, at which the state of plane strain is kept.

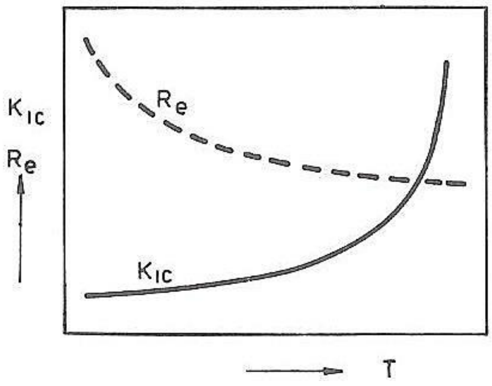

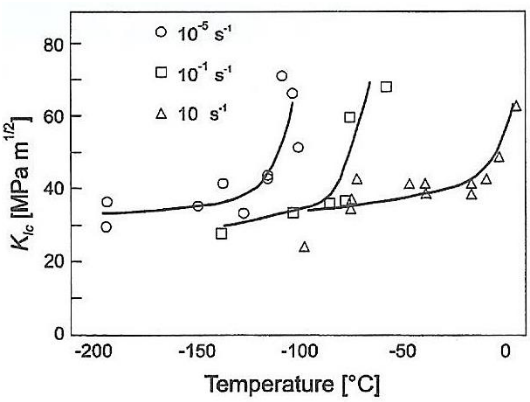

***Fig. 3.3**. Temperature dependence of fracture toughness K_{Ic} and yield strength R_e. Effect of strain rate on the transition behaviour of fracture toughness*

Value of fracture toughness is also dependent on thickness of a body. The known fact that brittle fractures occur preferentially in thick-walled structures can be explained as follows. The greater thickness of a stressed body, the greater is stress in the thickness direction σ_z, which creates favourable conditions for plane deformation. The dependence of fracture toughness on thickness of a body is schematically shown in **Figure 3.4**. At smaller thicknesses under given conditions (temperature, material properties), the state of plane strain (RD) is not achieved, but only the state of plane stress (RN). In this area, the fracture toughness value is termed as K_c and its value depends on the material thickness.

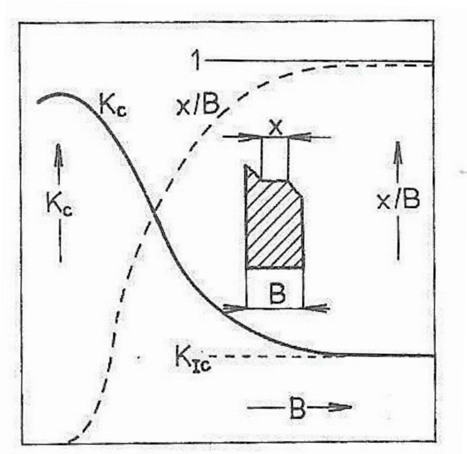

***Fig. 3.4.** Dependence of fracture toughness and proportion of a flat fracture on the thickness of a body*

State of plane strain in a body is achieved when thickness (B) and crack length (a) meet the condition: $\mathbf{a, B} \geq \mathbf{2{,}5}\left(\frac{K_{Ic}}{Re}\right)^{2}$.

The figure also shows that in the state of plane stress, the value of K_c decreases with increasing thickness and levels off at the value of K_{Ic} at the thickness corresponding to the stated condition. At further increase in thickness, the value of K_{Ic} is constant, independent of the material thickness. For comparison, there is also the course of the ratio of brittle fracture area to total thickness of the body x/a indicated in the figure. From the course of this curve, it also follows that at thickness a = a_{kr} , brittle fracture area x occupies the whole thickness of a body, that means there is the state of plane strain achieved in a body.

It follows from the above mentioned that K_c becomes a valid value of fracture toughness K_{Ic} in the state of plane strain of a body which is exposed to stress according the mode I, when not dependent on the body thickness. The state of plane strain and thus valid K_{Ic} values may be reached also in less thick bodies at lower temperatures, when values of yield strength are higher and the condition for the state of plane strain is easier to be satisfied.

K_{Ic} values also depend on loading rate, which in this case is expressed as the rate of growth of the stress intensity factor $\acute{K}$= dK_I/dt. With increasing values of $\acute{K}$, the curve K_{Ic} – T is shofted toward higher temperatures, **Fig. 3.5**. In dynamic load, K_{Ic} is usually referred to as K_{ID}. Under dynamic load, conditions for plane strain can be achieved on thinner samples, compared with static load.

Comparison of **loading rate** of a cracked body:

- Quasi-static loading dK_I/dt ≤ 1 MPa.$m^{1/2}$.s^{-1}
- Fast loading dK_I/dt = 10-10^4 MPa.$m^{1/2}$.s^{-1} (K_{Ic}(τ))
- Dynamic loading dK_I/dt ≥ 10^5 MPa.$m^{1/2}$.s^{-1} (K_{Id})

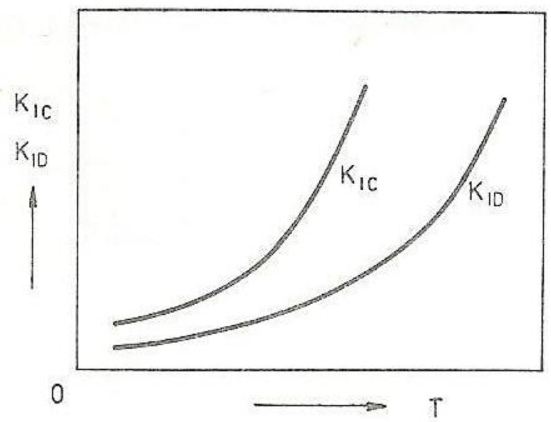

Fig. 3.5. *Temperature dependences of static (K_{Ic}) and dynamic (K_{ID}) fracture toughness.*

The criterion of K_{Ic} can only be used for materials and conditions for loading, when the LEFM principles are fulfilled, i.e. linear relations between stress and strain.

The value of K_{Ic} is a measure of the material resistance to brittle failure of a body with a defined crack. In engineering practice, there is a tendency to use materials with the highest values of K_{Ic} where possible. In the designer's work, the concept of fracture toughness can be also applied to other types of fractures, such as a fatigue fracture, a fracture during corrosion cracking, hydrogen embrittlement, etc. In the technology of metals, the criterion of K_{Ic} can be used with proper choice of alloying elements and heat treatment, especially for structural steels of middle and higher strength and greater thicknesses, that are welded in practice (pressure vessels, pipings, thick-walled structures).

Fracture toughness K_{Ic} enables to assess the body resistance to a brittle fracture. Cracked material does not fail, if $K_I < K_{Ic}$. Knowledge of fracture toughness enables to solve a number of problems in brittle failure of materials.

For the measured length (a), we calculate the critical stress σ_c by the equation $\boldsymbol{K_{Ic} = \sigma_c\sqrt{2\pi a}.Y}$, i.e. material (a part, a component) does not fail by an unstable brittle fracture if the true stress $\sigma < \sigma_c$.

Or for the stress σ, we calculate the critical length of a defect a_c according to equation $\boldsymbol{K_{Ic} = \sigma\sqrt{2\pi a_c}.Y}$, material resists an unstable brittle fracture, if $a < a_c$. The real crack length (a) can be measured by a non-destructive method, usually by ultrasound one.

3.3. Fracture Toughness Testing

Experimentally fracture toughness K_{Ic} can be determined on samples according to standards, e.g. **ČSN EN ISO 12737:** *Metallic materials - Determination of fracture toughness in plane strain (2010).* It is necessary to create a sharp fatigue crack with prescribed parameters prior to the test.

For the fracture toughness test, tensile testing machines that meet the requirements of standards are used, particularly in terms of stiffness and crosshead speed. Requirements to accessories for fixing test specimens are also included in the standard. In principle, this is a three-point bending test (type A) and eccentric tensile test (type B), **Fig. 3.6.**

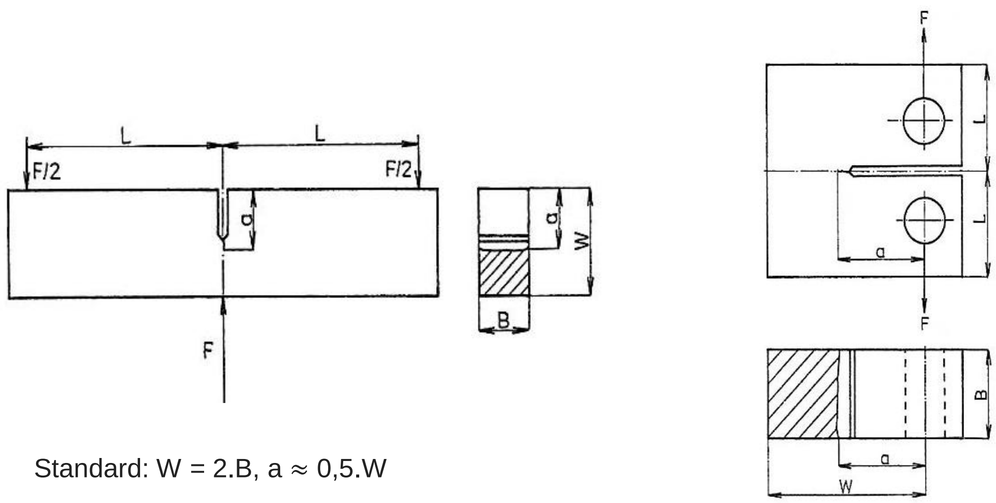

Fig. 3.6*. The specimen type A (3PB) loaded by three-point bending. The specimen type B (CT-compact tension) stressed by eccentric tension.*

During the test, which consists in uniform sample loading up to failure, dependence of the force *F* on opening of the *V* notch is scanned. To measure the opening, clip gages that are mounted into recesses in the notches or into attachments screwed onto surface of the body are used, see **Figure 3.7**.

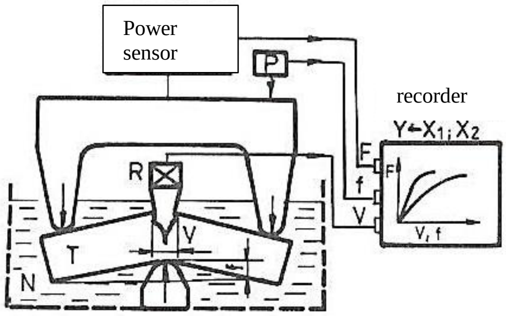

Fig. 3.7*. Configuration diagram of fracture toughness test on the specimen of type A*

According to the test material and test conditions, different types of F-V dependence may be obtained. Three kinds of records, at which a sudden brittle fracture occurred during the test, can be used to determine K_{Ic}, **Fig. 3.8**.

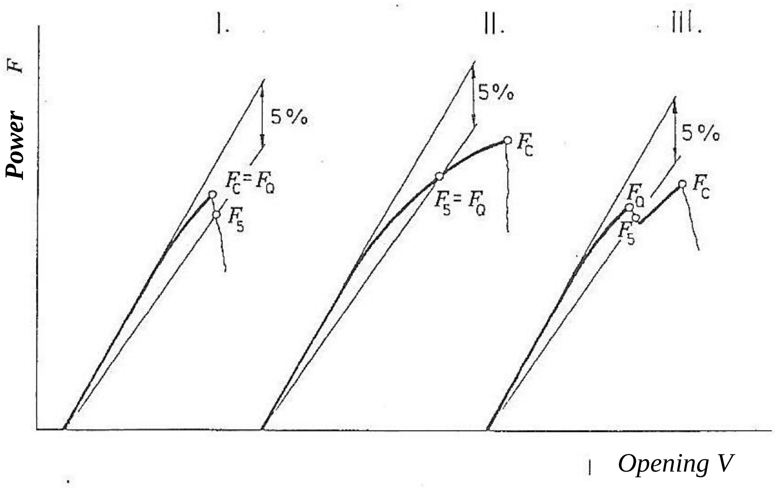

Fig. 3.8*. Characteristic types of the force F – V-notch opening dependence when measured fracture toughness*

Evaluation according to standard is carried out as follows:

1) The force, at which an unstable fracture initiated, is marked F_c.
2) At the intersection of the linear part of the record with the axis of opening *V*, a secant with the tangent by 5% lower than the tangent of the linear part is plotted. The intersection of the secant with the record may be indicated F_5.
3) Of the records, force F_Q is then determined for further calculation as follows:
   a) if the force at each point of the record prior to the intersection is lower than F_5, then $F_5=F_Q$. (mode II),
   b) if there is a maximum of the force on the record, which is higher than F_5, then the value of the maximum is equal to F_Q (mode I and III),
   c) the ratio F_C/F_Q (for mode II) is calculated. The force F_Q can be used for further calculation only if $F_C/F_Q \leq 1,1$.

Fulfilment of the condition ensures that from the force F_Q, not only plastic deformation but also a slow crack growth occurs. If the condition is not met, then it is necessary to evaluate the test record by other procedures (using the quantities introduced by elastic-plastic fracture mechanics.

4) From the value of the force F_Q determined by the above mentioned steps and from dimensions of the specimen, provisional value of fracture toughness K_Q is calculated according to the relation

$$K_Q = (F_Q.Y_1)/BW^{1/2} \quad \text{or} \quad K_Q = (F_Q.Y_2)/BW^{3/2}, \tag{3.3}$$

where Y = f (a/W) is a shape factor (function) dependent on the type of a body. In **Table 3.1,** there are listed formulas for K_Q calculation, where (a) is the total crack length including a notch, measured on the fracture surface of a broken body, other dimensions are shown in **Figure 3.6**.

Tab. 3.1. Relations for K_Q, resp. K_{Ic} calculation (ASTM E399, ASTM E1820-99)

Specimen	
Type A	$K_Q = \frac{F_Q L}{BW^{\frac{3}{2}}} \cdot \frac{3\left(\frac{a}{W}\right)^{\frac{1}{2}}\left[1{,}99 - \frac{a}{W}\left(1-\frac{a}{W}\right)\cdot\left(2{,}15 - 3{,}93\frac{a}{W} + 2{,}7\left(\frac{a}{W}\right)^2\right)\right]}{\left(1+2\frac{a}{W}\right)\cdot\left(1-\frac{a}{W}\right)^{\frac{3}{2}}}$
Type B	$K_Q = \frac{F_Q}{BW^{\frac{1}{2}}} \cdot \frac{\left(2+\frac{a}{W}\right)}{\left(1-\frac{a}{W}\right)^{\frac{3}{2}}}\left[0{,}886 + 4{,}64\left(\frac{a}{W}\right) - 13{,}32\left(\frac{a}{W}\right)^2 + 14{,}72\left(\frac{a}{W}\right)^3 - 5{,}6\left(\frac{a}{W}\right)^4\right].$

5) The provisional value of K_Q represents a valid value of fracture toughness K_{Ic} in plane strain, if the condition for plane strain is fulfilled. This condition may be expressed by two inequalities; for thickness of the specimen B and the total crack length and it must be applicable

$$B \geq 2{,}5(K_Q/R_p)^2, \quad a \geq 2{,}5(K_Q/R_p)^2 \ \text{[m]}, \quad W - a \geq 2{,}5(K_Q/R_p)^2 \tag{3.4}$$

In the case that the above listed inequalities are not fulfilled for the test, then it is necessary to use a thicker body (if the actual thickness of a part allows that) or to evaluate the test on the basis of other characteristics - usually by J-integral or critical crack opening. Methodology for the calculation of these parameters is again described in the relevant standards.

In steels for which the test was originally developed, non-compliance depends on both the temperature and the strain rate. Therefore when measuring fracture toughness, the temperature dependence of K_{Ic} is usually determined, or the temperature dependence of fracture toughness for fast loading $K_{I\tau}$ or shock loading K_{Id} (dynamic fracture toughness measured by the instrumented pendulum hammer).

With regard to the complexity of performing the test of fracture toughness, attempts to determine their values by using smaller samples with shock load are made, by means of results of the impact strength or tensile test under defined conditions. Fracture mechanics describes stability of a crack using one or more parameters. It enables to transfer measured data of K_{Ic} from test samples to real structures, **Fig. 3.9**.

If the conditions for plane strain are not met, fracture toughness is referred to as K_c and its size is affected by thickness of a body, at the same time $K_c > K_{Ic}$ (Fig. 3.4).

.

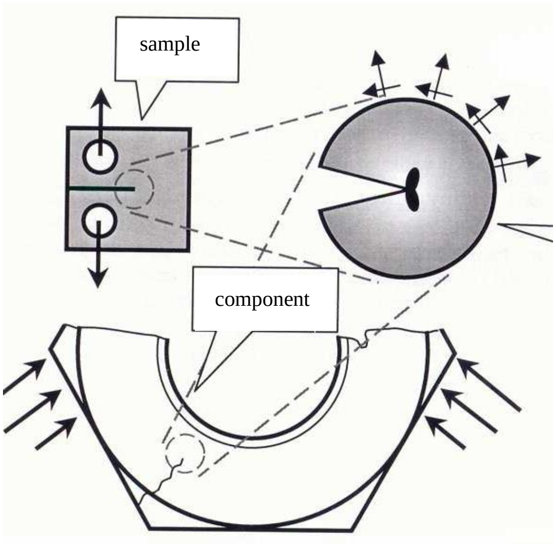

Fig. 3.9. *Fracture toughness of a sample material and of a component is the same. Stress intensity factors are different by distribution of load, a crack geometry and shape of a body.*

Example – Evaluation of measurement results of fracture toughness

When tested fracture toughness of the structural alloy AlCu4Mg1 on a body of type B (CT) 50 mm wide, 12,5 mm thick, critical force magnitude F_Q = 9,05 kN was measured. During subsequent fractographic analysis of the fracture surface of the disrupted body, the average crack length a = 25 mm was found. Engineering yield strength of the material is $R_p0,2$ = 390 MPa.

After substituting F_Q, a, W, and B into the equation for K_Q, we get provisional value of fracture toughness K_Q = 31,3 MPa.m$^{1/2}$. Empirical conditions for maintaining the state of plane strain require that thickness of the body B is greater than the minimum value B_{min} = $2,5(K_Q/R_p)^2$ = 2,5(31,3/390)2 = 0,0161 m = 16,1 mm.

From the inequality B = 12,5 mm < B_{min} = 16,1 mm, it is apparent that the value K_Q = 31,3 MPa.m$^{1/2}$ cannot be considered fracture toughness in the state of plane strain $K_{Ic.}$ From dependence of fracture toughness on thickness of a body, a one-sided estimate follows $K_{Ic} < K_Q$ = 31,3 MPa.m$^{1/2}$.

The material should have the value of $K_{Ic} \leq$ 27,6 MPa.m$^{1/2}$ so that the value of K_{Ic} is valid and thus the condition B ≥ 2,5 (KQ / Rp)^2 is applicable for B=12,5 mm.

The range of fracture toughness values of important groups of technical materials, are compared in **Tab. 3.2**. The highest values of K_{Ic} (K_c) are reached in austenitic steels.

Tab. 3.2. The fracture toughness values of selected materials

material	K_{Ic}		material	K_{Ic}	
	$[MPa\sqrt{m}]$			$[MPa\sqrt{m}]$	
Steels	30 – 220		Cast Iron	5 - 20	
Ni alloys	70 - 160		Technical ceramics	2 - 10	
Ti alloys	50 - 150		Technical polymers	0,5 - 7	
Al alloys	10 - 50		Glass	0,5 – 1,2	
Mg alloys	10 - 20		Concrete	0,15 – 0,3	

Generally, with increasing values of strength or yield strength, toughness values in the group of metallic materials show a decreasing trend.

Ashby maps are used for comparing properties and choosing material. In **Fig. 3.10**, there are depicted connections between fracture toughness and characteristic strength (yield strength for metals and polymers, compressive strength for ceramics and glass, tensile strength for composites).

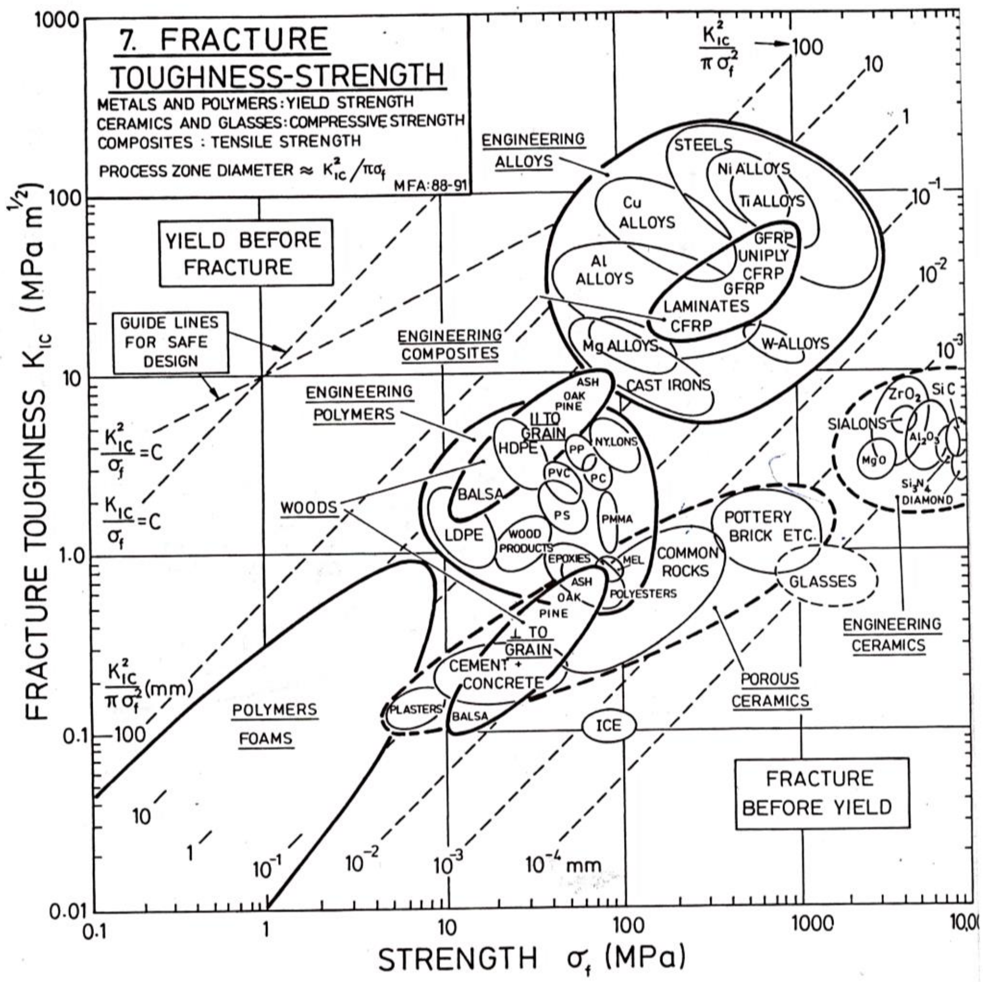

Fig. 3.10*. Relations between fracture toughness and characteristic strength values (Ashby)*

For graphical interpretation of the relation between fracture toughness, a crack length and tension, graphical dependences shown in **Figure 3.11** are used.

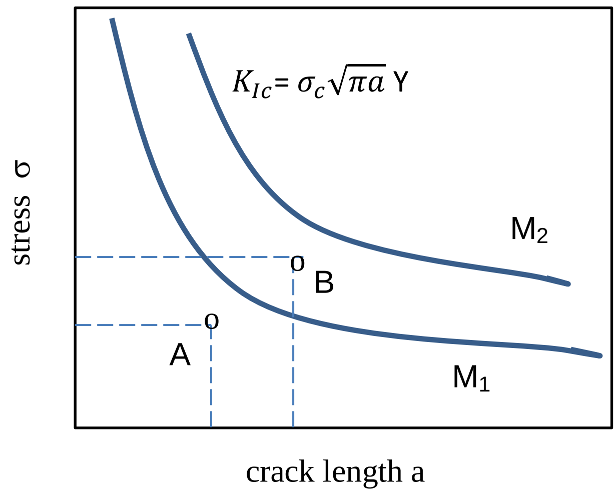

Fig. 3.11. *Graphical representation of the critical stress on a crack length at given fracture toughness*

When combined tensile stresses and a crack length under the curve (point A), the crack will be stable and the sudden brittle fracture will not occur. When achieved or exceeded the curve, the fracture would occur (point B, the material M1, not the material M2). Generally, the material M2 is more resistant to the brittle unstable fracture compared to M1.

Σ Summary of Terms

After reading this chapter, you should understand these terms and concepts.

- **A critical value of the stress intensity factor, fracture toughness K_{Ic}, critical stress, a critical crack length, conditions for plane strain, plane stress (K_c) effects.**
- **Static and dynamic fracture toughness, temperature dependences of toughness.**
- **Specimen types A (3PB) or B (CT), clip gage, provisional force magnitude.**

? Questions to Chapter 3

3.1 How is fracture toughness K_{Ic} defined?
3.2 Which metal materials reach the highest values of fracture toughness?
3.3 What are conditions for validity of K_{Ic} values during testing of samples according to the standard?
3.4 What is the effect of dynamic loading on temperature dependence of fracture toughness of steels?
3.5 What trend in general is valid for fracture toughness K_{Ic} and value of yield strength $R_{p0,2}$ (R_e) at the same metallic material (e.g. some steels after various processing)?
3.6 How does fracture toughness change depending on thickness of a body?
3.7 In what interval are usually values of fracture toughness K_{Ic} for ceramic materials?
3.8 What are advantages of using values of fracture toughness compared to notch toughness?

3.9 What are metallurgical (technological) steps to increase toughness?
3.10 What are disadvantages of fracture toughness testing according to standards?

Exercises to the Chapter

3.1. At the temperature drop from 25°C to -50°C, value of fracture toughness decreased 4 times. How will critical crack length a_c change at the same load?

3.2. A sample of 4340 steel with fracture toughness of 54,8 MPa.m$^{1/2}$ shall be subjected to stress of 1030 MPa. Will this material rupture, if it is known that the largest surface crack has length of 0,5 mm? The shape function (the shape factor) has the value of 1,12 for relatively short surface cracks.

Solution: The specified parameters: K_{Ic} = 54,8 MPa.m$^{1/2}$, σ = 1030 MPa, a = 0,5 mm, Y = 1,12. We shall calculate critical stress σ_c and compare it with stress σ. We use the basic equation for fracture toughness $K_{Ic} = \sigma_c \sqrt{\pi a}$ .Y, from which we calculate σ_c. E.g. directly from the equation 54,8 = $\sigma_c \sqrt{\pi . 0{,}0005}$.1,12 we get σ_c = 1235 MPa > σ = 1030 MPa, it means that a fracture will not occur.

3.3. Calculate in a simplified way a critical size of a sharp internal crack in steel with fracture toughness of 30 MPam$^{1/2}$, if a part of the steel is loaded by tensile stress of 100 MPa perpendicularly to the crack.

3.4. Estimate the theoretical fracture strength of a brittle material, if it is known that the fracture arises from a surface crack of an elliptical shape of length of 0,5 mm and with radius of curvature of 5.10^{-3} mm if tensile stress of 103,5 MPa is applied.

3.5. A sharp crack of a circular shape with a diameter of 25 mm was completely hidden in material. A catastrophic fracture occurred at tensile stress of 700 MPa.

a) What is fracture toughness of the material (let us assume this value for plane strain conditions).

b) If sheet metal (7,5 mm thick) of the material is ready for fracture toughness testing (B = 7,5 mm, a = 37,5 mm), would be the fracture toughness value valid (the yield strength of the material is 1100 MPa)?

c) What would be the sufficient material thickness for valid determination of K_{Ic}?

3.6. A slab is made of steel having fracture toughness of 82,4 MPa.m$^{1/2}$ in the state of plane strain. If the board is exposed to tensile stress of 345 MPa during operation, determine minimum length of a surface crack that leads to a fracture.

3.7. Calculate the maximum length of a crack admissible for a component of the titanium Ti-6Al-4V alloy, which is loaded to a half of yield stress (1000 MPa) and its fracture toughness $K_{Ic} = 80$ MPa.m$^{1/2}$. The geometrical factor has a size of 1,5.

3.8. Fracture toughness of ceramic materials can be determined from the size of cracks (a) that propagate from the peaks of an indentation when measuring HV hardness according to the relation $K_{Ic} = 0{,}022(E/HV)^{2/5}(F/a)^{3/2}$.
Used load F = 150 N at the end of the indentation created a crack of the length a = 400 μm. What is toughness of ceramics with the modulus of elasticity E = 120 GPa and hardness of 700HV?

Answers to the Questions

3.1 The critical value of the stress intensity factor for initiation of an unstable fracture under tensile loading in plane strain conditions.
3.2 Austenitic steels, nickel alloys, titanium alloys, some fibre composites
3.3 For K_{Ic} in the state of plane strain: $B \geq 2{,}5(K_{Ic}/R_p)^2$, $a \geq 2{,}5(K_{Ic}/R_p)^2$,
3.4 Dynamic load decreases toughness K_{Ic} (transition temperature is shifted above) .
3.5 With growing yield strength, fracture toughness decreases.
3.6 According to Figure 3.4, in the area of plane strain it is minimal, with decreasing thickness in the region of mixed state of stress, resp. plane stress, toughness K_c increases, for relatively small thicknesses it decreases again due to shear failure.
3.7 For technical ceramic materials, it is usually K_{Ic} = 1- 10 MPam$^{1/2}$
3.8 Possibilities of design calculations made for bodies with a crack or a sharp defect.
3.9 Alloying of Ni, Mn; decrease in content of C, S, P; increase in purity, refining of structure is not unequivocal.
3.10 Costly production of samples (preparation of a sharp crack by cyclic loading), ensuring the conditions of plane stress.

Results of the Exercises

3.1. Critical crack length drops 16 times.
3.2. The component will not rupture.
3.3. For the state of plane strain, a_c = 9,7 mm
3.4. Estimation σ_t = 2174 MPa
3.5. a) K_{Ic} = 139 MPam$^{1/2}$, b) thickness B = 7,5 mm does not comply, c) min B = 40 mm.
3.6. Minimum length of a surface crack a_c = 14,5 mm (on the surface Y = 1,12).
3.7. Length a_c = 3,62 mm.
3.8. Toughness K_{Ic} =1,3MPam$^{1/2}$.

4. PLASTIC ZONES AND CRACK OPENING

Time dedicated to the study of this chapter is approximately 2 hours.

Objective: After studying this chapter, you will be able to

Assess plastic zones for resistance of material to a brittle fracture.
Distinguish shapes of a plastic zone according to the method (mode) of loading.
Apply the method of opening the crack tip on the fracture behaviour of material.
Express or detect dependences between a critical value of the crack tip opening (δ_c) and other critical parameters of fracture mechanics.

Interpretation

4.1. Plastic Zones

Emergence of a plastic zone at a crack tip is shown schematically in Fig 4.1. To simplify considerations and calculations, we assume an elliptical shape of a zone with radius r_p. Distance of r_p from the front of a crack determines course of stress σ_y with level of stress on yield strength R_e. Stress σ_y' illustrates rearrangement of stress at the crack tip after creation of a plastic zone.

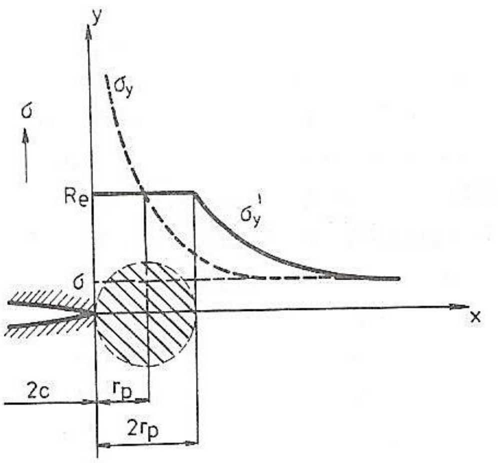

Fig. 4.1*. A simplified plastic zone (mode I)*

By the relation $\sigma_y = \frac{K_I}{\sqrt{2\pi r}}$ for $\sigma_y = R_p$ and $r = r_p$ we get easily dimension of the zone

$$\boldsymbol{r_p} = \frac{1}{2\pi}\left(\frac{K_I}{R_p}\right)^2, \qquad (4.1)$$

i.e. a size of the plastic zone in the axis x direction for the state of plane stress RN (on a surface).

Similarly for the state of plane strain RD (inside the thicker wall)

$$r_p = \frac{1}{6\pi}\left(\frac{K_I}{R_p}\right)^2. \tag{4.2}$$

For a more precise analysis of a shape of the zone, it is necessary to consider the shear stress components and criteria for beginning of plastic deformation. At the crack tip, a plastic zone is created with a real shape according to the type of loading (mode).

Part of the elastic energy is consumed for creation of a plastic zone; a **plastic zone increases the surface energy of a fracture** and thus toughness of material. A plastic zone leads to reduction in stress concentration, deadening peaks of stress before the crack tip, and thus reduces or prevents formation of a brittle fracture.

More accurate calculations of a shape of a plastic zone on the basis of components of the stress tensor, triaxial state of stress and criteria of beginning of yielding (HMH) lead to the result in **Figure 4.2**, where differences between the state of plane strain and plane stress in mode I and II are apparent.

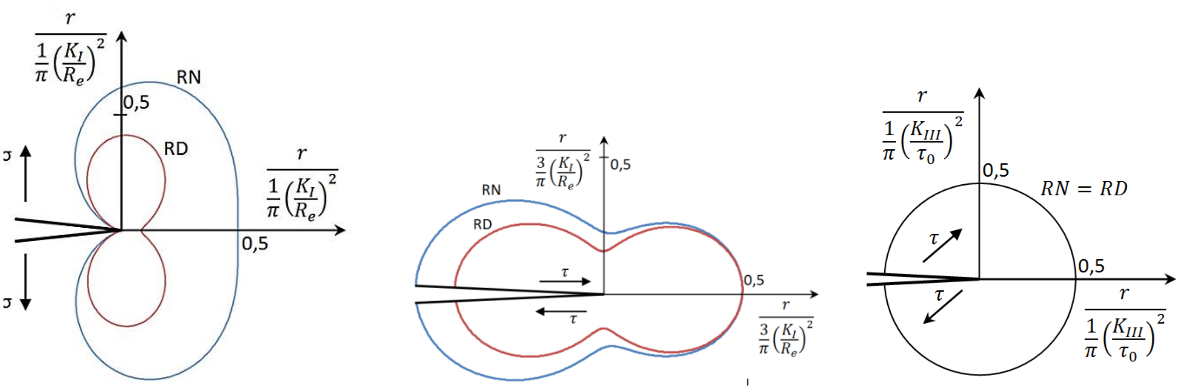

Fig. 4.2. Shapes of a plastic zone for mode I, II and III, for the state of plane strain (RD) and plane stress (RN). For more general comparison, the proportional coordinates are used.

In the state of plane strain, a smaller plastic zone arises with higher stress concentration before the crack tip (**Fig. 4.3**).

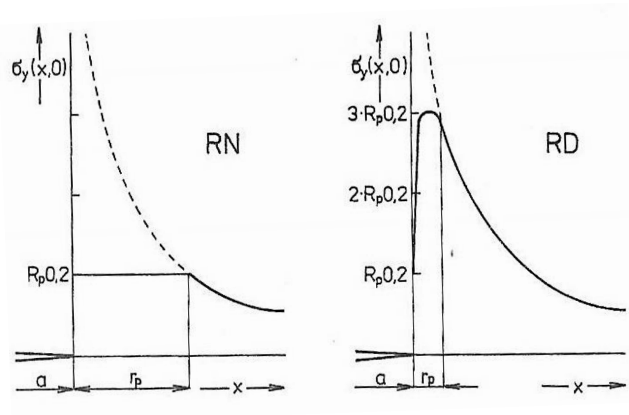

***Fig. 4.3.** Courses of stress σ_y before a crack tip in the state of plane stress (RN) and plane strain (RD). Comparison of a shape and proportional size of a plastic zone for mode I (tension)*

Also Mohr's circle is used to explain differences of the above mentioned findings, **Figure 4.4**; Possibilities of plastic deformation are determined by values of the shear stress components.

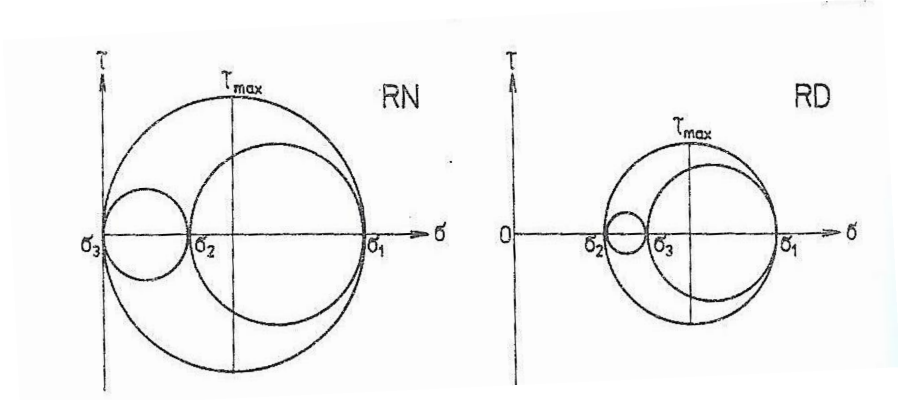

Fig. 4.4*. Mohr's circle of main stresses at the crack tip, maximum shear stress (the state of RN and RD)*

At the surface in the state of RN, there are multiple active slip systems and easier plastic deformation than for the state of RD (where triaxial tensile stress state prevails in the middle of the wall), **Fig. 4.5.**

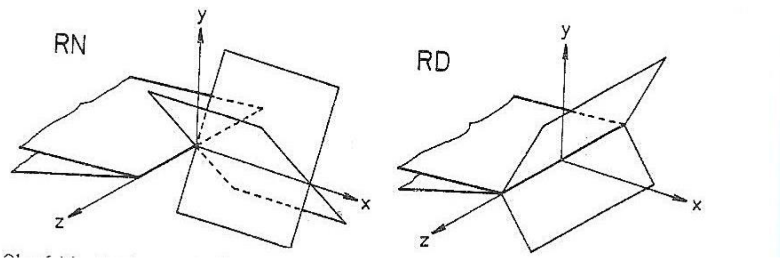

Fig. 4.5*. Planes of maximum shear stress before the crack tip in the state of RN and RD.*

There is a schematic dimensional model of a plastic zone shape at a sharp crack depicted in **Figure 4.6**. In the central part of thickness (b), there is the state of plane strain, which produces a small plastic zone. A plastic zone grows in marginal and subsurface areas due to the state of plane stress.

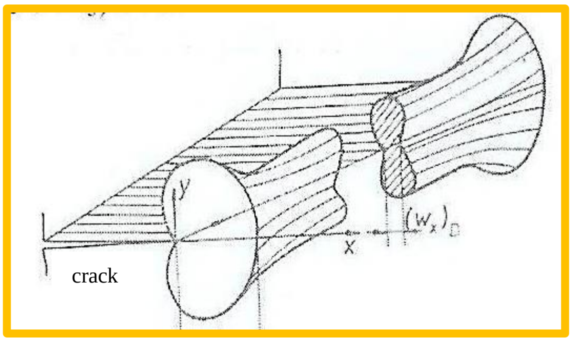

Fig. 4.6*. Spatial representation of a plastic zone in a plate with a crack. Comparison of a size and shape of the state of plane stress (RN, surface) and plane strain (RD, centre)*

From these relations for the size of a plastic zone, it follows for the tensile stress mode (mode I, a in the plane of the crack, y = 0, in the x direction), that in the state of plane strain, the plastic zone is about three times smaller than in the state of plane stress.

Experimental methods for determination of a plastic zone: a) etching method, b) roentgenographic methods, c) tensometric methods, d) recrystallization methods, e) monitoring on the electron microscope, f) moiré patterns, g) interference microscopy (holographic interferometry), h) fotoelasticimetry, i) stereometry, j) infrared thermography, k) microhardness measuring.

Steel structures are usually made of steels of lower and medium strength, which fail by brittle fracture, especially at lower temperatures and dynamic load. At the materials and under conditions in which they are loaded, it is necesary to allow for emergence of larger plastic deformation before the crack tip, which forbids the use of linear elastic fracture mechanics. Since in the context of elastic-plastic fracture mechanics we consider real size of a plastic zone, size of energy of plastic deformation, which is spent on its creation, must be reflected in relations to critical parameter values.

Energy of plastic deformation in the area of a plastic zone γ_p is 2 - 3 orders of magnitude higher than the value of its own surface (elastic) energy γ. The sum of both surface energy represents an **effective surface energy**

$$\boldsymbol{\gamma_{ef} = \gamma + \gamma_p}. \tag{4.3}$$

Original formula for calculation of critical stress (σ_c) of brittle fracture was adjusted to the

$$\sigma_c = R_f = \sqrt{\frac{2\gamma_{ef}\,\boldsymbol{E}}{\boldsymbol{\pi . a}}}. \tag{4.4}$$

Comparison of the size of the plastic zone at yield strength of material $R_p0,2$, and the stress intensity factor for a selected group of steels and alloys of nonferrous metals is depicted in **Figure 4.7**.

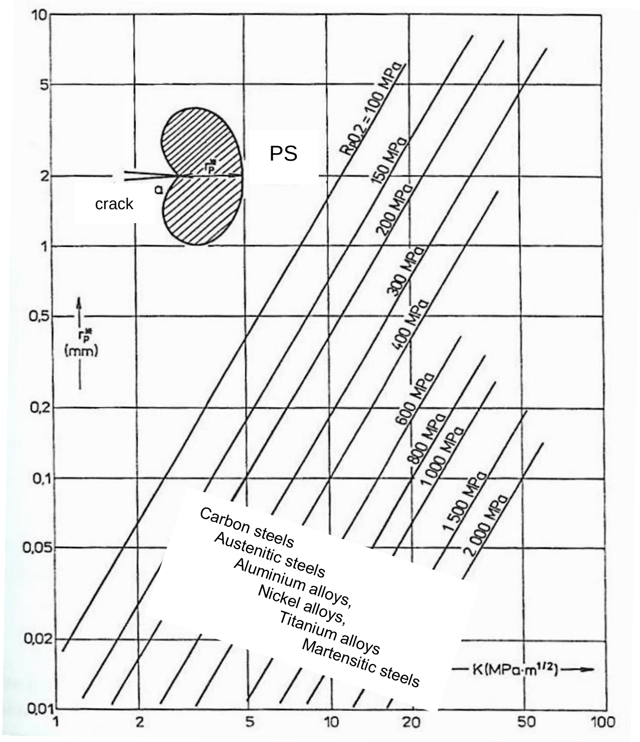

Fig. 4.7. Dependences of a plastic zone before the crack tip on the stress intensity factor K_I and yield strength of material $R_p0,2$

Inside a plastic zone, there is a smaller process zone, where the disruption of cohesion of material during initiation or crack growth (through microcavities, microcracks) occurs.

4.2. Crack Opening

The size of plastic deformation at a crack tip is proportional to the size of opening of the facing surfaces of a crack and can be determined experimentally. From there the name of crack opening came, which in the professional literature is marked δ or COD (crack opening displacement).

This approach is based on the condition that a crack will propagate unstably when the **crack opening δ**, proportional to the plastic deformation, reaches a critical value δ_c.

Scheme of gradual opening of a crack is shown in **Figure 4.8**. A body with an initial sharp crack is in the state indicated in Figure 4.8a without load and crack opening size is $\delta_o = 0$

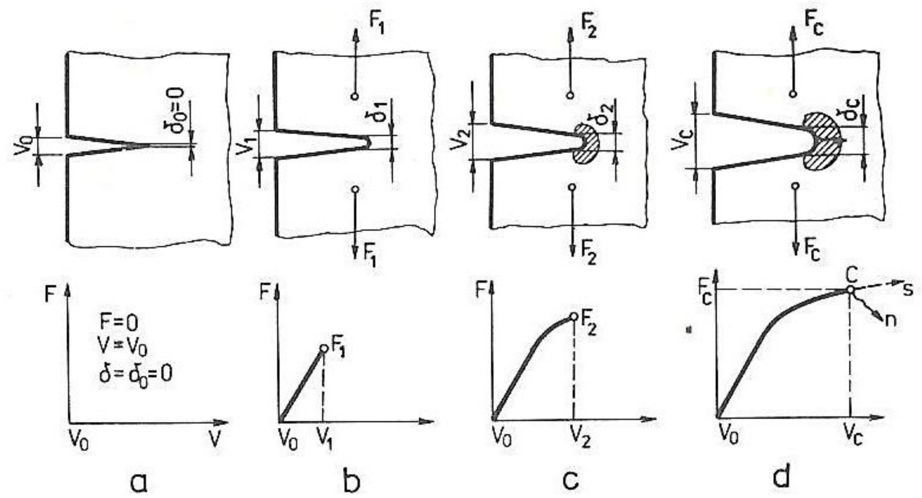

***Fig. 4.8**. Scheme of gradual opening of a crack at growing load.*
a – an unloaded state, b – under loading by force F_1, only elastic crack tip opening occurs, c – at a force F_2, a plastic zone is formed, d – moment of critical crack opening $\delta = \delta_c$ at a force F_c, and the crack starts to propagate. Crack opening size at the surface (V) can be easily measured.

Under loading by force F_1, the crack tip opens (deforms, state b) to the value δ_1, which crack mouth opening V_1 corresponds to. With greater force F_2 (state c), stress at the front exceeds the yield strength and plastic deformation, respectively plastic zone, occurs. In this case, the value of opening δ_2 represents the sum of elastic and plastic deformation at the tip and the value of V_2 corresponds to this. A critical moment occurs during loading by force F_c (state d), when the total deformation in the crack tip reaches a critical (limit) value $\delta = \delta_c$, while $V = V_c$. At that time, the crack begins to propagate:

- unstably, if initiation of a fracture takes place at concurrent sharp drop in a force (the case n in the F-V scheme in Fig. 4.8d),
- stably (slowly, sub-critically), if the crack propagates at a constant or slightly increasing strength (direction s).

The moment of the state of crack instability is defined by:

a) the value of critical crack opening δ_c,
b) nominal fracture stress σ_f, ascertained from a critical value of the force F_c.

Criterion of δ_c is of practical importance, when its value is determined in the context of fracture stress σ_f, which causes an unstable fracture. Therefore dependences between mentioned and other parameters have been derived. For the state of plane stress $\delta_c = \frac{\pi.c.\sigma_f^2}{E.R_e} = \frac{K_c^2}{E.R_e} = \frac{G_c}{R_e}$, and similarly for the state of plane strain

$$\delta_c = \frac{K_{Ic}^2\,(1-\nu^2)}{E.R_e} = \frac{G_{Ic}}{R_e}. \tag{4.5}$$

These relations determine interdependence between the parameters of linear FM (K_{Ic}, G_{Ic}) and the criterion of elastic-plastic FM (δ_c).

A requirement that the value of δ_c detected in a laboratory on test samples corresponds to the value at crack instability in a real structure at the same temperature, loading rate and state of stress is a prerequisite for application of the δ_c criterion for assessment of material resistance to brittle failure. At the same time, the size of plastic deformation at the front of an initial crack must be smaller than the thickness of a test body, which means that the fracture must occur before plastic deformation of entire cross-section before the crack. The value of δ_c depends on temperature, similarly to K_{Ic}.

Criterion of crack stability: **CTOD < CTODc** (CTODc – a critical value for unstable initiation of a fracture) or in short **$\delta < \delta_c$**.

The use of transformation relations between CTOD = δ and K_I, e.g.

$$\delta = \frac{K_I^2}{\lambda E R_p} \tag{4.6}$$

where $\lambda = \pi/4 - 2$ (RN), enables **indirect determination of fracture toughness** K_{Ic} by means of $\boldsymbol{\delta_c}$ (CTODc), e.g. according to the relation $\delta_c = \frac{K_{Ic}^2}{\lambda E R_p}$ **,** at the same time, it is necessary to verify the conditions for validity of K_{Ic} for plane strain and stated dimensions of the body B, a, W - a $\geq 0{,}1\,\frac{K_{Ic}^2}{R_p^2}$**.** (B – a sample width, a – a crack length, (W – a) a dimension of the part of a sample before the crack).

Determination of crack opening by means of two clip gages is depicted in **Fig. 4.9**.

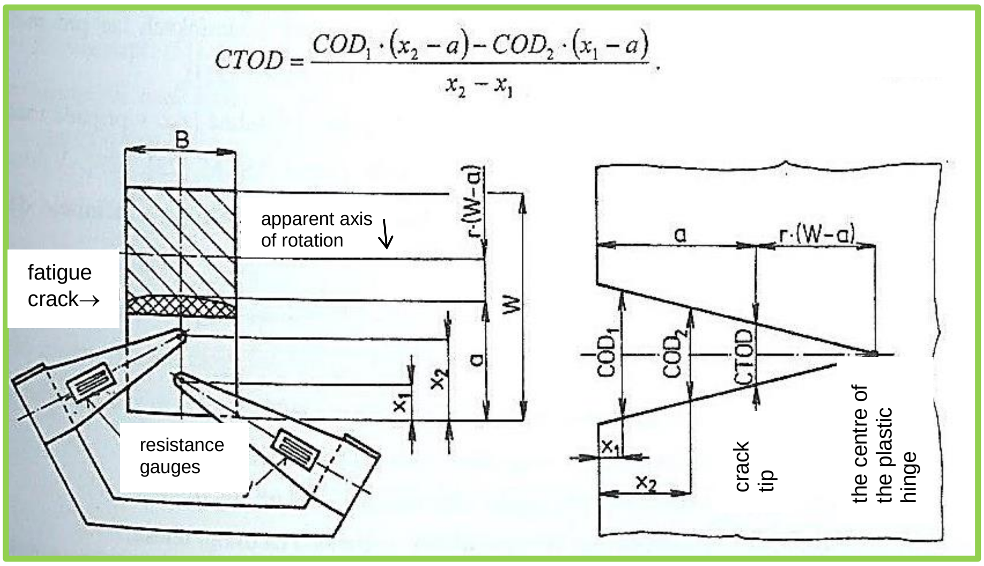

Fig. 4.9. *COD measurement in two places of a body, a crack face. Relation between COD_1, COD_2 and CTOD*

Summary of Terms

After reading this chapter, you should understand these terms and concepts.
A plastic zone, a size and a shape of a plastic zone, conditions for plane stress or plane strain, effective surface energy.
Crack opening (δ, COD), critical crack opening, criterion of δ_c, dependences of force - opening (F- V),

Questions to Chapter 4

4.1 What is the importance of a plastic zone for material resistance to a brittle fracture?
4.2 Why are there differences in the size of a plastic zone on a surface and inside a body with greater wall thickness?
4.3 What impact does a plastic zone have on the maximum values of tensile stress at the front of a crack?
4.4 What is the dependence between a size of a plastic zone and crack tip opening?
4.5 How do we determine fracture toughness by crack tip opening?
4.6 Suggest a way to determine the parameter λ in equation (4.6).

Exercises

4.1. Compare the size of a plastic zone before a crack tip for loading mode II and III at the condition $K_{II} = K_{III}$, $\tau_o = R_e/2$.

4.2. A large machine component made of steel having fracture toughness of 50 MPa $m^{1/2}$ and yield strength of 650 MPa burst. How large plastic zone was formed at a propagating crack?

4.3. Determine the angle associated with the maximum dimension of the plastic zone for mode I (Fig. 4.2).

4.4. What is the size of a plastic zone of a titanium alloy with the yield strength of 700 MPa at K_I = 30 $MPam^{1/2}$

4.5. Calculate the size of crack front opening of an aluminum alloy with the yield strength of 400 MPa under load of K_I = 20 $MPam^{1/2}$

Answers to the Questions

4.1 A plastic zone reduces the maximum stress at a crack and increases fracture surface energy.

4.2 On the surface, there is the biaxial stress state with the higher shear component and multiple slip systems.

4.3 In a plastic zone, the maximum stress (σ_y) is reduced and shifted under the surface. The maximum stress in the state of plane strain is about 3 times higher than in the state of plane stress (Figure 4.3)

4.4 The direct proportion $\delta = 4R_p.r_p/E$ (for $\lambda = \pi/2$) is true, according to relations (4.1) and (4.6).

4.5 By measuring the critical value of crack opening δ_c and the equation $K_{Ic} = (\lambda E R_p .\ \delta_c)^{1/2}$

4.6 For known values of K_I, E and R_p, we measure δ and calculate the parameter λ according to equation (4.6).

Results of the Exercises

4.1. For the angle φ =0, it is $r_p(II) = 3/4\ r_p(III)$, that means $r_p(II) < r_p(III)$,

4.2. Size of the zone is r_p = 1,9 mm.

4.3. For plane stress (RN) approximately φ = 70°, for plane strain (RD) φ = 85°.

4.4. Dimension of the zone is r_p = 0,292 mm for RN, resp. r_p = 0,097 for RD

4.5 Crack tip opening δ = 18,2 μm (for $\lambda = \pi/4$)

5. ENERGY CONCEPTS AND APPROACHES

Time dedicated to the study of this chapter is approximately 4 hours.

Objective: After studying this chapter, you will know

- Griffith theory of a brittle fracture and possibilities of its application
- The driving force of a crack and resistance to crack propagation
- Density factor of strain energy
- J-integral for crack stability assessment.

Interpretation

5.1. Griffith's Theory

Griffith's theory of a brittle fracture (1920) provides the basis for future energy concepts of initiation or propagation of fractures. It assumes for crack propagation that the decrease in elastic energy in a body depending on a length of a crack is greater than the increase in surface energy of a newly formed crack. For individual forms and items in the energy balance, it can be written (simplified derivation according to **Fig. 5.1**):

W_a – energy of a plate with a crack of length (a)

U_e – decrease in elastic energy by crack growth $\mathbf{U_e} = \frac{\pi a^2 . \sigma^2}{E}$

W_s – surface energy of a crack, $\mathbf{W_s = 4.\gamma.a}$, where γ [Jm^{-2}] is surface energy of material

W_o – energy of a system with no crack (W_o = const.). It is applicable:

$$\mathbf{Wa = Wo + Ws - Ue} \tag{5.1}$$

Crack stability condition: $\frac{dWa}{da} = 0 = 4.\gamma - \frac{2\pi.a.s^2}{E}$, thence after adjustment critical crack length

$$a_c = \frac{2E\gamma}{\pi\sigma^2}, \tag{5.2}$$

for (real) crack length $a < a_k$ an unstable fracture does not occur at the external stress σ.
Similarly, the critical stress can be derived:

$$\sigma_c = \sqrt{\frac{2\gamma.E}{\pi.a}}, \tag{5.3}$$

while a fracture does not arise for the stress $\sigma < \sigma_c$; an unstable fracture occurs immediately for $\sigma \geq \sigma_c$, at the given length of a sharp crack. Stated relations for critical parameters (a_c or

σ_c) and inequalities form **Griffith's criterion** of brittle failure. Its validity was confirmed first on glass, and later on other brittle materials.

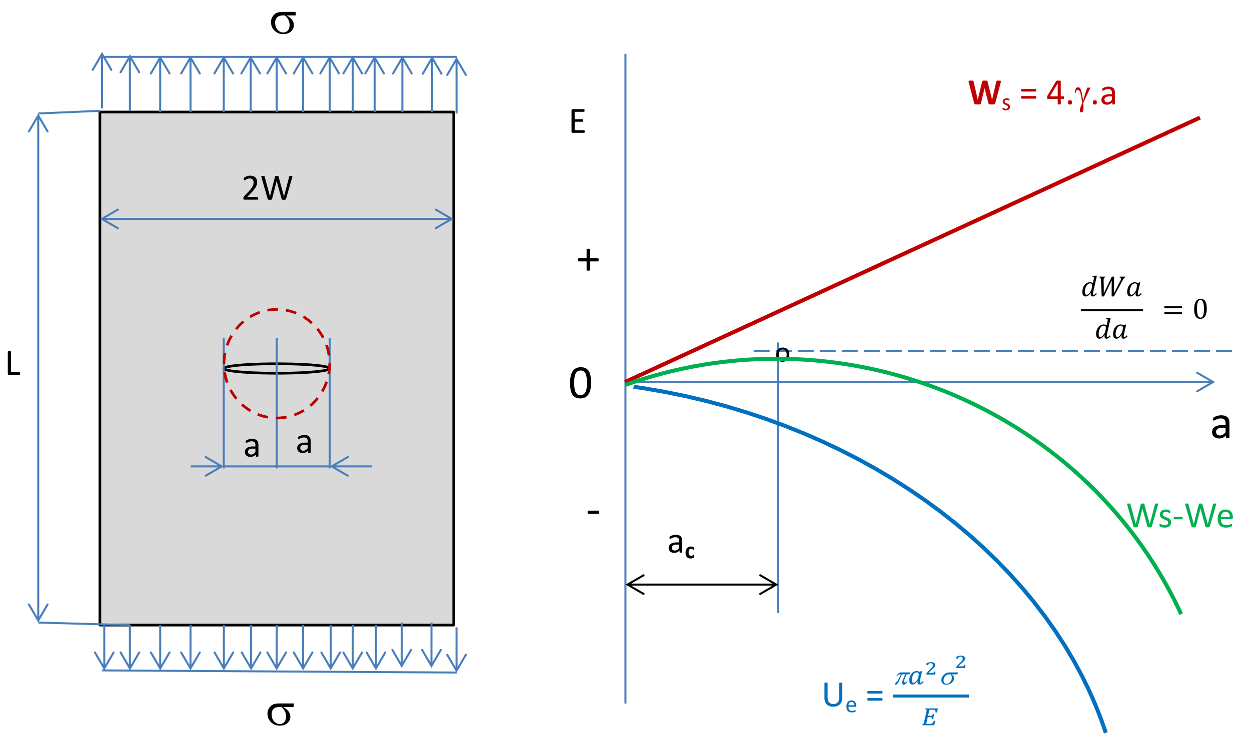

***Fig. 5.1**. We consider a plate of brittle material (e.g. glass) with a central crack of a length of 2a, oriented perpendicularly to the applied tensile stress σ. Prerequisites: a < < W, a < < L, (thickness B = 1): Critical crack length – a_c.*

Surface energy of a fracture of brittle materials ranges between limits of the order of γ = 1-10 [Jm^{-2}], therefore, we talk about low-energy fractures.
For comparison, high-energy ductile fractures have the effective values of surface energy of the order of $\gamma_{ef} = 10^3\text{-}10^4$ [Jm^{-2}].

5.2. The Driving Force of a Crack, Resistance to Crack Propagation

This energy approach extends the original Griffith concept to materials with partial plastic deformation and to so-called quasi-brittle fractures.
By adjustment of the energy concept of the beginning of brittle crack propagation (by Griffith), we get the relation

$$\frac{\pi a \sigma^2}{E} = 2\gamma. \tag{5.4}$$

The left side of this equation has a physical meaning and represents intensity of the release of elastic strain energy per unit of area of a crack surface at very (infinitely) small crack growth. Internationally, it is denoted by the letter G and is also called the **driving force of a crack** (according to the unit J/m = N). The value of G at stable (subcritical) crack propagation increases continuously and at the time, when the crack length reaches the critical value a_k, the value of G reaches the critical value G_c. After this time, crack propagation continues to the detriment of elastic energy that has accumulated in a body in the process of loading and preceding growth of a crack. Such crack propagation is referred to as unstable and is characterized by uncontrollable course that ends with a brittle fracture of a component or a structure.

The right side of equation (5.4) represents material property and expresses resistance to unstable crack propagation, denoted by the letter R. Perhaps it is true R = 2γ and $G = \frac{\pi c \sigma^2}{E}$.

Taking into account the stress intensity factor $K = \sigma\sqrt{\pi c}$, we get the relation between the parameters G and K in the form $G = \frac{\pi c \sigma^2}{E} = \frac{K^2}{E}$, that is valid for plane stress conditions. Similarly, for the state of plane strain and I. type of loading, it applies

$$G_I = \frac{K_I^2}{E}(1-\nu^2). \tag{5.5}$$

Thence it follows, that the G_I and K_I quantities are equivalent in assessing a body with a crack.

The second, **more general approach** to derive G and R: Crack driving force is the rate of release of elastic energy that enters into the process of crack propagation. Driving force of a crack is expressed by the equation

$$\mathbf{G = -\frac{dWc}{da}}, \tag{5.6}$$

where the total mechanical energy $W_c = W_e + W_p$ and then W_e – elastic energy, W_p – potential energy of external forces, $W_p = W_F$ – work of external forces.

For the area of the crack tip, it can be derived $G = \frac{a.\sigma^2}{E} = \frac{\boldsymbol{K_I}^2}{\boldsymbol{E}}$ for RN, $G = \frac{a.\sigma^2}{E}(1-\nu^2) = \frac{\boldsymbol{K_I}^2}{\boldsymbol{E}}(1-\nu^2)$ for RD.

The resistance to crack propagation

$$\mathbf{R} = \frac{\boldsymbol{dW\gamma}}{\boldsymbol{da}} \ (\mathrm{J}/m^2), \tag{5.7}$$

where $\boldsymbol{W_\gamma}$ - energy of a crack (J/m), $\boldsymbol{W_\gamma} = \frac{\boldsymbol{\gamma.S}}{\boldsymbol{B}}$ includes surface energy, also energy for plastic deformation, for a temperature increase, kinetic energy of material. Stability condition for elastic-plastic materials: $\mathbf{G_c = R}$

The resistance to crack propagation $\mathbf{R} = \frac{\boldsymbol{dW\gamma}}{\boldsymbol{da}}$ (J/m^2) is energy needed to create fracture surfaces of unit size, characterizes fracture toughness of material.

$$R = G_{Ic} = \frac{ac.\sigma^2}{E}(1-\nu^2) = \frac{\boldsymbol{K_{Ic}}^2}{\boldsymbol{E}}(1-\nu^2) \text{ for RD, and for RN: } \mathbf{R = G_{Ic}} = \frac{\boldsymbol{ac.\sigma^2}}{\boldsymbol{E}} = \frac{\boldsymbol{K_{Ic}}^2}{\boldsymbol{E}}. \tag{5.8}$$

R-curves represent dependences of the resistance R to the crack length (a) or the increment (Δa), i.e. R = f(Δa).

Appropriate graphical representation of some of the aforementioned relations $(G = \frac{a.\sigma^2}{E})$. Diagram of the subcritical growth of an initial crack (of a length a_i) to a critical size (a_c) is shown in **Figure 5.2**.

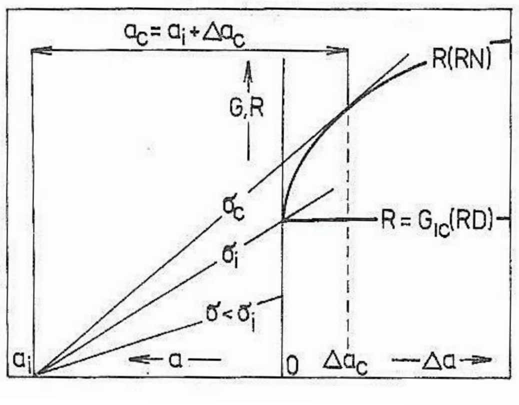

Fig. 5.2. Comparison of R-curves and critical crack lengths for RN and RD. Easier crack propagation in the state of plane strain (RD) compared to plane stress (RN).

Possibilities of crack propagation with respect to the values of G and R are shown in **Figure 5.3**.

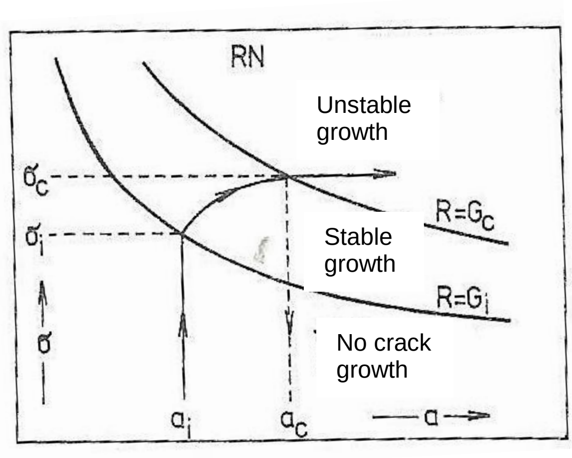

***Fig. 5.3**. Dependence of crack length a on stress σ in the state of RN, individual stages of crack propagation: a) $G < G_i$ – a crack does not propagate, b) $G_i \leq G < G_c$, a crack propagates stably (subcritically), c) $G \geq G_c$ a crack propagates unstably.*

Considerations on density distribution of elastic strain energy at the crack tip led to the creation of S-factor of elastic energy density, which can be used to predict direction of unstable crack propagation.

For materials and components with a larger size of plastic deformation under load, resistance to the initiation of stable and unstable fracture can be characterized using so-called J-integral, which is well-founded and used in the context of non-linear (elastic-plastic) fracture mechanics.

5.3. Density Factor of Strain Energy

Unlike previous parameters of linear elastic FM, this parameter allows to predict direction of crack propagation, is useful for assessing the effect of crack orientation on values of the stress intensity factor and to assess the effect of combined types of load.

According to Sih's theory, a **density factor of strain energy** is defined by the relation **S = r** $\boldsymbol{\frac{dU}{dV}}$, where $\frac{dU}{dV}$ is strain energy density. $w_e = \frac{dU}{dV} = \sum_{ij}^{3} \frac{\sigma ij \varepsilon ij}{2}$. In deriving, 3D Hooke's law was used $\varepsilon_{ij} = f(\sigma_{ij}, G, \nu)$ and the relations $\sigma_{ij} = \sigma_{ijI} + \sigma_{ijII} + \sigma_{ijIII}$ (the superposition of stress components), while generally $\sigma_{ij,k} = K_k \frac{f_{ijk}(\theta)}{\sqrt{2\pi r}}$, (i, j = x, y, z; k = I, II, III).
Following relations has been derived within FM for the S-factor:

$$\mathbf{S} = \boldsymbol{a_{11} K_I{}^2 + 2 a_{12} K_I K_{II} + a_{22} K_{II}{}^2 + a_{33} K_{III}{}^2} \;, \tag{5.9}$$

where the coefficients a_{ij} =f(G,ν,θ) are presented in **Table 5.1**.

When applying Sih's **S-factor, two hypotheses** are applied:

Hypothesis 1 – crack propagation occurs in direction θo, where **min. S = S(**$\boldsymbol{\theta_o}$**)**, hence

$$\frac{\delta S}{\delta \theta} = 0 \quad \text{and} \quad \frac{\delta^2 S}{\delta \theta_2} > 0, \tag{5.9a}$$

Hypothesis 2 – an unstable propagation occurs when the S reaches a critical value S_c, i.e.

$$\mathbf{S}(\boldsymbol{\theta_o}) = \boldsymbol{S_c}. \tag{5.9b}$$

Table 5.1. The coefficients for expressing S-factor.

$a_{11} = \frac{1}{16\pi G}\left[(3-4\nu-\cos\theta)\cdot(1+\cos\theta)\right]$	pro stav RD
$a_{11} = \frac{1}{16\pi G}\left[\left(\frac{3-\nu}{1+\nu}-\cos\theta\right)\cdot(1+\cos\theta)\right]$	pro stav RN
$a_{12} = \frac{1}{8\pi G}\sin\theta\cdot\left[\cos\theta-(1-2\nu)\right]$	pro stav RD
$a_{12} = \frac{1}{8\pi G}\sin\theta\cdot\left[\cos\theta-\frac{1-\nu}{1+\nu}\right]$	pro stav RN
$a_{22} = \frac{1}{16\pi G}\left[4(1-\nu)\cdot(1-\cos\theta)+(1+\cos\theta)\cdot(3\cos\theta-1)\right]$	pro stav RD
$a_{22} = \frac{1}{16\pi G}\left[\frac{4}{1+\nu}(1-\cos\theta)+(1+\cos\theta)\cdot(3\cos\theta-1)\right]$	pro stav RN
$a_{33} = \frac{1}{4\pi G}.$	

Simple Examples of the Application of S-Factor

1) **For the tensile mode I** , $K_I = \sigma\sqrt{\pi a}$, $K_{II} = K_{III} = 0$, that means there remains only $S = a_{11}K_I^2$ and after calculation $S_{min} = S(0) = a\sigma^2 \frac{1-2\nu}{4G}$, $\theta = 0°$, which proofs that a crack will propagate perpendicularly to tensile principal stress and for the critical parameters we get $\boldsymbol{S_c = \frac{1-2\nu}{4\pi G} K_{Ic}^2}$.

2) **The shear mode II**, $K_{II} = \tau\sqrt{\pi a}$, $K_I = K_{III} = 0$, $S = a_{22}K_{II}^2$, $S_{min} = S(\theta_0) = a\tau^2 \frac{2(1-\nu)-\nu^2}{12G}$, $\boldsymbol{S_c = \frac{2(1-\nu)-\nu^2}{12\pi G} K_{IIc}^2}$. Here the propagation direction θ_o is dependent on Poisson's ratio ν, **Fig. 5.4**

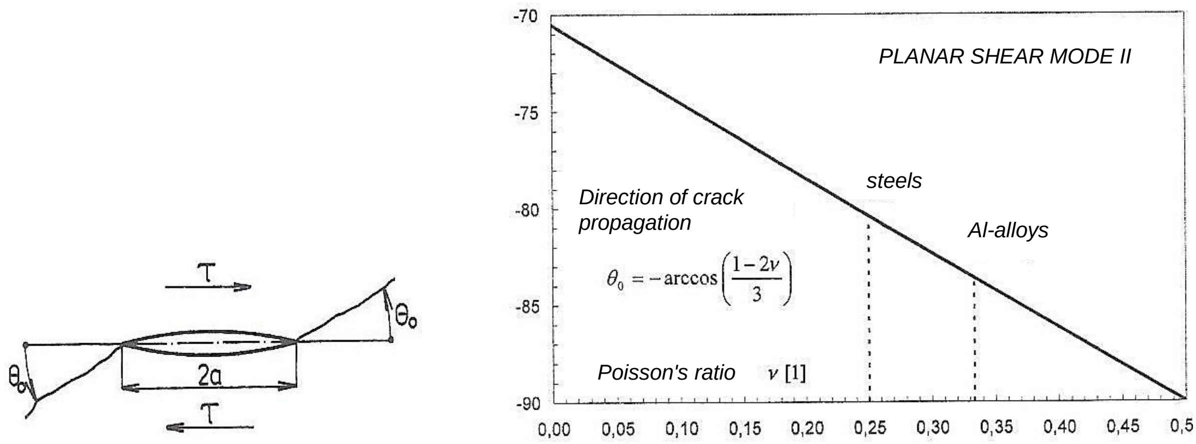

Fig. 5.4. *General plotting of direction of propagation after the loss of crack stability in the case of the mode II. Dependence of direction of crack propagation θ_o on Poisson's ratio ν*

3) Biaxial Stress, Mixed Mode I + II,

We consider a body with an internal crack length 2a (whose dimensions are very small relative to the size of the plate) loaded by biaxial load σ_1 and $\sigma_2 = k.\sigma_1$, where k is a real number. The axis of a crack forms an angle β with the direction of applied stress σ_1, **Fig. 5.5.**

Using Mohr's circle and the superposition principle, tensile stress acting perpendicularly to the crack (in the y-direction) and the shear stress acting in the x-direction can be derived and these stresses cause corresponding stress intensity factors K_I and K_{II} for the tensile and shear mode. Results are presented next to **Figure 5.5**.

Relations for K_I and K_{II} may be substituted into S-factor and after lengthy mathematical adjustments it is possible to identify trends of θ_0, in which cracks will propagate.

Graphical functional dependences $\theta_o = f(\beta,\nu)$, $S = f(\beta,\nu)$, $\sigma_c = f(\beta,\nu)$ are then clearly arranged, simplified for k = 0.

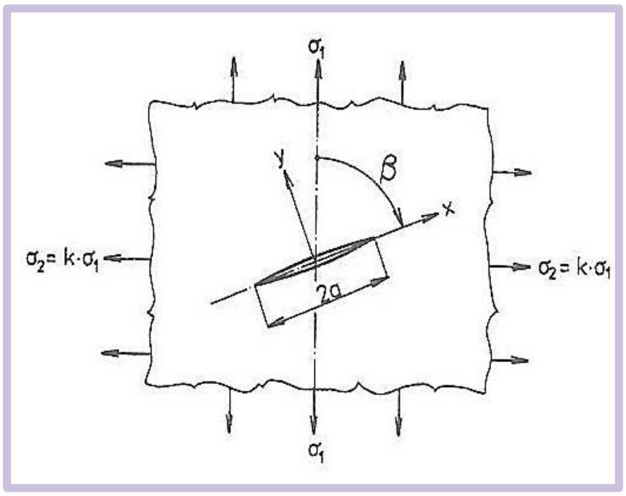

$$\sigma_I = \sigma_{I1} + \sigma_{I2} = \sigma_1\left(\sin^2\beta + k\cos^2\beta\right)$$

$$\tau_{II} = \tau_{II1} + \tau_{II2} = \sigma_1(1-k)\sin\beta\cos\beta\,,$$

$$K_I = K_{I1} + K_{I2} = \sigma_1\sqrt{\pi a}\left(\sin^2\beta + k\cos^2\beta\right)$$

$$K_{II} = K_{II1} + K_{II2} = \sigma_1\sqrt{\pi a}(1-k)\sin\beta\cos\beta$$

$$K_{III} = K_{III1} + K_{III2} = 0\,.$$

Fig. 5.5. *A plate with a crack loaded by biaxial stress in mixed mode*

For k = 0 (σ_2 = 0) we get dependences of the intensity factors K_I and K_{II} on the angle β.

5.4. J –Integral

The **total energy balance** of a disrupted body at given external stress is an objective basis for assessing stability of a crack. Griffith's criterion, which was originally derived for perfectly brittle materials, i.e. linear elastic state of stress in the vicinity of a crack tip, is the basic criterion for crack stability, based on energy considerations. This criterion was gradually extended to real structural materials at which the local plastic deformation occurs in the vicinity of a crack tip, i.e. formation of a plastic zone of a small size. In these cases, crack driving force G, whose calculation was based on the elastic solution of stress state in the vicinity of a crack, is a parameter characterizing stability of a crack.

However, if **plastic deformation of a larger size** emerges in a deformed body, criteria of crack stability described by the driving force G cannot be used, because this plastic deformation significantly affects the stress-strain field in the vicinity of a crack. The outlined problem was removed to some extent by introducing a new fracture parameter, called J-integral (Rice’s integral). This **J-integral** is a generalization of the crack driving force G and can also be used in cases of plastic deformation of greater extent.

J-integral is a **line integral** which expresses integration of the strain energy density for a body with a crack, within the closed path (curve) from one surface of a crack to the other around the crack tip (Fig. 5.6) and is defined as

$$J = \int_\Gamma \left(\mathrm{w}dy - T_i\frac{\partial u_i}{\partial x}ds \right), \qquad (5.10)$$

where Γ - any closed curve,

w - bulk density of strain energy, w = $\frac{W}{V} = \int_0^{\varepsilon m} \sigma_{ij}\,d\varepsilon_{ij}$, T - stress vector T = (T_x,T_y,T_z), it is vector of forces on the integration path, the force acting in a direction of a normal to the curve

ū - displacement vector, ū = (u,v,w) or ū = (u_1,u_2,u_3)

ds - element of the curve with the normal n

B = 1 (applicable to the unit thickness of a body).

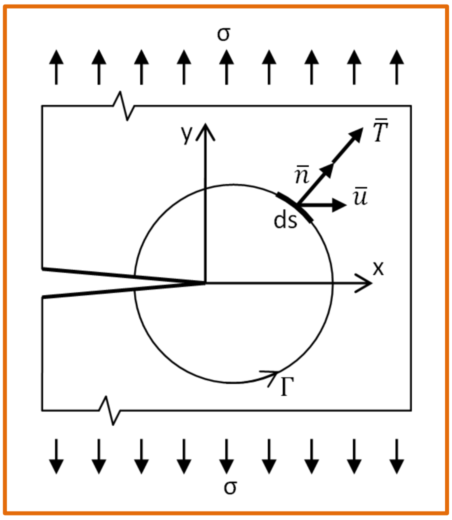

Fig. 5.6*. Identification of parameters for determining the J-integral*

When the integration path Γ is placed into the crack tip, it means that it aligns with the arc of curvature of the crack tip, then T = 0, since on free areas there cannot be normal stresses. Then, the value of J-integral represents the change (decrease) in potential energy dW_{el} at crack growth by the value *dc*, hence J = $\frac{dW_{el}}{dc}$. From this it also follows that at the condition of linear elastic deformation, it is possible to write J = G. J-integral has the unit J/m^2, resp. kJ/m^2.

For materials that are deformed by the linear or non-linear patterns of deformation it was theoretically proved that the value of J-integral does not depend on the integration path. This also means that for different integration paths, the difference will be $J_1 - J_2 = 0$, resp. $J_1 = J_2$.

The value of J-integral for a given body may be determined by calculation or experimentally. In real materials with elastic-plastic deformation, the determination of J-integral value is more complex. If the integration path is chosen close to the crack tip so as to pass both the elastic and the plastic region, then the value of J represents average properties of a deformation field in the vicinity of the crack tip.

The critical value of J-integral, at which unstable crack propagation begins, is determined experimentally and used as a fracture criterion of resistance to brittle failure

For the area of linear elastic FM, it holds (for the state of plane strain)

$$J_{Ic} = G_{Ic} = \frac{K_{Ic}^2\,(1-\nu^2)}{E}. \tag{5.11}$$

Experiments have shown that under certain boundary conditions (for a sample loaded in three-point bending), critical value of J-integral may be determined from the diagram of force F - displacement of force f (Fig. 3.16) according to the relation:

$$J_{Ic} = \frac{2}{B(W-a)} \int_0^{f_c} F dv = \frac{2A_c}{B(W-a)} \tag{5.12}$$

where B is sample thickness, W - sample width, f_c – critical value of displacement f, at which unstable crack propagation occurred, a – crack length, A – area under the curve, respectively work of force F along the path f.

In practical tests, there may arise three possibilities of failure of a test body, **Figure 5.7.**

a) Failure arises by a sudden fast fracture at force F_c. The value of J-integral is proportional to the area under the F-f curve.
b) Sudden failure occurs after previous slow growth by the value of Δa (which can be found on a fracture surface). The value of J is represented by the area under the F-f curve up to point C, where rapid crack propagation began.
c) Failure occurs after previous macroscopic deformation, resulting in a decrease in a force. To calculate the value of J, the area A_m under the F-f curve to its maximum point is considered.

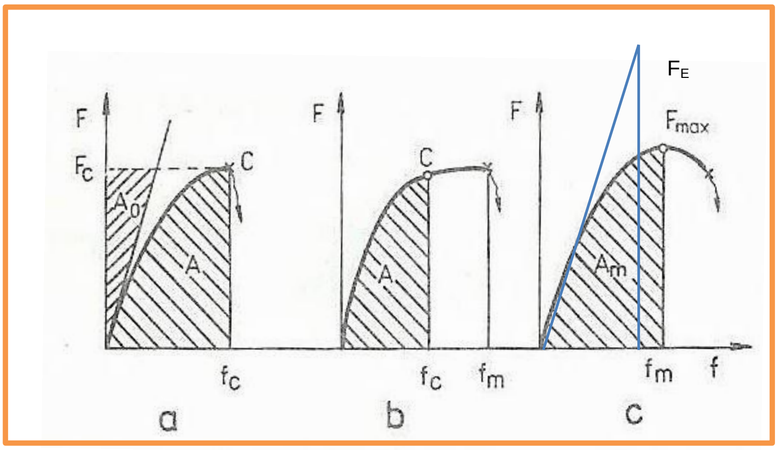

Fig. 5.7. *Characteristic dependences of F-f during testing J_{Ic}: a – failure by a sudden fracture, b – failure preceded by slow (subcritical) crack growth from the point C, c – failure preceded by macroscopic deformation*

For a more accurate determination of the critical value of J_{Ic}, it is recommended to divide the total area (energy) under the curve to the elastic (A_{el}) and plastic (A_{pl}) part, by **Figure 5.8,** i.e. $A_c = A_{el} + A_{pl}$.

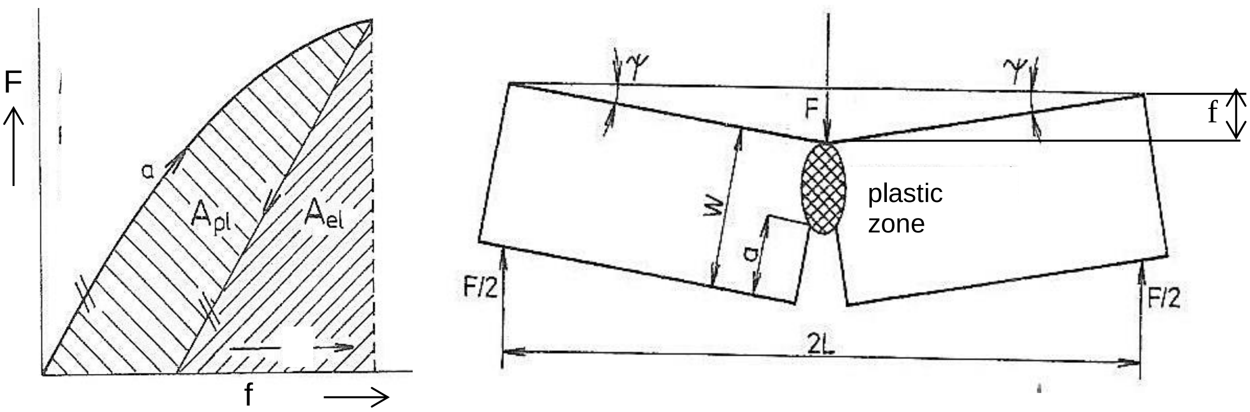

***Fig. 5.8**. Scheme of force F – bending f at biparametric expression of J-integral. Division of J-integral to the elastic and plastic component. A cracked body loaded by three-point bending, remaining load-bearing cross-section is plasticized.*

The value of fracture toughness J_{Ic} for load in three-point bending is then given by the relation

$$\mathbf{J_{Ic} = J_{ce} + J_{cp}} = \frac{K_c^2\,(1-\nu^2)}{E} + \frac{2A_{pl}}{B(W-a)}, \tag{5.13}$$

while $K_c = \frac{Fc.Y}{B\sqrt{W}}$, where Y is a shape factor (the shape function for calculating K_I).

J-integral method enables to determine the elastic-plastic value of fracture toughness J_{Ic} under test conditions in which values of K_{Ic} would not meet the conditions of validity (smaller thickness of test samples higher test temperatures, lower values of yield strength).

J-integral is a generalization of a crack driving force, enabling application also in cases of plastic deformation of greater extent. J-integral is defined just as a driving force for a crack, only that it is not limited to a linear elastic material:

$$\mathbf{J} = \frac{d(A-U)}{da} \tag{5.14}$$

A – work of external forces acting on a body, U – strain energy of a body.
J-integral is defined as a line integral independent of the integration path.

Comparison of the extent of validity of the main fracture mechanics parameters, depending on temperature and a size of plastic deformation (proportional to crack tip opening and a size of the plastic zone), is clearly shown in **Figure 5.9.**

Note: The parameter K_E (according to the method of equivalent energy) was used for bodies with the occurrence of plastic deformation. The area under the force F – displacement f curve (e.g. Fig. 5.7 c) was converted to the area of a right triangle with the same area as the measured hatched area, while one side of the triangle passed through the linear part of the record. So-called equivalent critical value K_E was then calculated by means of the force F_E, proportional to the height of the triangle, as fracture toughness.

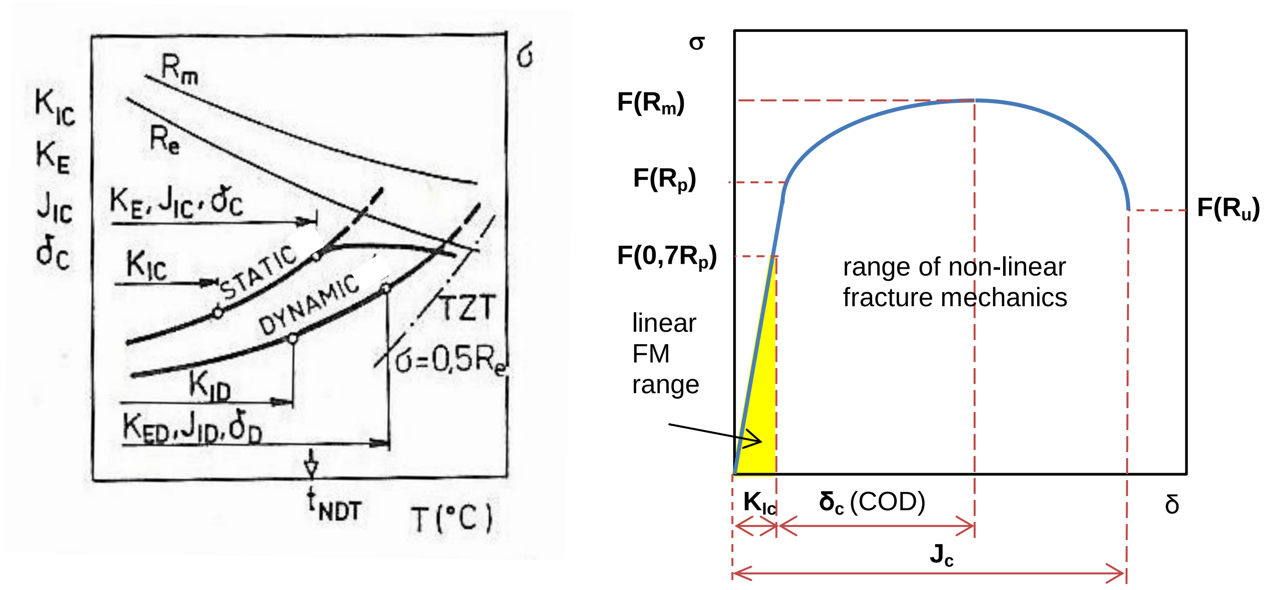

Fig. 5.9. *Validity range of fracture mechanics criteria based on temperature and strain rate. Graph of dependence between tensile stress and crack tip opening with schematic representation of the field of linear elastic and non-linear fracture mechanics (K_{Ic} – fracture toughness, δ_c – critical crack opening, J_c – critical value of J-integral).*

Summary of Terms

Reading this chapter, you learned the following terms:

- **Energy balance, surface energy, Griffith's criterion, critical stress, a critical crack length, effective surface energy.**
- **A driving force of a crack G_I, elastic energy release rate (G_I), resistance to crack propagation, R-curves, critical values of G_{Ic},**
- **A strain energy density factor (S-factor), hypotheses for S-factor.**
- **J-integral, definition, force-displacement dependences, conditions for validity of FM parameters**

Questions to Chapter 5

5.1. What can we calculate by means of Griffith's relation?
5.2. How can we characterize surface energy of a fracture?
5.3. How can we define driving forces of a crack?
5.4. What does resistance to crack propagation R mean?
5.5. What does the critical value of the crack driving force represent?
5.6. What tasks does S-factor of elastic energy density enable to solve?
5.7. What hypotheses are related to S-factor?
5.8. What is the definition of J-integral?

5.9. For which regions of deformation can J- integral be used?
5.10. What are the possibilities of determining the critical value of J-integral?

Exercises to the Chapter

5.1. A relatively large pane of glass is subjected to tensile stress of 40 MPa. Surface energy of the glass is 0,3 J/m^2 and the modulus of elasticity E = 69 GPa. Determine the length of a surface defect (oriented perpendicularly to stress), that would cause a fracture.

Solution: For solving, it is possible to use Griffith's relation for calculation of the critical stress $\sigma_{\mathbf{k}} = \sqrt{\frac{\mathbf{2}\gamma.\boldsymbol{E}}{\pi.a}}$.

After adjustment for the critical crack length at the given stress σ, we get relation $a_{\mathbf{k}} = \frac{\mathbf{2}\boldsymbol{E}\gamma}{\pi\sigma^2} =$

$$= \frac{2.(69 \times 10^9\ \mathrm{N/m^2})(0{,}3\mathrm{N/m})}{\pi(40 \times 10^6\ \mathrm{N/m^2})^2} = 8{,}2 \times 10^{-6}\ \mathrm{m} = 0{,}0082\ \mathrm{mm} = \underline{8{,}2\ \mu\mathrm{m}}$$

Note: Numerical calculation should be also done with correct units.

5.2. A ceramic part must not crack at stress of 13,5 MPa. Determine the maximum allowable length of a surface crack, if the surface energy of MgO is 1,0 J /m^2.

5.3. Calculate the critical crack length in a toughened plastic, in which the crack driving force G_c = 2,5 kJ/m^2 and the modulus of elasticity E = 2,0 GPa was detected. The plate is loaded with tensile stress of 70 MPa, perpendicular to the plane of a crack.

5.4. Explain under what circumstances the toughness of metallic material a) increases b) decreases with increasing thickness t of plates with notches.

Solution: At very thin metal sheets $t < t_o$, where it is thickness for which toughness is maximum, fracture failure occurs by shear and $G_c = G_c(45°) \approx \sigma_{y.}\varepsilon_{f.}t$, and thus toughness with increasing thickness also increases. If $t > t_o$, fracture failure is a combination of a shear fracture and a fracture under conditions of plane strain. The driving force of the crack is then $G_c = SG_{Ic} + (1{+}S)G_c(45°)$, where 1-S is the proportion of a shear fracture on a fracture surface and toughness decreases with increasing sheet thickness (see Fig. 3.4).

5.5. Calculate the stress by which glass can be loaded if it contains a defect of a size of 2a = 30 μm. The modulus of elasticity of the glass is 70 GPa and the driving force of a crack G_c = 10 J/m^2.

Answers to the Questions

5.1 The critical stress magnitude (strength of a brittle material), which contains a crack. Or similarly calculate the critical crack length for given tensile stress.

5.2 Surface energy of a fracture – energy spent on creating a unit area of a fracture, consumed on a fracture γ [Jm^{-2}]. It includes material's own surface energy (γ_o) and surface energy (γ_p) in case of plastic deformation

5.3 A driving force of a crack (G) is the intensity of elastic strain energy release per unit area of the fracture surface at very small extension of the crack length.

5.4 The resistance to crack propagation $R = dW\gamma/da$ (J/m^2) is the energy needed to create a fracture surface of a unit size, it characterizes fracture toughness (R= $G_{Ic} = \frac{K_{Ic}{}^2}{E^{\check{}}}$)

5.5 A critical value of a driving force of a crack (G_{Ic}, G_c) represents the condition for crack instability, it is used to express fracture toughness of material.

5.6 S-factor is used for calculation, prediction of the direction of crack propagation, especially when combined loading, depending on the orientation of a crack (the angle between the crack and direction of loading).

5.7 First hypothesis: the crack will propagate in the direction θ_o, where the value is minimum S = S(θ_o).

Second hypothesis: unstable propagation will occur at the critical value S_c, i.e. S(θ_o) = S_c

5.8 Mathematically, using the line integral whose value is independent of the integration path (relation 5.10). Physically defined just as a crack driving force, while it is not limited to linear elastic material and smaller plastic zones: J = d(A-U)/da (relation 5.14).

5.9 J-integral is a generalization of a crack driving force and enables using also in cases of plastic deformations of a larger size. It is used for initiation (J_i), stable crack propagation (J(Δa)), an unstable fracture (J_c).

5.10 By calculation usually in simple symmetrical configurations of bodies within the linear FM and using the relation between J_I and K_I. Experimentally on bodies, through measurements of the force F- displacement f (δ) dependence to the critical size at a fracture and by determination of the spent work or energy proportional to the corresponding area under the measured F= f(δ)dependence (Fig. 5.8, relation 5.13, or 5.14).

Results of the Exercises

5.1. Length a_k = 8,2 μm
5.2. [a_{max} = 78,6 μm]
5.3. [0,325 mm]
5.5. [$\sigma_{max} = \sigma_f$ = 122 MPa]

6. INITIATION AND GROWTH OF MICROCRACKS

Time dedicated to the study of this chapter is approximately 1,5 hour.

In terms of a content and logically, this chapter could be included sooner prior to the chapter on unstable crack growth and fracture toughness. With regard to the historical development of research methods of material in microscopic volumes including the use of scanning electron microscopy, it is possible to include this chapter on micromechanisms of failure after the chapters on macroscopic approach to material failure.

Objective: After reading this chapter, you will be able to

Identify ductile and brittle failure at the microscopic level, the basic mechanisms.
Describe cleavage transcrystalline failure of material, intercrystalline brittle failure.
Characterize conditions for ductile microcavity failure of metallic material.
Distinguish low-energy and high-energy fractures according to fractographic observations.

Interpretation

6.1. Brittle Cleavage

In metallic materials with a body centred cubic lattice (Fe_{α}, Cr, Mo, W), transcrystalline cleavage occurs at low strain rates up to temperatures of about (0,1-0,15).T_m (melting temperature in K) and propagates along the cleavage planes of type of {100}. Cleavage was not observed in metals with a body centred cubic lattice (but Ir). Metals with a hexagonal lattice (Zn, Cd, Zr, Co, Ti_{α}) fail in a transcrystalline way in the (0001) plains up to temperatures of (0,1-0,2).T_m. Schematic comparison of fractures at various temperatures is shown in **Figure 6.1**.

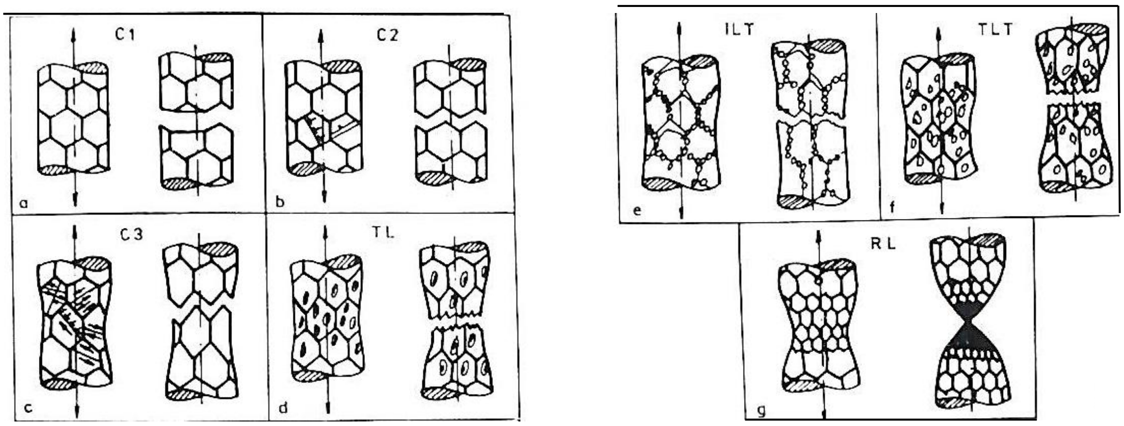

***Fig. 6.1**. Diagram of material failures and fractures in different stress-temperature conditions Brittle fractures (a, b, c), a ductile fracture (d), fractures at creep (e, f) and with recrystallization (g)*

In metal materials, initiation of microcracks can be explained through accumulation of dislocations, see dislocation models in **Fig 6.2**. Their further growth in brittle material is conditioned by occurrence of local tensile stresses, respectively by achieving a critical size of microcracks according to the energy balance (see below).

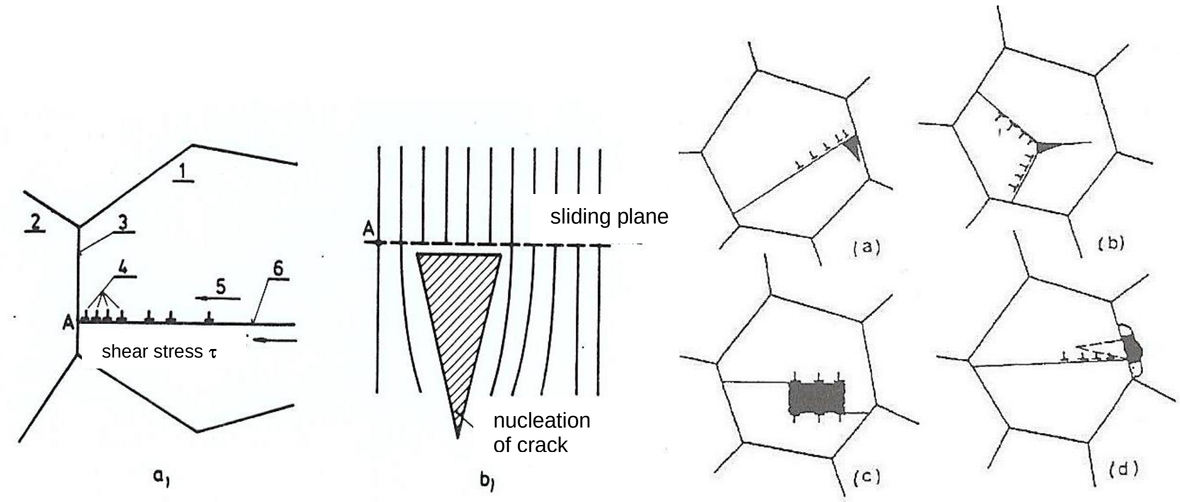

Fig. 6.2. *Micromechanisms of microcracks initiation by accumulation of edge dislocations: 1,2 - differently oriented grains, 3 – grain boundaries, 4 – accumulation of dislocations before a grain boundary, 5 – direction of dislocation motion, 6 – slip plane. Other possibilities of microcrack initiation by interaction of dislocation lines (case (c) characterizes rather formation of a microcavity)*

According to Cottrell's model (6.2b), nucleation of a cleavage crack occurs in metals with a body centred cubic lattice when accumulated dislocations (b = a/2[111] on slip planes (101)) when stress

$$\sigma_f = \frac{2G\gamma_{ef}}{k_y\sqrt{d}}, \tag{6.1}$$

where d is a grain size and γ_{ef} – effective surface energy, k_y- a constant in the Hall-Petch equation for shear stress ($\tau_y = \tau_o + k_y\sqrt{d}$).

Local cleavage strength in case of spherical particles (carbides, inclusions) of a diameter of 2r, that block dislocations, is given by the relation

$$\sigma_f = \sqrt{\frac{\pi\, E.\gamma_{ef}}{2(1-\nu^2)r}} \tag{6.2}$$

These relations (and similar others) imply that local cleavage strength decreases with an increasing size of structural components, mainly grains and particles. The decrease in σ_f may also occur due to segregation of surface active components along grain boundaries and decrease in the value of γ_{ef}.

In case of brittle material, cleavage failure usually occurs due to disruption of interatomic bonds, **Fig. 6.3a**. An initiated cleavage microcrack begins to propagate unstably by energy balance (by Griffith's criterion).

6.2. Ductile Fracture

Initiation of microcavities, their growth and **coalescence** (interconnecting, merging) occur in material with the possibility of plastic deformation. That consumes considerable amount of energy, a high-energy fracture is usually formed. For the critical value of plastic deformation during nucleation of a cavity to a particle of a radius ***r***, the following relation can be derived

$$\varepsilon_n = \sqrt{\frac{4\gamma_s}{E' r}}, \qquad (6.3)$$

where γ_s is surface energy of **decohesion** of a matrix and a particle, E′ is the modulus of elasticity of a particle.

Coalescence (i.e. mutual merging) of cavities occurs at the moment when a size of a cavity during loading reaches the inter-particle distance l_p. At the same time, fracture deformation can be calculated

$$\varepsilon_f = \frac{\ln\left(\frac{l_p}{2r}\right)}{0{,}28.\exp\left(\frac{1{,}5\sigma_m}{\sigma_{ef}}\right)}, \qquad (6.4)$$

where mean stress $\sigma_m = \sigma_1 + \sigma_2 + \sigma_3$, σ_{ef} - effective stress (for plastic deformation initiation according to the von Mises yield criterion)

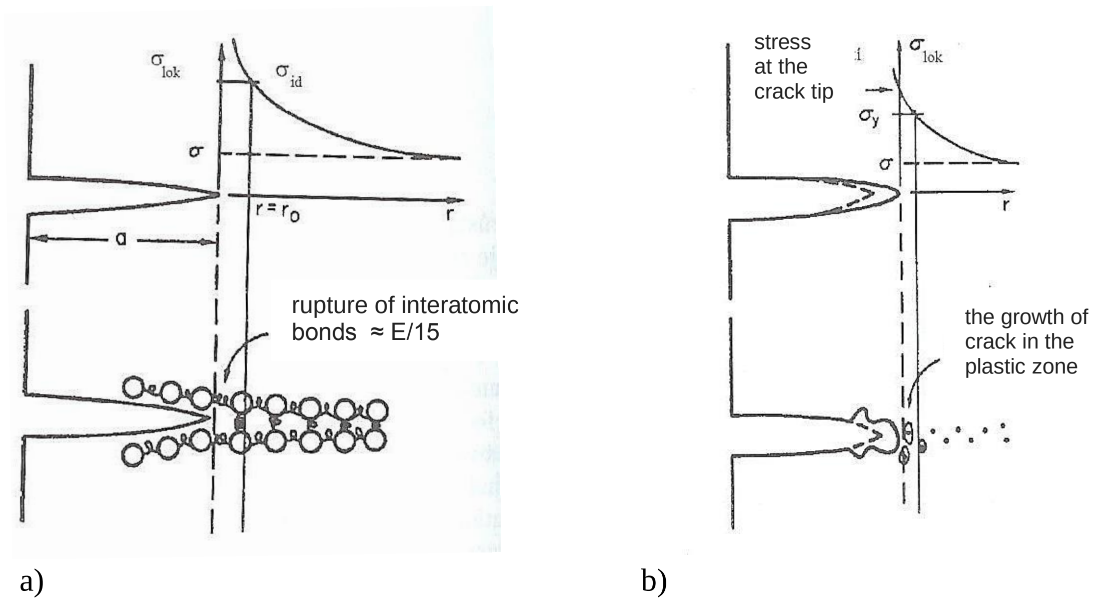

Fig. 6.3. *Crack growth by cleavage mechanism disruption of bonds between atoms in excess of mechanism, initiation and merging of the theoretical strength at a crack tip (a).*
Crack initiation and growth by ductile microscopic dimples (microcavities) before a crack tip in a process zone (b).

In front of main crack, there is a process zone where microscopic cracks or cavities are initiated and merged. **A process zone** is located inside a plastic zone.
Further development of a crack is dependent on the possibility of plastic deformation and the occurrence of a plastic zone.

Brittle transcrystalline cleavage failure and intercrystalline brittle failure are compared in **Fig. 6.4**. On cleavage transcrystalline facets that follow the cleavage planes {100}, there are small kinks which result from the intersection of a crack tip with screw dislocations. Between facets which reflect the size of grains, under certain conditions, there could be created small plastic bridging. On some facets, there can also be found areas of initiation of local microcracks. Due to low energy consumption on the formation and propagation of these fractures (in order of $10\text{-}10^2$ J/m^2), we talk about low-energy fractures.

Secondary microcracks between grains may arise at an intercrystalline brittle fracture, when cracks propagate along weakened grain boundaries, **Fig. 6.4 b**. Various impurities, inclusions, precipitates and other particles can also be observed with a scanning electron microscope on fracture surfaces.

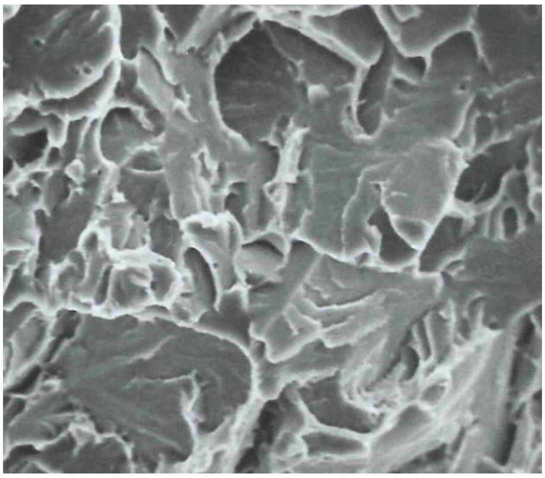
a)

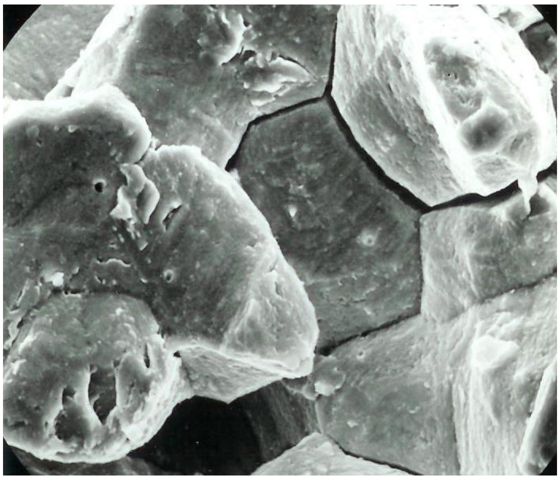
b)

Fig. 6.4*. Typical transcrystalline (a) and intercrystalline (b) brittle failure (magn. 1000x)*

Transcrystalline failure occurs in metals with a body centred cubic lattice at lower temperatures (below the transition temperature) or at high strain rates, when motion of dislocations and possibilities of creating a plastic zone are limited.

An example of microcavity material failure is documented in **Figure 6.5a**. In many cavities, there can be observed smaller particles. Intergranular facets slightly show themselves in some places of the fracture surface. Generally speaking, the smaller microscopic cavities, the less energy consumed for their formation and therefore the surface energy is smaller.
In **Fig. 6.5** there is documented the local area with a mixed fracture (ductile cavity approx. 70%, and brittle areas, above intercrystalline, right in the middle transcrystalline).

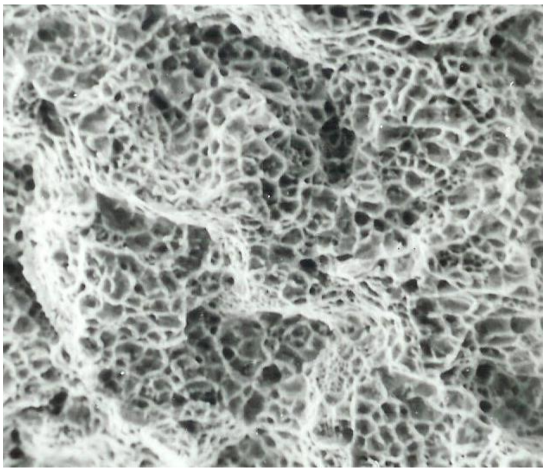
a)

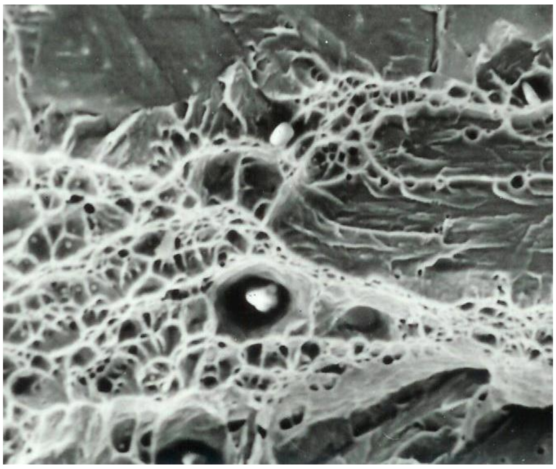
b)

Fig. 6.5. *Area of cavity ductile failure of steel REM, magn. 800x (a). Detail of a fracture surface with multiple mechanisms of failure (locally mixed fracture), 1000 x.*

Σ Summary of Terms

After reading this chapter, you should understand these terms:
Mechanisms of failure of metallic materials, Cleavage transcrystalline failure, dislocation models of microcrack initiation. Decohesion. Cavity transcrystalline or intercrystalline failure. Initiation, growth, merging of microscopic cavities. Low-energy and high-energy fractures, fractographic observation and assessment, analyses of failure.

? Questions to Chapter 6

6.1 Under what conditions do transcrystalline brittle fractures arise?
6.2 How do transcrystalline cleavage cracks and fractures propagate?
6.3 When does a brittle intercrystalline fracture form and propagate?
6.4 What are conditions for development of transcrystalline ductile failure?
6.5 When can intercrystalline ductile cavity failure arise?
6.6 How do micromechanisms of failure relate to energy consumption on crack propagation?
6.7 How can dislocations participate in initiation of a brittle fracture?
6.8 How does the size of a grain affect the local cleavage strength?
6.9 What effect does the particle size have on a value of plastic deformation for the initiation of cavities?
6.10 You shall evaluate a fracture surface of metal that was disrupted by coalescence of microcavities, and a vitreous polymer that showed the cleavage type of morphology. In terms of your knowledge of these fracture mechanisms, how would the mentioned fracture surfaces look like?

Exercises to the Chapter

6.1. What is the value of local cleavage strength of ferritic steel with the grain size of 30 μm, if surface energy for microcrack creation is 14 J/m^2 and the shear constant in the Hall-Petch equation k_y = 0,3 MPam$^{-3/2}$. The modulus of elasticity in shear G = 85 GPa.

6.2. Calculate the critical thickness (c) of a carbidic film at grain boundaries of non-eutectic steel, which leads to initiation of a microcrack, if the stress, by which steel is loaded, is 1000 MPa. Surface energy of the steel is 14 J/m^2 and modulus of elasticity 2,1 . 10^5 MPa.

6.3. Calculate local fracture deformation in ductile failure of hardened and tempered carbon steel in whose structure carbidic particles of a spherical shape are released, in area before a blunted and tensile-stressed crack where the stress state σ_m/σ_{ef} = 1,5. Average distance between carbides is 6,0 μm and their average size is 1,2 μm.

6.4. Calculate the deformation necessary for nucleation of a cavity on an inclusion of a spherical shape in steel with ferritic pearlitic structure, if surface energy of decohesion of the inclusion and matrix is 6,0 J/m^2, the modulus of elasticity of the inclusion is 270 GPa and its diameter 2r = 10 μm.

6.5. In the picture of a fracture surface detail, name micromechanisms of material failure, determine roughly the sizes of the structural components of the material (grains, particles) or the dimensions of fractographic features (facets, cavities). A scanning electron microscope. Magnification 1000x.

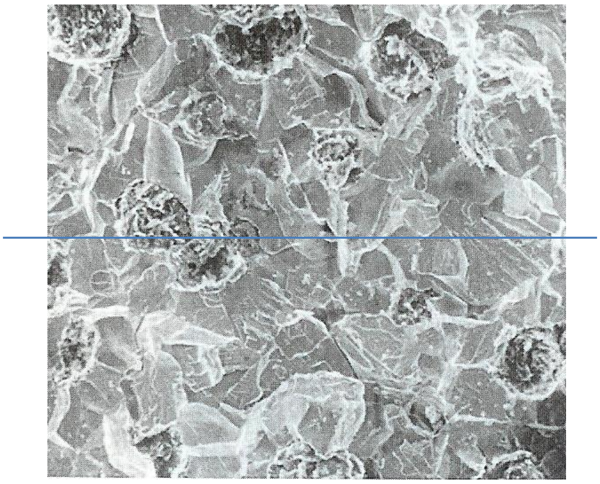

6.6. Draw schematically micro-mechanisms of failure shown in the photograph of Exercise 6.5. Draw schematically a fracture line (in the middle of the image, horizontal section).

6.7. Show that the intersection of a cleavage crack with a screw dislocation forms a kink (step) on a fracture surface and that no kink will be formed in the interaction of this crack with an edge dislocation.

Answers to the Questions

6.1 At relatively low temperatures up to 0,1- 0,2 T_m [K] in metals with a bcc and hcp lattice, at high strain rates, this area extends.

6.2 Propagation of transcrystalline cracks is usually along cleavage planes (min $\gamma(100)$) at high stress concentration, almost without plastic deformation.

6.3 Brittle intercrystalline fractures occur mainly when weakened grain boundaries (segregation of detrimental elements, elimination of brittle phases).

6.4 This failure occurs in the matrix with the ability of plastic deformation, with presence of particles.

6.5 Intercrystalline cavity failure occurs when on grain boundaries there are excluded particles and the surrounding matrix is capable of plastic deformation.

6.6 Transcrystalline cleavage and intercrystalline separation (cleavage) ranks among low-energy fractures. Cavity tough failure is usually high-energy. For very small shallow intercrystalline microscopic cavities, a fracture may be low-energy.

6.7 Accumulation of a number of dislocations before an obstacle causes local stress concentration (accumulation of elastic energy) and formation of a microcrack, see Figure 6.2

6.8 According to Cottrell's model, local cleavage strength increases at grain refinement.

6.9 On larger particles, nucleation of a cavity arises more easily, with smaller deformation, relation (6.3)

6.10 Scheme of coalescence of cavities is e.g. in Figure 6.3b (a surface appears matt); on vitreous polymer, a fracture surface will be smooth or slightly wavy (interaction of a crack tip with reflected elastic waves)

Guidelines and Results of the Exercises:

6.1. Guidelines for a solution: we use relation (6.1) for solving, the result σ_f = 1450 MPa.

6.2. Solution: According to the relation $\sigma_f = \sqrt{\frac{4\,E.\gamma_{ef}}{\pi(1-\nu^2)c}}$ (similar to 6.2), we calculate

<u>c = 4,2 μm.</u>

6.3. Solution: After substitution into the relation (6.4) and numerical calculation $\underline{\varepsilon_f = 0{,}60}$.

6.4. Solution: Substituting into the relation (6.3), we get $\underline{\varepsilon_n = 0{,}42\%}$.

6.5. Brittle cleavage failure, facets mainly intercrystalline (≈70% of a surface), less % of a transcrystalline facet and several regions (islets) probably with microcavities. The sizes of facets 5-10 μm, sizes of grains 10-20 μm, particles 1-3 μm.

7. TRANSITION FRACTURE BEHAVIOUR OF STEELS AND TRANSITION TEMPERATURES

Time dedicated to the study of this chapter is approximately 3 hours.

Some materials under changing conditions of loading (particularly temperature, state of stress and loading rate) pass suddenly from ductile to brittle state. Metals having a body centred cubic lattice have this tendency, especially low carbon and low alloy steels. On the contrary, metals having a face centred cubic lattice and some metals having a hexagonal lattice such transition from tough to brittle state do not evince.

Objective: After reading this chapter, you will be able to

1. Name and describe main impact fracture tests.
2. Apply methods for transition temperatures in impact tests.
3. Explain the procedure for determination of the NDT temperature (nil ductility transition temperature).
4. Assess the practical importance of results of the DWTT (drop weight tear test).
5. Describe the CAT tests (crack arrest temperature) and influences of the main parameters.

Interpretation

A temperature at which a sharp decrease in toughness (in yield strength) occurs and at which a failure mode starts to change from ductile to cleavage, is the **transient, resp. transition temperature**. Several models try to explain a mechanism of a transition from ductile to brittle behaviour by means of a possibility of dislocations motion. Also the role of a grain size is considerable.

From the practical point of view, the transition effect is a very unfavourable property of the most widespread unalloyed steels. Since the operating temperatures of components and structures may drop to very low temperature levels (-60 to -80°C), it is necessary to find appropriate criteria for assessing the resistance of these materials to brittle failure at low temperatures. Similarly to decrease in temperature, it is possible to achieve a brittle state of these materials by increasing the strain rate and stress concentration (three axis tensile stress state). Therefore, test conditions for determination of transition temperature are modified by dynamic load and test specimens are provided with notches or contain cracks.

7.1. Impact Tests

It is the oldest and easiest **test of toughness**, followed later by other impact or dynamic tests of materials. The test was devised by Charpy (in 1901) for testing of structural steels against a fracture at high strain rates, resp. rates of loading. It supplements basic mechanical properties determined by a tensile test and takes into account the resistance of material to brittle failure due to notches and impact load. Its objective is to determine the value of **notch toughness**, which is defined as work consumed by breakage of a test sample under specified conditions, which include:

a) mode of loading (three-point symmetric bending),
b) loading rate (impact velocity 4,5 - 7 m/s),
c) temperature of a test sample,
d) dimensions and a shape of a test sample (usually 10 x 10 x 55 mm)
e) depth, a shape and sharpness of a notch

Purpose of the test of toughness on the Charpy hammer is to determine the energy (impact work), which was consumed on deformation and breaking a sample. Work consumed on breaking a sample is given by the difference of potential energies of a hammer between the initial and final position of the hammer. $K = W_o - W_p = mg(H-h)$, where m is weight of a hammer, H – initial height of centre of gravity of the hammer, h – its extreme height after breaking a sample and a swing to the other side. Values of impact energy can be read directly on a scale of the hammer by means of a pointer. **Standard CSN EN 10045** lays down a basic sample for the impact toughness test with a cross section of 10 x 10 mm bearing a **V**-notch with a depth of 2 mm or a **U**-notch, 5 mm deep. Values of notch toughness are expressed by amount of impact energy, denoted according to the notch shape KV or KU [J]. Notch toughness values could be also presented as proportion of impact energy (K) and the initial cross-section of a sample below the notch (S_v), i.e. $KC = K/S_v$. [J/cm^2] and by the shape of a notch KCV or KCU.

Notch toughness as a criterion of resistance to brittle fracture is of practical importance as a transition (transient, Vidal) curve. By decreasing the test temperature in a certain temperature interval, toughness drops sharply from the maximum value K_{max} to minimum K_{min}. This interval is called a **transition region**, and the corresponding curve with a significant decrease in toughness - **transition** or **transient curve**. A steep part of the curve in the transition region constitutes an interface between the temperatures at which ductile or brittle failure occur. According to this part of the curve, transition (transient) temperature is also determined, as the temperature at which:

a) A notch toughness value corresponds to the mean value (of maximum and minimum of the curve, interspersed with a series of measured values of toughness at several temperatures),

$$KV_s = \frac{KVmax + KVmin}{2} \tag{7.1}$$

b) KV has an agreed value for certain types of structures or equipment, or it is determined by the yield strength, e.g. KV = 28 J (classical energetics).

Besides the energetic approach, also fractographical (morphological) evaluation of a fracture surface of a test bar can be used for determination of the transition temperature. Three characteristic fracture surfaces of samples broken at different values of notch toughness are plotted in **Fig. 7.1**. The figure shows that on a fracture surface there may be two areas:
1) the ductile (tough) fracture region, 2) the brittle (crystalline) fracture region.

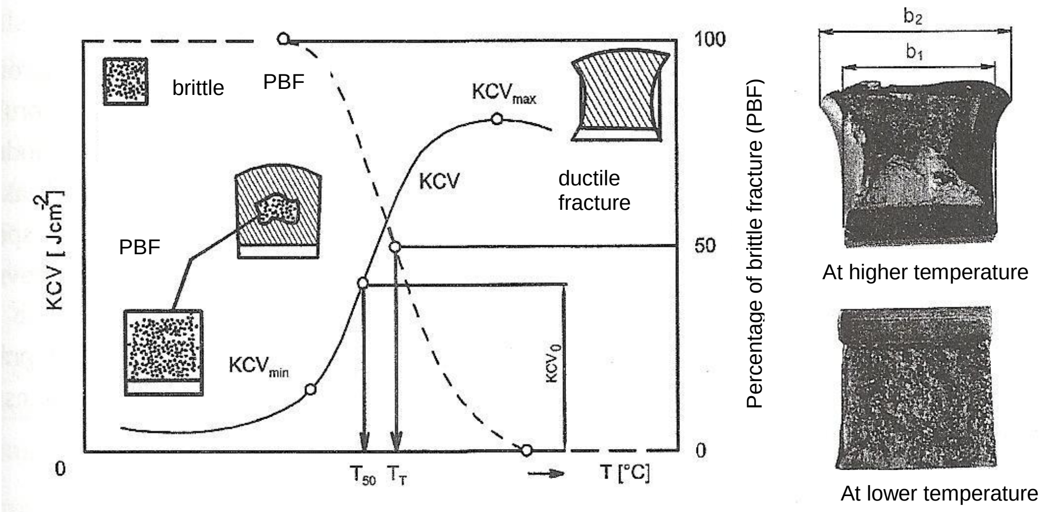

Fig. 7.1*. Transition curve of structural carbon steel and macrofractographic images of fracture surfaces at low and elevated temperatures. Lateral widening $\Delta b = b_2 - b_1$.*

The curves of notch toughness dependence on temperature for carbon steels are compared in **Fig. 7.2**. With increasing carbon content, the transition temperature increases and the maximum value of notch toughness decreases. A similar negative effect as carbon is exhibited by harmful elements (P, S, H), surface-active elements (Sn, Sb, Bi) and some alloying elements (Cr in high-alloy ferritic steels). Various impurities, segregation and excessive hardening affect adversely. The negative influence of defects (notches, cracks) is also reflected in the decrease of values of strength properties of material determined through tensile tests (Fig. 3.5).

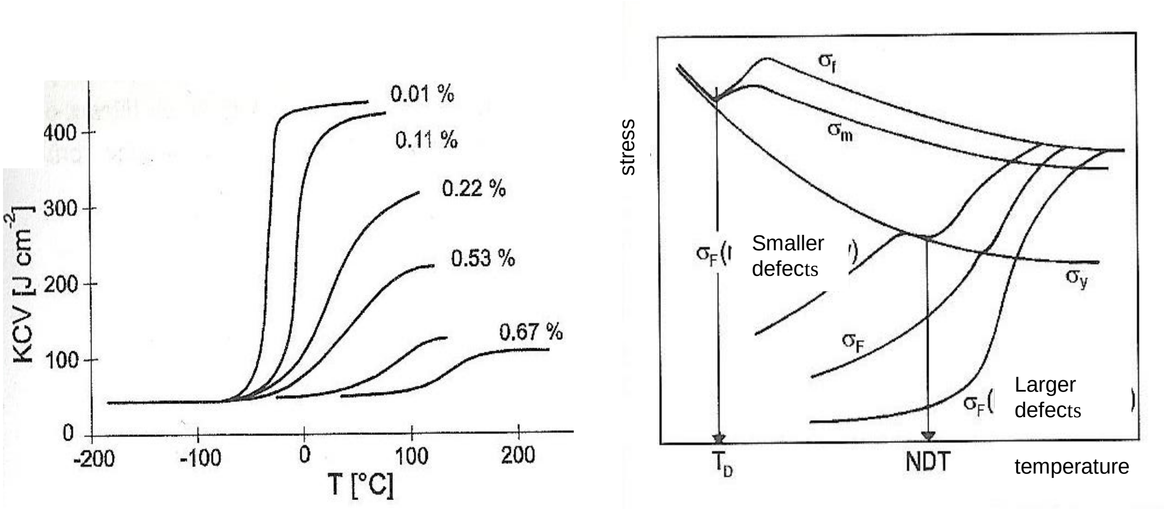

Fig. 7.2*. Dependence of notch toughness on temperature of carbon steels with different carbon content (wt. %). Effect of temperature on yield strength σ_y, ultimate strength σ_m and fracture stress σ_f (without defect) or σ_F with defects in tensile test of low carbon steel.*

With decreasing temperature, area (portion, percentage) of a brittle fracture PBF proportionally increases. Course of PBF values (also indicated by k), shows up as a dashed line in the diagram. Mixed fractures consisting of a brittle fracture area in the central part and a ductile fracture at the surface occur in the transition region.
The transition temperature, determined in accordance with appearance of a fracture is usually defined as a temperature at which PBF has a certain value, e.g. 50%.
Consumed work can also be measured indirectly by deformation at a fracture. It has been proved that the value of deformation work is proportional to deformation of a transverse cross-section $\Delta b = (b_2 - b_1)/2$, see **Fig. 7.1**.

An advantage of the impact test lies in its simplicity, speed and relatively low costs. The main area of application is in comparison of various states and processing of given steel or various steels mutually. Usually entire transition curves are evaluated, from which transition temperatures and also maximum values of notch toughness are determined. On the other hand, the impact test has the following shortcomings:

a) Value of the transition temperature T_T indicates only limit (lowest) temperature at which material can be stressed in operation. However, it does not indicate the stress that causes failure at given temperature,
b) ascertained data of T_T apply to a standardized laboratory test sample and are not applicable to larger material thicknesses,
c) a fracture surface is small for more accurate assessment and evaluation of a fracture,
d) results of this test are not applicable for structural calculations.

Therefore, this test is complemented or replaced by newer and in terms of physics more appropriate tests of brittle-fracture characteristics.

7.2. Nil Ductility Temperature Test

Principle of the test (**Figure 7.3**) consists in loading of flat (prismatic) steel test specimens by three-point bending with dynamic force (impact) with limited bend. The test specimen has brittle weld overlay on the side of tensile stresses. In the weld overlay, there is milled a notch which serves as an initiator of a fracture. Maximum bend of a body (YA) is limited by an underlay so that on the tensile side tensile stress equals to the value of yield strength in tension of material of the body. The test is performed at various temperatures. The aim of this test is to determine the nil ductility temperature, which expresses the resistance of material to unstable propagation of a brittle crack.

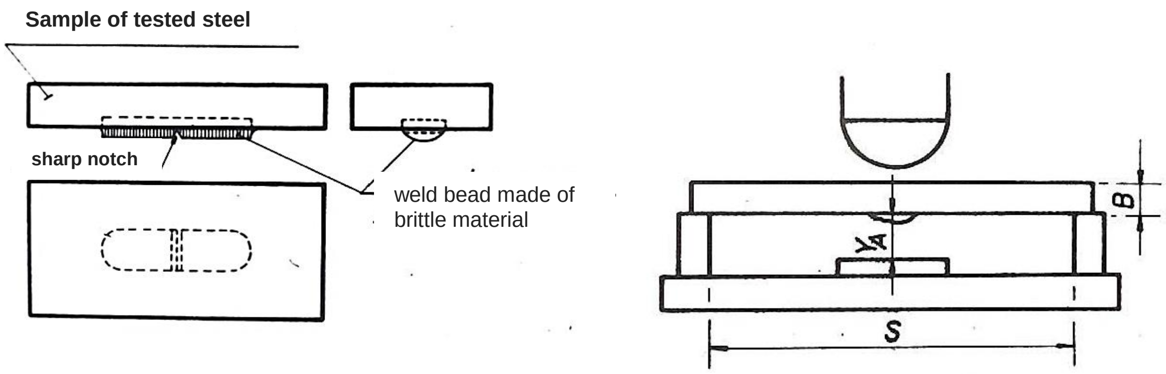

Fig. 7.3. Scheme of the nil ductility temperature (NDT) test

The highest temperature, at which a fracture still passes from a welded overlay into a base material, is called the **nil ductility temperature (NDT)**. NDT temperature is in a certain correlation with transition temperature. It is located in the lower part of the transition curve and its value does not depend on thickness of the tested material. The test is also suitable for welded structures.

7.3. Test of Large Bodies for Impact Bend – DWTT

The acronym DWTT stands for drop weight tear test (impact test by falling weight). The aim of the test is to determine the transition temperature of steel plates for pressure pipelines (gas pipelines). In this test, unlike the impact test, the metal plates are tested on large test specimens **with real thickness of a plate**. Principle of the test is shown in **Fig. 7.4**. Test plates (bars) are provided with a sharp pressed V-notch and are loaded by impact three-point bend to complete breakage. Tests are carried out on a falling dart or a large capacity pendulum hammer at various test temperatures. Impact energy must be such that failure occurs by one blow.

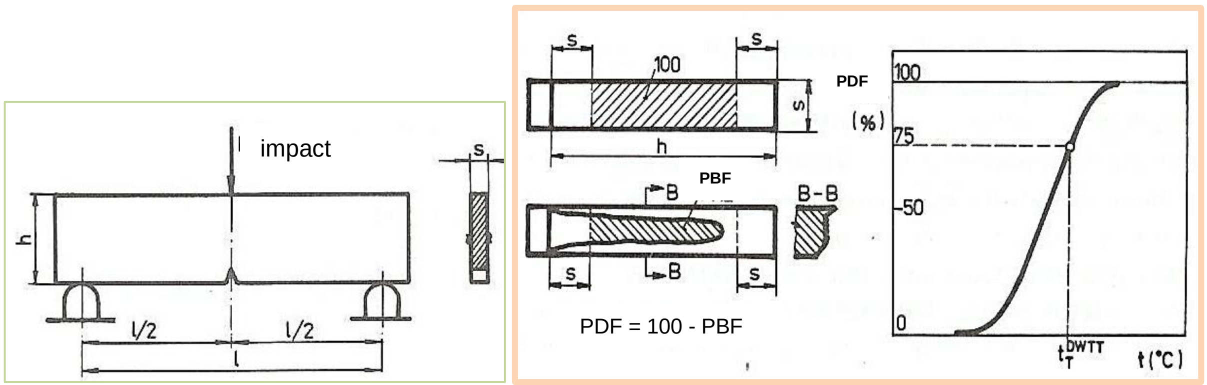

***Fig. 7.4**. A test specimen for DWTT test. Method of evaluating the DWTT test results*

After a fracture the proportion of ductile fracture (PDF) on a fracture surface is evaluated on test bars, **Fig. 7.4**. Transition curves are evaluated in the PDF - temperature coordinates.

DWTT test results are very important and have been proven through destructive tests on gas pipelines of a real size. These correlation tests have shown that it is possible to prevent formation and propagation of a brittle fracture on a pipeline if the operating temperature of the pipeline is higher than the transition temperature of metal plates, determined in the DWTT test. **Welded joints** and heat affected zones of a base material are critical points of failures in welded structures. Welded joints may contain defects such as incomplete penetration, cracks, bubbles, etc. In carbon microalloyed steel, there was found experimentally the value of DWTT = -30°C, on a quality weld 0°C and on a defective weld +30°C.

The above example shows that for welded structures, resistance to brittle failure is determined primarily by quality and properties of welded joints. With regard to the sharp pressed notch and hardening of material, energy for initiation of a fracture will be low. The major part of consumed energy will be used on crack propagation. Therefore, this test can be regarded as a test of resistance to crack propagation.

Impact bending test of large bodies DT (450x120x25 mm, with a sharp crack) is also standardized and when being carried out, it is measured with consumed energy by means of a large-capacity hammer (with max. energy of 10 kJ).

7.4. Crack Arrest Temperature Test

The aim of this test is to determine conditions under which an artificially created brittle crack is arrested. Ascertained conditions are expressed by dependences between stress and crack arrest temperature.

Principle of the test, devised by Robertson, is shown in **Fig. 7.5**. A flat test specimen of real thickness, provided on one side with a notch is loaded by tensile stress. It is concurrently cooled at one end (in the area of a notch) and heated at the other end. In a body, this creates course of the temperature, indicated in the lower part of the figure. The crack is induced by a blow to the place where a notch is located, and it propagates perpendicularly to the direction of tensile stress. In the material, where temperature is low (subtransient), a crack is of brittle nature and propagates rapidly (≈1000 m/s). In regions with higher temperature there are not suitable conditions for brittle crack propagation, therefore its velocity continuously decreases to complete stop at a certain point. The temperature at this point is the **crack arrest temperature** CAT that at a given nominal stress characterizes the ability of material to stop a propagating brittle crack.

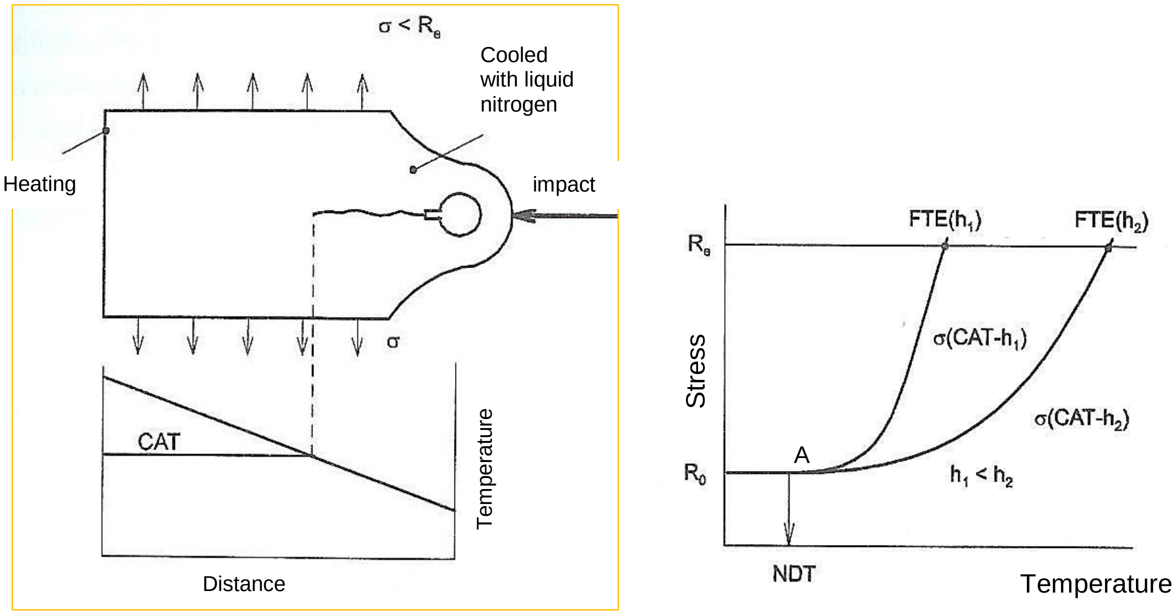

Fig. 7.5*. Scheme of Robertson's test of the crack arrest. Dependence of crack arrest temperature on acting stress and body thickness.*

Crack arrest temperature depends on acting tensile stress σ, on thickness of a tested material. In **Fig. 7.5** there is depicted dependence of CAT on acting tensile stress for two values of thickness h_1 and h_2. **The dependence of σ - CAT is of transient nature** and according to its author, it is called Robertson's transition curve of crack arrest temperature. The curve has two characteristic points. Point A is located at the lower bend of both curves, and has the coordinates (R_o, NDT).

Stress $\mathbf{R_o}$ represents **threshold (limit) stress**, below which neither at temperatures lower than NDT, brittle failure cannot occur because the energy of elastic deformation under stress R_o is insufficient to meet the conditions for crack propagation, nor at its maximum magnitude. Therefore, below the horizontal section of the curve (R_o-A) there cannot occur brittle fractures even at lowest temperatures and maximum defects.
The second characteristic point of the Robertson's curve is its intersection with the level of yield stress (R_p). This point represents the highest transition temperature of a fracture in the elastic region of deformation. It is denoted with the acronym **FTE (fracture transition elastic**). Above the FTE_{h1} temperature at a given material thickness h_1, a brittle (unstable) crack cannot propagate in the elastic region of a diagram, i.e. below yield strength. Inclination of the curve in the A-FTE section indicates that in this section CAT increases with increasing stress σ.

The second curve belongs to the thickness h_2 and deflects from the left curve behind point A to the right. At the same time, the two curves have the same NDT temperature. From the position of the two curves it follows that at larger thicknesses at the given conditions (σ c), brittle cracks arrest at higher temperatures. This difference is greatest at the stress at yield strength, at the same time it applies $\mathbf{FTE_{h1}<FTE_{h2}}$. It is explained by the fact that at larger

thicknesses the state of plane strain is more extensive, favourable to brittle failure at given temperatures.

On the basis of tests, it was found that by increasing thickness of a body, **Robertson's curve** shifts to the right, i.e. toward higher temperatures only to certain limit thickness which for structural steels is about 75 mm. Larger thicknesses do not further increase CAT temperatures. If the thickness h_2 >75 mm, TZT_{h2} curve may be considered a limiting transition temperature range LTTR of crack arrest temperatures. At temperatures and stresses lying to the right of this **limiting curve (LTTR)**, conditions for unstable crack propagation are not met.

Importance of Criteria Based on the Transient Temperature

The basic aim of the concept of transition temperature is to determine the temperature above which in a stressed component unstable growth of the allowable crack size cannot occur. The basis for determination of the temperature lies in transient temperatures by the relevant tests (standards) that have been described in previous chapters.

In terms of correlation between a test and real conditions, in application it is most appropriate to use the DWTT temperature for steel sheets and the CAT temperature for thick-walled components. Material for construction must comply with the condition $\mathbf{TZT_{\sigma pr} \leq T_{pr} - \Delta T_B}$, where $TZT_{\sigma pr}$ is crack arrest temperature at operating stress σ_{pr}, ΔT_B - increment of temperature to safety, T_{pr} – operating temperature.

Σ Summary of Terms

After reading this chapter, you should understand these terms:

Notch toughness. Transition (transient) temperature. Nil ductility temperature (NDT), Drop weight tear test, DWTT temperature, Crack arrest test, Robertson's test, CAT (Crack arrest temperature). FTE point (fracture transition elastic). Limiting curve LTTR

? Questions to Chapter 7

7.1 Explain why some materials show a sharp ductile-brittle transition at transient temperature, while others do not.
7.2 What methods may transition temperature in the impact test be determined by?
7.3 Which factors (agents) reduce the notch toughness value?
7.4 Which metallurgical measures improve toughness and transition temperature?
7.5 How does the fracture (critical) stress change with temperature and a defect size in the tensile test?

7.6 How is the nil ductility temperature determined?
7.7 Why the drop weight tear test is used?
7.8 What does the crack arrest temperature mainly depend on?
7.9 What relation shall be applicable among transition and operating temperature to avoid brittle fractures?
7.10 How the DWTT temperature is set?

Exercises to Chapter 7

7.1. When the temperature dropped from 20°C below the NDT temperature, a value of fracture toughness decreased 3 times. How does the critical crack length a_c change at the same load (stress)?

7.2. How will the critical stress change if a fracture toughness value decreased three times at temperature decrease? A crack length is independent of temperature.

7.3. Summarize relative advantages and disadvantages of the transition temperature approach in the analysis of material fractures.

7.4. For steel for bridges, it was found that the correlation K_{Ic} –KV in the transition region has the form:
$\frac{K_{Ic}^2}{E} = 655.KV$, where K_{Ic}, E and KV are in $Pa\sqrt{m}$, Pa resp. in J. Calculate fracture toughness of such steel if the transient value KV = 30 J is recorded.

7.5. What could happen for the relative position of the Charpy curve of impact energy (Vidal curve) of steel with yield strength of 275 MPa and 1380 MPa, if the samples were tested slowly in bending?

7.5. Toughness tests are to be carried out to evaluate quality of steel sheet of thickness of 6.0 mm. A standardized sample to the Charpy hammer has the dimensions 10 x 10 x 55 mm. What difference in impact energy can be expected, if the results for the steel sheet are compared with another plate of the same steel of thickness of 12.5 mm with identical structure?

7.6. Plot the impact of stress on CAT (crack arrest temperature) for a sample subjected to the Robertson's test.

Answers to the Questions

7.1 Metals with a lower number of slip systems and higher frictional stress exhibit transition behaviour at lower temperatures.

7.2 On the basis of a part of the Vidal curve in the transition region, according to the mean value of toughness, according to the prescribed value of KV_P, according to the percentage proportion of a brittle fracture (50%).

7.3 Toughness values are reduced by impurities (segregations, inclusions, the elements C, S, P, H, Sn, Cr), excessive hardening, radiation, high velocities of impact.

7.4 Increase in purity of steel, decrease in content of C, P, S etc., Ni and Mn alloying, suitable heat treatment contribute to increase in values of toughness and reduction in transition temperature.

7.5 Generally according to Fig. 7.2 (on the right); with decreasing temperature, fracture stress decreases.

7.6 Nil ductility temperature NDT - the highest temperature at which a fracture still passes from a weld overlay to base material, the test arrangement is shown in Fig. 7.3

7.7 The aim is to determine transition temperature (DWTT) of steel sheets of real thickness, especially for pressure pipelines (gas pipelines), usually with welded joints.

7.8 For the given material, CAT is dependent on tensile stress (above the threshold), and thickness of the body (up to the maximum thickness of approximately 75 mm), see Fig. 7.5.

7.9 Between transition temperature T_{tr} and operating temperature T_{prov}, the relation $T_{tr} \leq T_{prov} - \Delta T_B$ shall be applicable, where ΔT_B is an increment to safety, scattering of results.

7.10 According to the proportion of a ductile fracture of 75%.

Results of Exercises, Instructions for Solving

7.1. The critical crack length will be reduced 9 times (at the same load and configuration of a crack, we assume that the shape function and stress are independent of temperature).

7.2. By the relation $K_{Ic} = \sigma_c(\pi a)^{1/2}.Y$ and at the given condition $K_{Ic}(T_1) = 1/3\ K_{Ic}(T_2)$, where $T_1 < T_2$, after adjustment we get $\sigma_c(T_1) = 1/3\sigma_c(T_2)$, a, Y – independent of temperature.

7.3. The advantage consists in determination of the transition temperature at which the material loses its toughness and should not be used below this temperature. Examining and assessing the impact of technology. Disadvantage – transition temperature cannot be used for design calculations, results of some tests may differ significantly from real bodies.

7.4. After substituting into the mentioned relation and calculation $K_{Ic} = 64{,}2\ \mathrm{MPam}^{1/2}$

7.5. For the steel with lower yield strength at slow load, Vidal curve is considerably shifted toward low temperatures. For the steel with high yield strength, displacement is smaller.

8. APPLICATION OF FRACTURE MECHANICS IN THE FIELD OF FATIGUE

Time dedicated to the study of this chapter is approximately 2 hours

For the study of this chapter, it is assumed that students have been familiarized with basic knowledge of material fatigue in other subject, e.g. in material science.

Objective: After studying this chapter, you will be able to

Apply stress intensity factor in the field of fatigue crack propagation.
Compare initiation and propagation of short cracks.
Assess propagation of short fatigue cracks.
Describe effects of corrosive environment on limit values (amplitude) of stress intensity factor

Interpretation

Fatigue process takes place gradually during cyclic loading and includes the following stages.

1. Changes in mechanical properties

2. Initiation (nucleation) of microcracks

3. Propagation of microcracks and short cracks

4. Propagation of (macro)cracks - stable growth

5. Static fast fracture – unstable growth

Within this short chapter and the support, we will only mention some of the problems associated with possibilities of application of fracture mechanics parameters, namely the amplitude of the stress intensity factor. The knowledge of fracture mechanics is applied mainly in propagation of fatigue cracks and fast fractures.

8.1. Issues of Short Fatigue Cracks

In most cases, initiation occurs by slip process on material surface, due to a shear stress component whose maximum size is about 45° relative to tensile stress, **Fig. 8.1**. During cyclic loading, slip of a part of materials occurs and depressions into material (intrusions) adjacent to projections on material (extrusions). Intrusions represent stress concentrators and their further deepening forms fatigue microcracks propagating along slip planes. Grain boundaries represent a kind of obstacle to their further propagation.

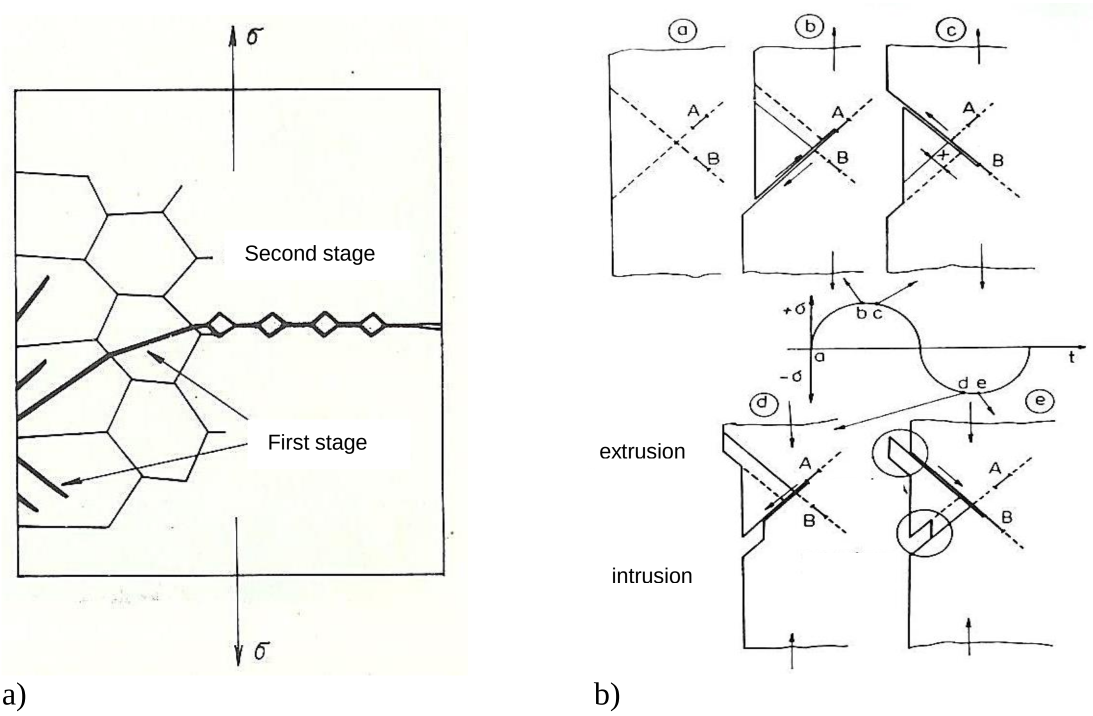

Fig. 8.1. *Scheme of stages of microscopic and short fatigue crack propagation (a). Scheme of intrusion and extrusion formation on a surface at cyclic loading and fatigue (b)*

In the first phase on the surface usually a number of microcracks arises, of which the largest or the most active cross grain boundaries and due to the interaction of shear and tensile cyclic stresses they gradually turn to a plane perpendicular to the principal stress. In the second phase, propagation of fatigue cracks is carried out perpendicularly to tensile stress, and is driven by cyclic plastic deformation, caused by shear stress components associated with tensile stress. The first phase of propagation is usually in the range of 5-10 grains, depending on level and nature of load. Initiation and propagation of microcracks may occur even under fatigue limit, while cracks of macroscopic dimensions do not arise here.

For **short cracks** whose size is comparable to grain size, amplitude of stress intensity factor can be formally applied in expressing velocity of propagation. Such an approach, however, is not correct. Directly in relations for velocity of propagation of short fatigue cracks, there are present lengths of these cracks and sizes of grains having borders which hinder or slow short crack propagation, **Fig. 8.2**.

For short cracks whose length is comparable to grain size, we can write formally $K_I = \sigma\sqrt{\pi a}$, or for amplitude of stress in the field of thresholds $\Delta K_I = \Delta\sigma\sqrt{\pi a}$, but the value of upper stress σ_h may exceed yield strength of material and classic deformation of a cross-section occurs. For application of linear elastic fracture mechanics, the condition for stress $\sigma_h < 2/3\ R_p$ should be met, while a very small plastic zone arises. Short fatigue cracks are hindered by grain boundaries, and also their propagation rate is at minimum when crack length equals the size of a grain. For a description of velocity, it is necessary to leave the K factor and use directly length of a crack or fracture mechanics parameters applicable to plastic deformation (J-integral).

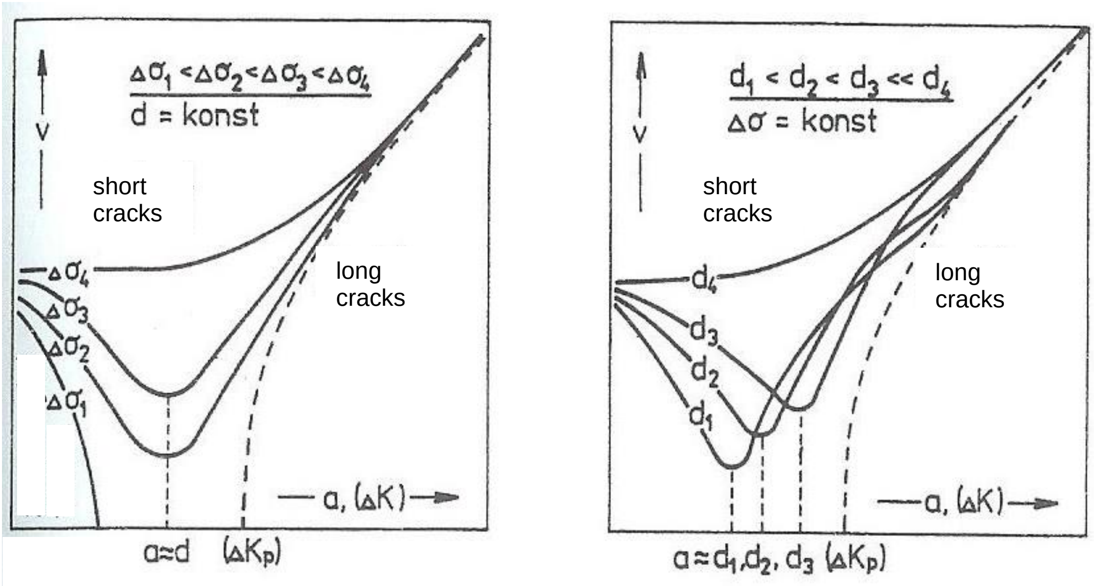

Fig. 8.2. *Effect of stress range ($\Delta\sigma$) grain size (d) on propagation rate of short cracks depending on ΔK_I formally.*

In the first downward branch of velocity dependence of a crack v = da/dN on its length (a) or ΔK_I , plastic deformation of surface grains is critical, and effect of a crack as a notch is negligible. Relations of linear elastic fracture mechanics do not apply here, the rate of crack propagation can be here expressed in the form

$$\mathbf{da/dN = Ca^{\alpha}(d-a)^{1-\alpha}} , \qquad (8.1)$$

where d is grain size and exponent α is an empiric parameter, which can reach values of $-0{,}27 < \alpha < 0{,}08$.

In the second rising branch (a > d) notch effect of a crack begins to play an important role, Fig. 8.2. Similar to long cracks, a plastic zone at the crack tip is crucial here. Fatigue crack propagation ceases to be affected by local conditions on a surface of a body and begins to follow the patterns of fracture mechanics. For speed of a crack, it is possible to write (relation of Klesnil and Lukáš)

$$\mathbf{v = da/dN = C(\Delta K_I^{\,n} - \Delta K_{Ip}^{\,n})}, \qquad (8.2)$$

where ΔK_{Ip} is the threshold of the amplitude of stress intensity factor, n – exponent (n = 2-5) in Paris relation (8.3) $da/dN = C(\Delta K_I)^n$.

8.2. Fatigue Crack Propagation

The typical mechanism of fatigue crack propagation through local cyclic plastic deformation is presented in **Figure 8.3**. When a fatigue crack propagates, a crack opens and closes alternately, while on the surface there are formed grooves, called striation. One loading cycle usually corresponds to crack tip displacement of the distance of neighbouring grooves. By measuring the spacing of striations (grooves), we can thus ascertain the rate of crack propagation in a given local area.

From the macroscopic point of view and according to fracture mechanics, fatigue crack propagation rate depends on the amplitude of stress intensity factor $\Delta K = \Delta\sigma(\pi a)^{1/2}Y$ or the amplitude of stress intensity factor K_a ($\Delta K = 2.K_a$). In **Fig 8.3**, there is presented the general dependence of fatigue crack propagation rate $v = dA/dN$ on the amplitude of stress intensity factor ΔK. According to size of ΔK and course of the curve, three phases (stages) of crack development are distinguished. At very low values of ΔK below the threshold ΔKp, cracks do not propagate. The propagation of fatigue (macroscopic) crack takes place above the threshold in the first stage (I).

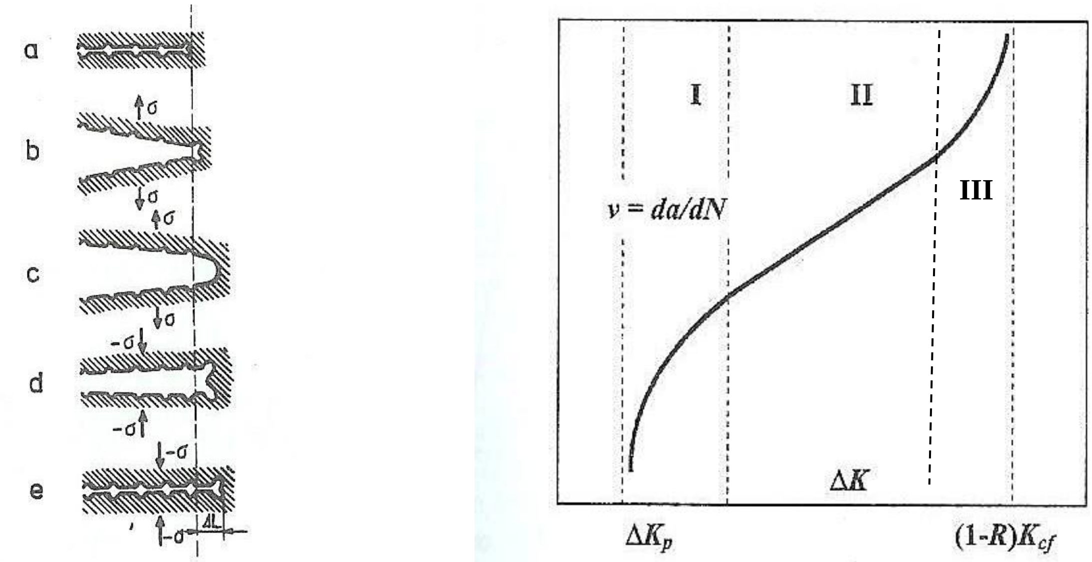

Fig. 8.3**. Mechanism of grooves creation in the stage II of fatigue crack propagation. General dependence of velocity of fatigue crack propagation v = dA/dN on the amplitude or range of ΔK. K_{cf} – fracture toughness at cyclic loading. Dependence is depicted in logarithmic scales of log**ΔK** - log **v.

To describe the stage *II* of stable crack propagation, Paris equation is used:

$$\mathbf{v = da/dN} = \boldsymbol{C}(\Delta\boldsymbol{K})^{\boldsymbol{n}}, \tag{8.3}$$

where C – material constant, parameter n = 2 - 5, $\Delta K = K_{max} - K_{min}$ the range of stress intensity factor or its amplitude $K_a = \Delta K/2$. More precisely, instead of ΔK it is necessary to consider **the effective value of the amplitude ΔK_{ef}**, defined by a tensile part of stress and by effect of compressive stresses from the cyclic plastic zone. Using that relationship according to fracture mechanics is possible when a plastic zone at a crack tip is small compared with crack length ($r_p \leq a/50$) and thence it follows $\sigma_h \leq R_p/3$.

In the zone of stage III, development of fatigue crack propagation accelerates in connection with overload of material in reducing a residual load-bearing cross-section. In addition to the grooves, ductile cavities or cleavage facets are formed here that contribute to accelerated crack propagation to the critical size. When reached the value of fracture toughness, affected by cyclic loading (due to cyclic hardening or softening of material), unstable, usually brittle, fracture occurs.

In the first phase of fatigue crack propagation, microstructure, mean stress and environment, which at this stage of slow growth acts for a longer time, have great impact. In the second phase, relatively small influence of microstructure, mean stress, environment and thickness is shown. In the third phase of accelerated development of cracks, microstructure, mean stress and thickness have significant influence, while the environment has little effect. Temperature effect is not unequivocal; usually in the stage I at temperature increase (relative to the normal room temperature), the threshold (ΔK_p) decreases and velocity of a crack increases, contrarily in stage III the value of fracture toughness increases with temperature and concurrently crack propagation rate decreases.

Unlike statically stressed materials, plastic zone of fatigue cracks is composed of a part corresponding to the maximum values of tensile stress σ_h and a cyclic part, whose dimensions are about 4 - 5 times smaller than those of static zone, **Fig. 8.4**. Effect of these zones is reflected in changes in crack propagation rate at changes in the amplitude of stress.

Rate of fatigue crack propagation is affected by alternating amplitude or mean value under cyclic loading. If the stress amplitude at the same mean value decreases in blocks of a large number of cycles, at first the rate of crack propagation significantly reduces and then it gradually increases to a value corresponding to smaller stress amplitude. Conversely, when the stress amplitude increased, fatigue crack growth rate significantly transiently increases, followed by a decrease to a value corresponding to stationary loading by higher amplitude. These transient changes in speed can be explained by cyclic plastic zone, which a crack must cross at changes in stress levels.

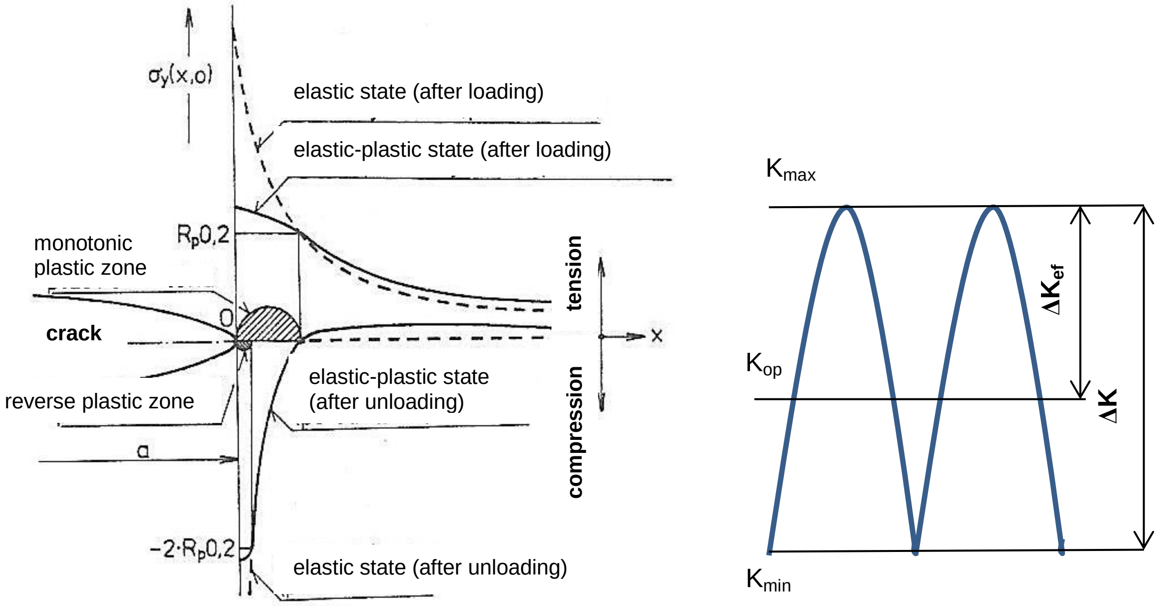

Fig. 8.4. *Comparison of monotonic and reverse (cyclic) plastic zone at the crack tip. Closing the crack tip due to the reverse plastic zone leads to introduction of effective amplitude of stress intensity factor (ΔK_{ef}) when describing the fatigue crack propagation rate.*

Due to the plastic zone, a crack also closes (in the compressive part of the cycle) and later it opens, which results in reduction of the effective stress amplitude. Instead of the original amplitude ΔK_I, **the effective amplitude ΔK_{ef}** $< \Delta K_I$ is to be considered.

Larger plastic zone under cyclic loading means larger crack opening and the higher rate of crack propagation in malleable metal material.

.

8.3 Effects of an Environment and Frequency on Crack Propagation

Combined effect of mechanical fatigue and corrosive environment reduces the fatigue cyclic lifetime at a given cyclic loading or it reduces fatigue limit, resp. fatigue strength (for a specified number of cycles), see **Wöhler's curves** in **Fig. 8.5.**

Influences of selected environments (deaerated water, water saturated with 98% of N_2 + 2% of O_2, water saturated with air and oxygen) on fatigue life curves are shown in **Figure 8.5**.

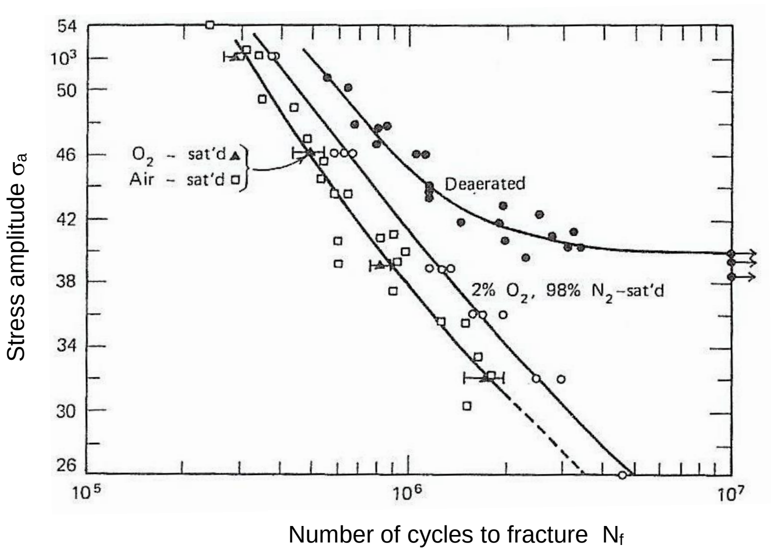

Fig. 8.5. *Effect of dissolved oxygen in a solution of 3% NaCl at 25°C on fatigue behaviour of carbon steel*

Basic possibilities of increasing fatigue crack propagation rate in a corrosive environment are shown in **Figure 8.6**.

In the first case (A), the rate of fatigue crack propagation is affected by environment to above the threshold K_{ISCC} for **stress corrosion cracking**. In the second case, aggressive environment reduces the threshold of amplitude of stress intensity factor K_{ap} (for purely mechanical fatigue) and increases the rate of crack propagation in entirety of K_a, resp. K_{max} (Fig. 8.13 b), represents corrosion fatigue as such. The third case is a certain superposition of the two previous.

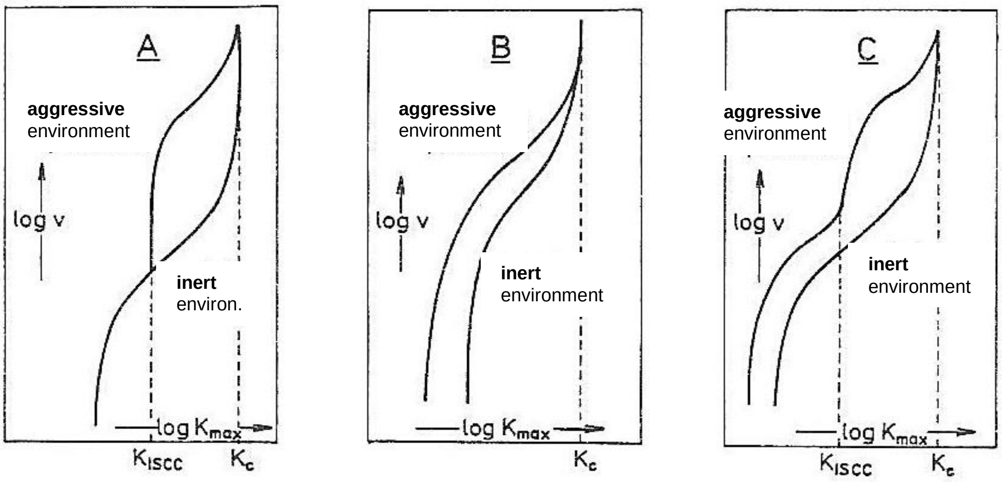

Fig. 8.6. *Combination of mechanical fatigue with corrosive environment on increase in the crack growth rate: A – Effect of corrosion cracking, resp. hydrogen embrittlement on fatigue crack propagation. B – Corrosion fatigue of material, as such (interaction of effects), C – Combination of the mentioned mechanisms*

In **Tab. 8.1** for comparison, there are stated fracture toughnesses K_{Ic} of structural materials and thresholds for stable development of cracks with the assistance of corrosive environment K_{IEAC} (EAC – *environmental assisted cracking*). Generalized designation K_{IEAC} includes corrosion cracking (K_{ISCC}) or hydrogen (K_{IHIC}, or K_{ISH}) embrittlement and cracking.

Tab. 8.1. Examples of the critical values of K_{IEAC} for selected materials and some environments

Material	solution	$R_p0,2$	K_{Ic}	K_{IEAC}
		MPa	$MPa.m^{1/2}$	$MPa.m^{1/2}$
Al – alloy 2024-T351	3,5% NaCl	325	55	11
Al – alloy 2024-T852	Sea water	370	19	15
Al – alloy 7075-T6	3,5% NaCl	505	25	21
Al – alloy 7075-T7351	3,5% NaCl	360	26	23
Steel 18Ni(300)-maraging	solution NaCl	1960	80	8
CrNiMo steel 4340	solution NaCl	1335	79	9
Stainless steel 300M	3,5% NaCl	1735	70	22
Ti – alloy TiAl6V4	3,5% NaCl	890	99	45
Ti – alloy TiAl8Mo1V1	3,5% NaCl	745	123	31
Ti – alloy TiAl8Mo1V1	water	855	105	29

Effects of cycle asymmetry ($R= \sigma_d/\sigma_h$) and frequency of loading (f) on fatigue crack propagation are also significant, **Fig. 8.7**, especially in corrosive environments. With increasing cycle asymmetry coefficient, mean value of stress increases (σ_m) at a given amplitude of stress ($\Delta\sigma = 2.\sigma_a$, $\Delta K = \Delta\sigma\sqrt{\pi a}.Y$). With increasing frequency, the rate of fatigue crack v = da/dN (in a unit μm/cycle) generally decreases, in contrary the rate v = da/dt (μm/s) increases.

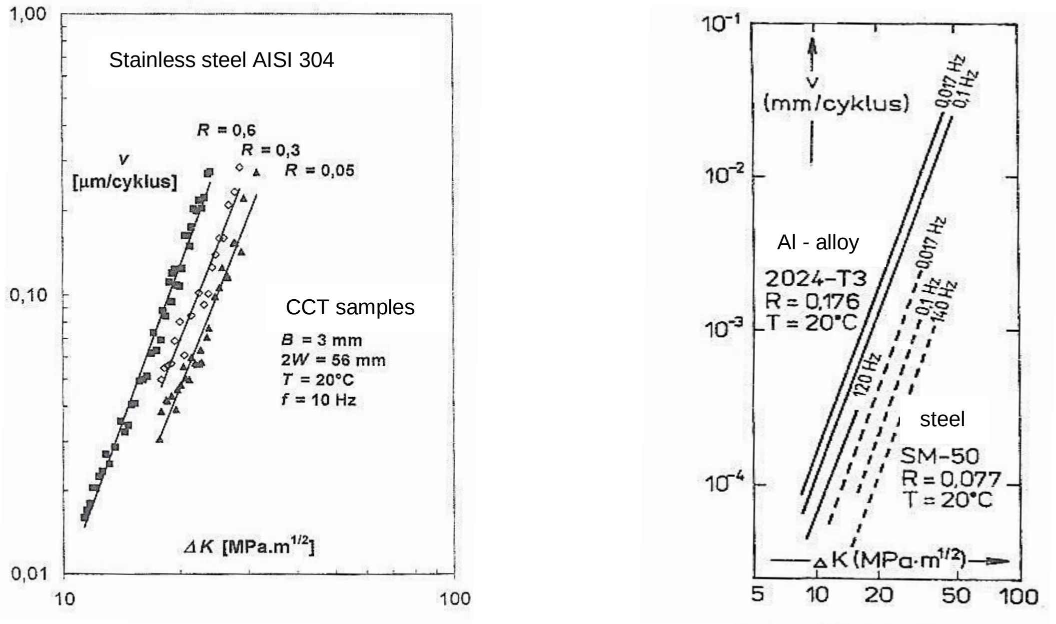

***Fig. 8.7**. Examples of the effect of cycle asymmetry R and frequency f [Hz] on crack propagation rates.*

Influence of frequency (f) on crack propagation rate can be described by the equation

$$v = Cf^{-\lambda}(\Delta K_{ef})^{n}, \qquad (8.4)$$

where the material constant λ = 0,08-0,09 for Al alloys, and λ = 0,12-0,14 for steel.

8.4. Fractography of fatigue failures

According to the purpose of research and observation techniques used, the fatigue fractography can be divided into three separate areas:

a) **Fractography** of fatigue crack propagation, which examines some aspects of fatigue damage in terms of the kinetics of its development. This information has practical significance, since it allows to assess the risk of developing crack, which can lead to fracture and crash.

b) **Makrofraktography** provides an integral image of the fracture process, the macroscopic characteristics of the fracture surface (Fig. 8.8), visible to the naked eye using a magnifying glass or optical microscope (stereomicroscope, SEM), the maximum magnification of 100 x.

Unstable fracture surface (final fracture) is usually rough and rugged as compared with the stable fatigue crack propagation, characterized by a smoother surface (Fig. 8.8). Fractography of fatigue cracks is used for research purposes and to determine the causes of components damage in operation. According macroscopic analysis we can qualitatively determine load levels, in some cases, the type of load (tension, bending, torsion, etc.), or the level of stress concentrators, see Appendix (p. 93). In simple and logically true: the larger the area of final fracture, i.e. critical crack length is shorter, the higher was applied cyclic stress. There are monographs and handbooks to determine the stress intensity factors.

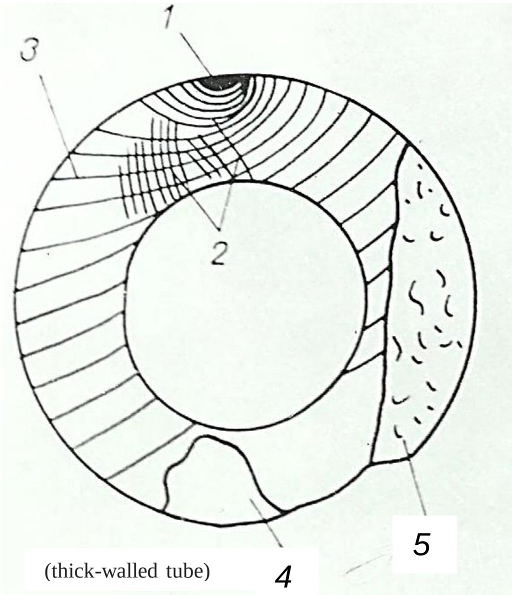

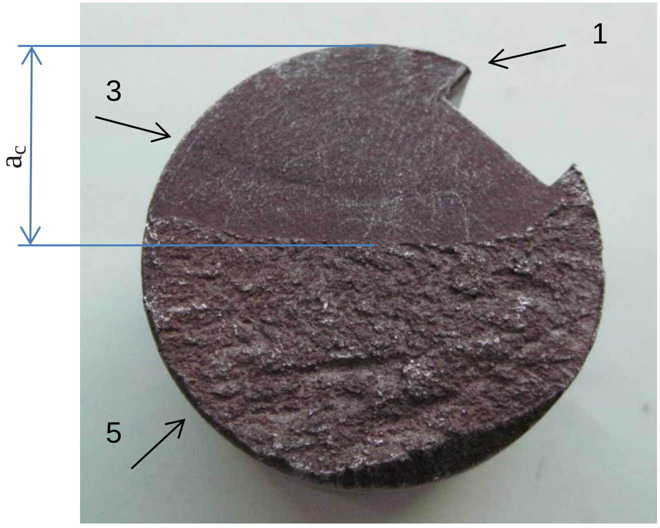

Fig. 8.8 *Diagram of fatigue fracture with typical characteristics: 1 - Initiation and short cracks propagation, 2 - Secondary steps and hems, 3 - Fatigue lines (beach marks), fatigue crack growth area, 4 - Zone of accelerated crack growth, 5– Final unstable fracture. Shaft (∅45 mm) with the surface groove and fatigue fracture,* a_c *– critical fatigue crack length.*

In many cases, the fatigue crack front, including the critical size, has a semi elliptical shape or a partially elliptical one. Calculating the value of stress intensity factor is then quite complex.

c) **Mikrofraktography** studying the fracture surface at high magnification and obtains information about the failure mechanism and material based on microscopic traces such as striations (fatigue grooves, Fig. 8.9.), the position of grain boundaries and slip planes due to the crack, or an occurrence of intergranular facets, etc. By measuring the range of striations we can determine the local velocity of crack propagation. One loading cycle typically causes the increase in length of the crack size about size of striation (0,01-100 μm). Local direction of crack propagation is at right angle to the striations.

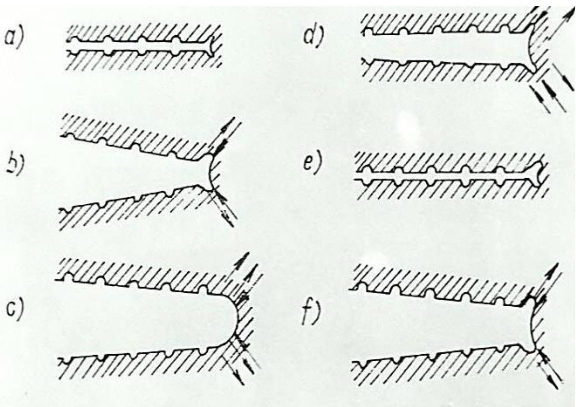

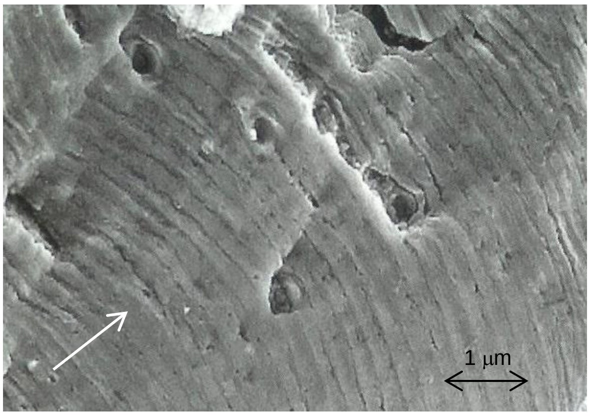

Fig. 8.9 *Geometric changes at the top of fatigue cracks during a deformation cycle: a) no load, b) low tensile load, c) the maximum tensile load, d) small compressive load, e) the maximum load pressure, f) a small tension load. Typical microscopic striations (grooves) on the fracture surface. Traces of particles or intersection by fatigue crack.*

Summary of Terms

Based on the brief interpretation of relatively large issue of material fatigue, it is necessary to know these basic terms:

- Wöhler curve, fatigue strength, fatigue limit, a cyclic lifetime, corrosion fatigue

- The stage of crack initiation, intrusion, extrusion, short cracks, crack propagation, striation,

- Paris relation, thresholds of amplitude of stress intensity factor ΔK_p (ΔK_{Ip}) effective amplitude ΔK_{ef}.

- Thresholds (limit values) for stress corrosion cracking (K_{ISCC}, K_{IHIC}, K_{IEAC}) and corrosion fatigue.

Questions to Chapter 8

8.1 How are intrusions and extrusions formed under alternating stress of metallic materials?

8.2 Why short crack propagation cannot be described by the amplitude of the stress intensity factor?

8.3 What methods of reducing or suppressing initiation of fatigue failure do you know?

8.4 How are fatigue striations formed and how do they relate to crack propagation rate?

8.5 What does the rate of fatigue crack propagation in metallic materials depend on?

8.6. Indicate the main factors that may cause dispersion of values of a fatigue lifetime.

8.7. What calculations is Paris relation used for? Indicate possibilities of use and limitations of this relation.

8.8. How does the corrosive environment affect fatigue characteristics of material?

8.9. How can the stress intensity factor be used in describing influence of a corrosive environment on crack propagation?

8.10. How does the fatigue crack propagation rate change with frequency of loading?

Exercises to the Chapter

8.1. Rather thin leaf spring is subjected to simple bending in one direction and on the tensile side, a semi-elliptical defect arises (a/2c = 0,15). As may be expected, the defect plane is oriented perpendicularly to the bending stress. Cyclic loading causes crack propagation. Discuss whether the ratio of ellipticity (a/2c) will increase or decrease.

8.2. Determine the time to fracture of a steel plate of a width of 200 mm and a thickness of 3,0 mm, wherein a central crack of length of 10 mm occurs. Fracture toughness of steel is K_{Ic} = 48 MPam$^{1/2}$ and the yield strength Re = 1400 MPa. The plate is loaded by repeated force F_{max} = 80 kN with frequency of 3,0Hz. We assume that a fatigue crack propagates from the initial central crack according to Paris relation with the constants $C = 10^{-10}$ $MPa^{-3}m^{-1/2}$ and n = 3,0.

Solution:

The initial crack is relatively short compared with the width of the sample (2a/W=10/200 =0,05), thus geometric factor Y=1. Maximum, upper stress is $\sigma_h = F_{max}/S = 80.10^3/200.3$ = 133 MPa = 0,095.Re. Minimum, lower stress is $\sigma_d = 0$. The fatigue crack will propagate stably from the initial length a_o = 5,0 mm (to both sides) to the critical length a_c, which we calculated from the equation for K_{Ic} : $K_{Ic} = \sigma_h\sqrt{\pi a_c}$.Y, to simplify the calculation we assume Y = 1 (otherwise Y = f(a/W) and the calculation is more complicated). Then the critical length of the crack a_c = 41,3 mm.

According to Paris relation: $da/dN = C.\Delta K^n$ it is formally $dN = \frac{da}{C.\Delta K^n}$ and we calculate a lifetime by means of integrals from both sides. Integration limits shall be chosen such that zero number of cycles $N_o = 0$ corresponds to the initial crack length a_o, and a number of cycles N_c, i.e. the cyclic lifetime corresponds to the critical final length of the fatigue crack a_c.

$N_c = \int_0^{N_c} dN = \int_{a_o}^{a_c} \frac{da}{C.\Delta K^n}$, where the amplitude $\Delta K = \Delta\sigma\sqrt{\pi a}.Y = \sigma_h.\sqrt{\pi a}Y$, after adjustment we get $N_c = \frac{1}{C(\Delta\sigma\sqrt{\pi})^n}\int_{a_o}^{a_c}\frac{da}{(\sqrt{a}Y)^n}$, To simplify the calculation Y = 1 (or Y = const.> 1), and for the specified n = 3,0 we get $N_c = \frac{1}{C(\Delta\sigma\sqrt{\pi})^3}\int_{a_o}^{a_c}\frac{da}{(\sqrt{a})^3} = \frac{1}{C(\Delta\sigma\sqrt{\pi})^3}\left[\frac{1}{\sqrt{a_o}} - \frac{1}{\sqrt{a_c}}\right]$.

After substituting and numerical calculation N_c = 13970 cycles. Time to fracture $t_f = N_c/f$ = 77.6 min.

Note: More precise calculation of the critical crack length, taking into account the function Y= f(a), leads to the result a_c = 34,9 mm and for the mean value Y = 0,5.(Y(a_o) + Y(a_c)) > 1 we get approximately N_c = 12500 cycles. The shape function (the shape factor) is possible here in the form: $Y = Y(\frac{a}{W}) = 1+0,128(\frac{a}{W}) - 0,288\,(\frac{a}{W})^2 + 1,525(\frac{a}{W})^3$, it is true for a/W ≤ 0,7 with an accuracy of 0,5 %.

8.3. In 1CrMoV steel for the manufacture of rotors of energy devices, afatigue crack propagation rate was experimentally determined according to the relation: $\frac{dc}{dN} = 7,7.10^{-12}.\Delta K_I^3$.

Calculate approximately the cyclic remaining useful lifetime of a component when a semi-elliptical crack of a depth of 5 mm and a width of 20 mm, lying in a plane passing through the axis of the rotor, was detected by means of defectoscopy on a surface of the cylindrical rotor. Amplitude threshold of stress intensity factor is ΔK_{Ith} = 5,0 MPa $m^{1/2}$ and fracture toughness of the steel is 115 $MPam^{1/2}$, nominal alternating bending stress is 90 MPa.

8.4. The threshold of ΔK_p decreases with increasing R according to the relation $\Delta K_p = (1-R)^{\gamma}\Delta K_{po}$, where γ is a parameter dependent on material and environment ($0 < \gamma < 1$, e.g. for pearlitic steels γ = 0,93, for high-strength steels γ = 0,71, for martensitic steels γ = 0,53, in dry air).
Calculate the threshold of stress intensity factor amplitude ΔK_p for pearlitic steel for cycle asymmetry R = 0,9, and the value of $\Delta K_{po,}$ when ΔK_p = 4,0 MPa$\sqrt{m}$ for R = 0,7. What is the importance of the parameter ΔK_{po}?

8.5. A component of an energy device of steel having fracture toughness K_{Ic}= 54 MPa.m$^{1/2}$ was subjected to nondestructive ultrasonic testing and it was found that it contains a crack of a depth of 2,0 mm and of a width of 5,5 mm, and a defect of a depth of 1,5 mm and of a width of 10,2 mm, both of almost semi-elliptical shape, oriented perpendicularly to circumferential stress. Tests have shown that the rate of crack propagation under cyclic loading follows Paris law with the constants C = 4,0.10^{-13} MPa^{-4}m^{-1} and n = 4 (for R=0). Calculate the number of cycles to fracture when amplitude of the stress at repeated load is $\Delta\sigma$ = 150 MPa.

8.6. Determine how the critical crack length of CrNiMo (4340) steel will change according to Tab. 8.1 in aqueous solution of NaCl due to corrosion cracking. Consider the same tensile stress in an inert environment and in the solution.

Answers to the questions

8.1. Intrusions (microscopic depressions) arise at cyclic slip of dislocations and narrow bands due to shear stresses. Extrusions protrude above a surface adjacent to intrusions; they are formed by a similar slip mechanism as intrusions (Fig. 8.1).
8.2. At the amplitude $\Delta K = \Delta\sigma(\pi a)^{1/2}Y$ and for very short cracks $\Delta\sigma$, resp. σ_h, it exceeds the yield strength and then relations of linear elastic fracture mechanics are not applicable.
8.3. Fatigue failure initiation of metals can be generally hindered by motion of dislocations. The measures taken: reducing stress concentration, increase in quality of a surface (polishing, fine grinding), introducing compressive stresses on a surface and surface hardening (carburizing, nitriding, surface hardening, shot peening, rolling, etc.)
8.4. Fatigue striations are formed by cyclic plastic deformation as microscopic grooves (one groove occurs per one cycle), indicate local positions of a front of a growing crack. They enable determination of the local speed of crack propagation.
8.5. Mainly on amplitude of the stress intensity factor, i.e. on the size of cyclic plastic deformation, then on temperature, frequency, stress state, corrosive environment.
8.6. Variance of a fatigue lifetime is caused mainly in the stage of initiation and propagation of microcracks. Random local concentrations of stress on a surface and random occurrence of defects in material are significant at initiation; particularly, different grain sizes are applied in growth and dispersion of microcracks. Dispersion of the fatigue

lifetime is further increased by random course of loading, random changes in the environment and temperature.

8.7. Paris relation (law) is used for estimates or calculations of the fatigue lifetime, the remaining cyclic lifetime, then to compare the speed of crack propagation in different materials or in certain material after different treatment options.

8.8. Corrosive environment usually reduces fatigue strength and a lifetime, increases a crack propagation rate especially in the stage I and II of growth, reduces thresholds (ΔK_{Ip}) – corrosion fatigue.

8.9. The stress intensity factor can be used to express thresholds under static or cyclic loading (K_{ISCC}, K_{IHIC}, ΔK_{Ipc}), to describe and compare an increase in crack propagation speed in a corrosive environment.

8.10. Speed of fatigue crack propagation (da/dN) in μm/cycle generally decreases with increasing frequency. Contrarily, the speed v = da/dt = f.(da/dN) in μm/s increases with frequency.

Results of some exercises:

8.1. The ellipticity ratio will rise during bending.

8.3. The lifetime $N_f = 1{,}7.10^7$ cycles, according to simplified calculation.

8.4. $\Delta K_{po} = 12{,}3\ \mathrm{MPa}\sqrt{m}$ and $\Delta K_p = 1{,}45\ \mathrm{MPa}\sqrt{m}$ for R = 0,9, where ΔK_{po} indicates the threshold of stress intensity factor amplitude at the parameter of cycle asymmetry R = 0.

8.6. The critical crack length reduces ≈77 x.

References

- ANDERSON T. L: Fracture Mechanics. Fundamentals and applications, BAE, 2005, 621 p.

- CALLISTER D. W., Materials Science and Engineering. An Introduction. University Iowa, John Wiley& Sons, 2007,721 p.

- FELBECK, D. K., ATKINS A.G.: Strength and Fracture of Engineering Materials. Prentice Hall, Englewood, 1984, 542 p.

- ASHBY M. F.: Mechanical selection in mechanical design. Pergamon Press, 1992, 311 p.

- STRNADEL, B. et.al. New methods of damage and failure analysis of structural parts. Workshop, VŠB-TU Ostrava, 495 s. 2012.

- FRACTURE MECHANICS – internet teaching programs and informations.

- ENGINEERING FRACTURE MECHANICS – international journal, covers a broad range of topics in fracture mechanics to be of interest and use to both researchers and practitioners.

- MURAKAMI, Y., Stress Intensity Factors Handbook. Pergamon pr., 1999, 1566 p.

- BROEK, D., Elementary Engineering Fracture Mechanics. Kluwer Academic Publishers, Dordrecht, 1986, 516 p.

- The online version of Engineering Fracture Mechanics at ScienceDirect.com

- ASTM E399-09: Standard Test Method for Linear-Elastic Plane-Strain Fracture Toughness K_{Ic} of Metallic Materials, ASTM International, West Conshohocken, PA, 2012.

- ASTM B645-10: Practice for Linear-Elastic Plane-Strain Fracture Toughness Testing of Aluminum Alloys

- ASTM D5045- 99: Standard Test Methods for Plane-Strain Fracture Toughness and Strain Energy Release Rate of Plastic Materials.

- ASTM E647-91. Standard Test Method for Measurement of Fatigue Crack Growth Rates, 1991. In Annual Book of ASTM Standards, pp. 654-681.

APPENDIX

Test specimens and elements subjected to different loading conditions. Schematic examples of the appearance of typical fatigue failures which allow to deduce the type and level of stress and/or stress concentration, or assess the cause of damage. Shaded area - the final unstable fracture.